



МИНИСТЕРСТВО НА ЗЕМЕДЕЛИЕТО, ХРАНИТЕ И
ГОРИТЕ



This study was carried out thanks to the financial support of the European Commission under Regulation (EC) No.199 / 2008 and Regulation (EU) 2017/1004 of the European Parliament and of the Council establishing a Community framework for the collection, management and use data in the Fisheries sector and support for scientific advice on the Common Fisheries Policy, the National Agency for Fisheries and Aquaculture – Ministry of Agriculture and Forests Bulgaria, and:

Institute of Oceanology – BAS, Varna, Bulgaria

Project No BG14MFOP001-3.003-0001, "Collection, management and use of data for the purpose of scientific analysis and implementation of the Common Fisheries Policy for the period 2017-2019", funded by the Maritime and Fisheries Program co-financed by European Union through the European Maritime and Fisheries Fund."

The survey was carried out during the period X-XI 2019 in Bulgarian Black Sea area on board of R/V HAITHABU" in execution of National Programs of Bulgaria for data collection in 2019.

List of authors:



BULGARIAN ACADEMY OF SCIENCES
INSTITUTE OF OCEANOLOGY
VARNA

Assoc.Prof. Dr. Violin Raykov; Assoc. Prof. Maria Yankova Assoc. Prof. Dr. Petya Ivanova Assoc. Prof. Veselina Mihneva, PhD; Assoc. Prof. Dr. Dimitar Dimitrov; Assoc. Prof. Dr. Kremena Stefanova; Chief Assist. Dr. Elitsa Stefanova; Dr. Ilian Kotsev; Dr. Nina Dzembekova; Technician Nelly Valcheva; Technician Dobroslav Dechev; Technician Hristina Stamatova; Technician Svetla Koleva; Logistics Peter Trandafilov;

1----- www.eufunds.bg -----

Проектно предложение № BG14MFOP001-3.003-0001, „Събиране, управление и използване на данни за целите на научния анализ и изпълнението на Общата политика в областта на рибарството за периода 2017-2019 г.“, финансирано от Програмата за морско дело и рибарство, съфинансирана от Европейския съюз чрез Европейския фонд за морско дело и рибарство.



МИНИСТЕРСТВО НА ЗЕМЕДЕЛИЕТО, ХРАНИТЕ И
ГОРИТЕ



Contents

1.	Results from pelagic survey in October-November 2019	4
1.1.	Summary	4
2.	R/V vessel and gears	6
3.	Material and Methods	7
3.1.	Sampling design	8
3.2.	Onboard sample/processing	9
3.3.	Laboratory analyses	10
3.4.	Statistical analyses	10
3.5.	Age estimation	14
3.5.1.	Otolith preparation for sprat	17
3.5.2.	Preperation of the otoliths for the age determination	17
3.5.3.	Age readings and commenting on annuluses	18
3.5.4.	Sprat (<i>Sprattus sprattus</i>)	19
3.5.5.	Age reading protocol	21
3.6.	Sex and Maturity Estimation	22
3.6.1.	Sprat	22
3.6.2.	Maturity Stages of Sprat	23
3.6.3.	Batch fecundity	31
3.7.	Feeding of sprat (<i>Sprattus sprattus</i> , L) in October – November 2019	33
3.8.	Selectivity of the fishing gear	34
4.	Results	37
4.1.	Selectivity of the fishing gear	37
4.2.	Abundance and biomass indices	41
4.3.	Catch per unit area	47



МИНИСТЕРСТВО НА ЗЕМЕДЕЛИЕТО, ХРАНИТЕ И
ГОРИТЕ

4.4. Catch per unit of effort	49
4.5. Size structure of <i>Sprattus sprattus</i> , Red mullet and Whiting.....	52
4.6. Age structure	57
4.7. Growth.....	59
4.8. Body growth.....	61
4.8.1. Sex Ratio.....	64
4.9. Fertility and fecundity.....	66
4.10. Gonado-somatic index.....	68
5. Length-weight dependence, Index of stomach fullness (ISF)	70
6. Forecasts and Operational Opportunities	88
7. Maximum sustainable yield.....	92
8. Conclusions	93
9. References	97
ANNEXES.....	101
Pictures.....	130



МИНИСТЕРСТВО НА ЗЕМЕДЕЛИЕТО, ХРАНИТЕ И
ГОРИТЕ



1. Results from pelagic survey in October-November 2019

1.1. Summary

Pelagic Trawl Survey was accomplished in October-November 2019 in the Bulgarian Black Sea area. Scientific team has produced a biological analysis of the results obtained in the marine area. Biological analysis is based on the biomass of the species found during the study. In addition, an analysis of the distribution and abstraction of the other species caught as by-catch is presented. The Black Sea Sprat (*Sprattus sprattus*) is a key species for the Black Sea ecosystem. Together with the anchovy, sprat is one of the most abundant, planktivorous, pelagic species. The level of its stocks depends on the conditions of the environment mainly and on the fishing effort. (Raykov, 2007; Raykov et al., 2007; Raykov et al., 2011).

The changes in the environment due to anthropogenic influence, affect the dry land as well as the world ocean. The level of the sea pollution and its "self-purifying" ability are completely different. There is a clear indication of changes in the nature equilibrium in the corresponding ecological niches (Prodanov et al., 1997). The greatest impact in the world ocean has the commercial fishery, which directly devastates a significant part of the given species populations. As a result of this some of the species stocks are declined or depleted. As a result of the excessive exploitation, altered habitats and climatic variations numerous of the commercial species are critically endangered or vulnerable. The abundance of the given fish species generations is dependent on different abiotic and biotic factors. With great importance are: the level of fishing mortality, changes in trophic levels due to mass occurrence of the ctenophore *Mnemiopsis leidyi*, algal blooms which lead to hypoxia

4-----

www.eufunds.bg

Проектно предложение № BG14MFOP001-3.003-0001, „Събиране, управление и използване на данни за целите на научния анализ и изпълнението на Общата политика в областта на рибарството за периода 2017-2019 г.“, финансирано от Програмата за морско дело и рибарство, съфинансирана от Европейския съюз чрез Европейския фонд за морско дело и рибарство.



МИНИСТЕРСТВО НА ЗЕМЕДЕЛИЕТО, ХРАНИТЕ И
ГОРИТЕ



in the shallower waters with mass mortality of the bottom dwelling organisms and etc. Recent state of the sprat stock biomass (aggregations) off Bulgarian Black sea coast show relative stability i.e. taking into consideration almost constant level of exploitation (in western and north-western part of the Black Sea) in the last years the stock possibly is underexploited yet. Estimates of the numbers and size distributions of fish stocks based on experimental trawling have become a necessity in fisheries management (Godø et al., 1990). The main assumption in these studies is that the level of catches are constant, no matter how long the trawling is. Any deviation from the linear dependence between the catch and the magnitude of the effort applied to the fishery can have a significant impact on the composition of the catches and the estimates of the numbers and to deviate from the results of the trawl studies (Wassenberg et al., 1998). The duration of the fishing effort during the trawling period may last up to 200 min (Godø et al., 1990), but for economic reasons, together with the need for multiple reps and maintaining statistical validity, the duration of trawling is reduced. Thus, the standard trawl duration varies from 30 to 120 minutes for each selected station. Some authors (Godø et al., 1990; Somerton et al., 2002; Wassenberg et al., 2002) allow larger specimens to swim in the trawl without entering the bag and that trawls of varying lengths may affect the levels of the catches and the size distribution of the trawl. In this way, some size groups may not be captured in shorthaul trawls. The average catch (in units of weight or in units) per unit of effort or per unit area is the inventory of the stock (assumed to be proportional to the stock) (Beverton and Holt, 1957). This index can be converted into an absolute measure for biomass by the so-called Area Method ". The "area method" is the so-called holistic methods (www.fao.org). All analyses are based on the biomass and density estimates and by geographical strata. All the teams calculated their standard statistical estimates using the same software.

This report presents successively the results obtained at these two levels. The



МИНИСТЕРСТВО НА ЗЕМЕДЕЛИЕТО, ХРАНИТЕ И
ГОРИТЕ



regional reports are presented in an order following the coast, from the northern to southern part of the Black Sea. The document is completed by a series of tables and figures related to the biomass/abundance indices and length frequency distributions of the species included in the reference list.

2. R/V vessel and gears

The Pelagic Trawl survey (PT) was accomplished on board of research vessel "HaiHabu" (Pic. 2.1; 2.2). The main characteristics of the ship are given bellow:



Picture 2.1. R/V HaiHabu



МИНИСТЕРСТВО НА ЗЕМЕДЕЛИЕТО, ХРАНИТЕ И
ГОРИТЕ

R/V HaitHabu

- IMO: 8862686
- MMSI: 207139000
- Позивна: LZHC
- Flag: Bulgaria [BG]
- AIS Vessel Type: Other
- Gross Tonnage: 142
- Length Overall x Breadth Extreme: 24.53m × 8m Crew: 6



Picture 2.2. a,b Catch of the OTM

3. Material and Methods

Pelagic Trawl survey was accomplished in accordance with National Programs for Data Collection in Fisheries sector of Bulgaria for 2019. The study held during the period of X-XI 2019, in the area enclosed between Durankulak and Ahtopol (Bulgaria) with total length of coastline of 370 km. Study area encloses waters between 42°05' and 43°45' N and 27°55 and 29°55 E.

During the survey, total 38 mid-water hauls were carried out in Bulgarian area (X-XI



МИНИСТЕРСТВО НА ЗЕМЕДЕЛИЕТО, ХРАНИТЕ И
ГОРИТЕ



2019). The survey undergoes during the day and the following types of data were collected:

- Coordinates and duration of each trawl
- Sprat total catch weight
- Separation of the by-catch by species
- Composition of by-catch
- Conservation of the samples
- Hydroacoustic device (fish finder, bottom bathymetry)

3.1. Sampling design

To establish the abundance of the reference species (*Sprattus sprattus*) in front of the Bulgarian coast a standard methodology for stratified sampling was employed (Gulland, 1966). To address the research objectives the region was divided in 3 strata according to depth – Stratum 1 (15 - 30 m) Stratum 2 (35 – 50 m), Stratum 3 (50 – 100m).

The study area in Bulgarian waters was partitioned into 128 equal in size not overlying fields, situated at depth between 16 - 92 m. At 37 of the fields chosen at random, sampling by means of mid-water trawling was carried out (Pic. 3.1.1).





МИНИСТЕРСТВО НА ЗЕМЕДЕЛИЕТО, ХРАНИТЕ И
ГОРИТЕ



Picture 3.1.1. Trawling operation

Each field is a rectangle with sides 5' Lat × 5' Long and area around 62.58 km² (measured by application of GIS), large enough for a standard lug extent in meridian direction to fit within the field boundaries. The fields are grouped in larger sectors – so called strata, which geographic and depth boundaries are selected according to the density distribution of the species under study. At each of the fields only one haul with duration between 30 - 40 min at speed 2.7-2.9 knots was carried out.

As a result of the trawling survey a biomass index was calculated.

3.2. Onboard sample/processing

The number of processed individuals is presented on Table 3.2.1.

Table 3.2.1. Number of processed individuals

Species	Number
Sprat	1326
Whiting	893
Red mullet	925
Horse mackerel	294
Anchovy	135
Spiny dogfish	9

The data recorded and samples collected at each haul include (Gulland, 1966):

- Depth, measured by the vessel's echo sounder;
- GPS coordinates of start/end haul points;
- Haul duration;
- Abundance of sprat caught;



МИНИСТЕРСТВО НА ЗЕМЕДЕЛИЕТО, ХРАНИТЕ И
ГОРИТЕ



- Weight of total sprat catch;
- Abundance and weight of other large species;
- Species composition of by-catch;
- 4% Formaldehyde solution with marine water was used for conservation of sprat for stomach content examination.

3.3. Laboratory analyses

The samples collected onboard were processed in the laboratory for determination of age and food composition.

The age was established in otoliths under binocular microscope.

The food spectrum was determined by separation of the stomach contents into taxonomic groups identified to the lowest possible level.

3.4. Statistical analyses

Swept area method

This method is based on bottom trawling across the seafloor (area swept), weighted with chains, rock-hopper and roller gear, or steel beams. Widely used direct method for demercal species stock assessment (Foote, 1996).

The main point of the method: the trawl doors are designed to drag along the seafloor for defined distance. Trawling area was calculated as follows:

$$(1) \begin{aligned} a &= D * hr * X2 \\ D &= V * t \end{aligned}$$

(Where: a – trawling area, V – trawling velocity, hr* X2 – trawl door distance, t –



МИНИСТЕРСТВО НА ЗЕМЕДЕЛИЕТО, ХРАНИТЕ И
ГОРИТЕ



trawling

duration (h), D – dragged distance on the seafloor;

$$(2) D = 60 * \sqrt{(Lat_1 - Lat_2)^2 + (Lon_2 - Lon_1) * \cos(0.5 * (Lat_1 + Lat_2))}$$

$$(3) D = \sqrt{VS^2 + CS^2 + 2 * VS * CS * \cos(dirV - dirC)},$$

Where, VS is vessel velocity, CS - present velocity (knots), $dirV$ vessel course (degrees) and $dirC$ - present course (degrees).

Stock biomass is calculated using catch per unit area, as fraction of catch per unit effort from dragged area:

$$(4) \left(\frac{C_{w/t}}{a/t} \right) = C_{w/a} \text{ kg / sq.km}$$

Where: $C_{w/t}$ – catch per unit effort, a/t – trawling area (km^2) per unit time;

Stock biomass of the given species per each stratum could be calculated as follows:



МИНИСТЕРСТВО НА ЗЕМЕДЕЛИЕТО, ХРАНИТЕ И
ГОРИТЕ



$$(5) \quad B = (\overline{C_{w/a}}) * A$$

Where: $\overline{C_{w/a}}$ - mean CPUA for total trawling number in each stratum, A- area of the stratum.

The variance of biomass estimate for each stratum is (equation 4):

$$(6) \quad VAR(B) = A^2 * \frac{1}{n} * \frac{1}{n-1} * \sum_{i=1}^n [Ca(i) - \overline{Ca}]^2$$

Total area of the investigated region is equal to the sum of areas of each stratum:

$$A = A_1 + A_2 + A_3$$

Average weighted catch per whole aquatic territory is calculated as follows:

$$(7) \quad \overline{Ca}(A) = Ca_1 * A_1 + Ca_2 * A_2 + Ca_3 * A_3 / A$$

Where: Ca1- catch per unit area in stratum 1, A1 – area of stratum 1, etc., A- size of total area.

Accordingly, total stock biomass for the whole marine area to:



МИНИСТЕРСТВО НА ЗЕМЕДЕЛИЕТО, ХРАНИТЕ И
ГОРИТЕ



$$(8) \quad B = \overline{Ca}(A)^* A$$

Where: $\overline{Ca}(A)$ - average weighted catch per whole investigated marine area, A – total investigated marine area.

Estimation of Maximum Sustainable Yield (MSY)

The Gulland's formula for virgin stocks is used – equation 7:

$$(9) \quad MSY = 0.5 * M * B_v$$

where: M – coefficient of natural mortality; B_v – virgin stock biomass.

Relative yield-per-recruit model with uncertainties

$$(10) \quad Y'/R = E * U^{M/k} \left\{ 1 - \frac{3U}{(1+m)} + \frac{3U^2}{(1+2m)} - \frac{U^3}{(1+3m)} \right\}$$

where: $U = 1 - (L_c/L_\infty)$

$$m = (1-E)/(M/k) = k/Z$$

$E = F/Z$ – exploitation coefficient.

Length-converted catch curve

A number of methods are available with the help of which total mortality (Z) can be estimated from length-frequency data. Thus it is possible to obtain reasonable



МИНИСТЕРСТВО НА ЗЕМЕДЕЛИЕТО, ХРАНИТЕ И
ГОРИТЕ



estimates of Z from the mean length in a representative sample, or from the slope of Jones' cumulative plot. In this article, a variety of approaches for analysing length-frequency data are presented which represent the functional equivalent of [age structured] catch curves; these "length-converted catch curves" are built around assumptions similar to those involved in age-structured catch curves.

3.5. Age estimation

As it is well known, the Calcified Structures (CS) are usually used to assign age useful to obtain their growth model and so, to reconstruct age composition of exploited fish populations. Fish ageing implies the presences in the CS of a structural pattern, in terms of succession of opaque and translucent zones and the knowledge of the periodicity of this deposition pattern. Calcified structures available for fish ageing are different: otoliths (sagittae, lapilli, asterischi), scales, vertebrae, spines and opercular bones (Panfili et al., 2002). For the selected stocks the CS utilized is the sagittae. The most important aspects (difficulties, extraction, storage, preparation method, ageing criteria) regarding the age analysis are addressed by species. Otoliths are important for fish and fisheries scientists. Otoliths are playing role balance, motion and sound. These structures are effective from growth to death in entire life cycle. They are most commonly used for age in order to determine growth and mortality research. Research on otoliths began in 1970s and continues to 21st century. Periodic growth increments which in scales, vertebrae, fin rays, in cleithra, opercula and otolith are used to determine annual age in many fish species.

Researchers have used otolith reference collections and photographs in publications to aid in identifications (Pic. 3.5.1). Otoliths have a distinctive shape which is highly specific, but varies widely among species.



МИНИСТЕРСТВО НА ЗЕМЕДЕЛИЕТО, ХРАНИТЕ И
ГОРИТЕ



6 cm (0+)



7.5 cm (1+)



8.2 cm (1+)



9 cm (2+)



МИНИСТЕРСТВО НА ЗЕМЕДЕЛИЕТО, ХРАНИТЕ И
ГОРИТЕ



9.5 (3+)



10.7 (4+)

Picture 3.5.1. Otoliths of sprat

Biologists, taxonomists and archaeologists, based on the shape and size of otoliths determined fish predators feeding habits (Kasapoglu and Duzgunes, 2014). In teleost fishes, otoliths are the main CS for the age determination and it is widely used in fisheries biology. On the other hand analysing O₂ isotopes in their structure is useful to determine fish migrations between fresh water and sea as well as species and stock identification. Otoliths are the balance and hearing organs for the fish. They are in three types located on the left and right side of the head in the semi rings; "sagitta" in the saccular, "lapillus" in the lagena and "asteriskus" in the utricular channels. Place, size and shape of these three types are different by species, the biggest one is sagitta and the smallest one is asteriscus. So, sagitta is the one mostly used in age determination in bony fishes. Other reasons for the preference to otoliths are;

- Their formation in the embryonic phase which shows all the changes in the life cycle of the fish,
- Existence in the fish which have no scales,
- Giving better results than the scales and more successful age readings in older fish than their scales,



МИНИСТЕРСТВО НА ЗЕМЕДЕЛИЕТО, ХРАНИТЕ И
ГОРИТЕ



- No resorption or regeneration,
- Having same structure in all the individuals in the same species (Jearld, 1983).

On the other hand, their disadvantages are the obligation of dissecting the fish and some failures in age determination due to crystal like formations by irregular CaCO_3 accumulations on the otoliths.

3.5.1. Otolith preparation for sprat

Sampling of the fish for otolith extraction from the overall samples is very important to have representative samples for the catch. Number of otoliths needed is lower for the species having smaller size range than the species having larger size range. According to the availability 5 fish for each length group may be better for age readings to be representative for the population. Each of the individuals should be recorded individually with place of catch, date and ID number. These steps are useful for the process:

- For each fish total length ($\pm 0,1$ cm), total weight ($\pm 0,01$ g), sex, maturation stage (I-V), gonad weight ($\pm 0,01$ g) are recorded.
- Sagittal otoliths of each fish are removed by cutting the head over eyes after all individual measurements. Then, rinsed and immersed in 96% ethyl alcohol to get rid of organic wastes/residuals and finally kept in small chambers in plastic roomed boxes with the sample number and other operational information.

3.5.2. Preparation of the otoliths for the age determination

Otoliths are put into small black convex glasses containing 96% ethyl alcohol for age



МИНИСТЕРСТВО НА ЗЕМЕДЕЛИЕТО, ХРАНИТЕ И
ГОРИТЕ

readings under binocular stereo microscope which is illuminated from top and sides (Fig. 3.5.2.1) (Polat and Beamish, 1992). Magnifying level depends on the size of the otolith; X4 is good for sprat and X1 for turbot.



Figure 3.5.2.1. Binocular stereo microscope with top and side illumination

3.5.3. Age readings and commenting on annuluses

In order to prevent bias, during age reading reader should not refer length and weight of that fish. But information on the date of the catch and gonadal state is very important. First step is to clarify the place of the center and the first age ring. After



МИНИСТЕРСТВО НА ЗЕМЕДЕЛИЕТО, ХРАНИТЕ И
ГОРИТЕ



that, observation of the successive rings, whether they are continuous or not is important.

Finally, determination of the fish in growth or just at the end of the growth period by checking characteristics of the ring at the edge of the otolith to decide it is opaque or hyaline. After these procedures otoliths can be read under these protocols which are very important to provide data on age to determine realistic population parameters and reduce uncommon procedures and biases by standardized age reading criteria.

3.5.4. Sprat (*Sprattus sprattus*)

In sprat left and right otoliths shows isometric growth. These are small and transparent (Fig. 3.5.4.1). Age readings can be done over otolith surface by clear ring views. Due to summer and winter growths there are two different nucleus formation in the center; spring recruits has opaque, late fall recruits has hyaline rings which is taken into consideration during age readings (Pisil, 2006).



TL: *a* – 6.2 cm; *b* – 6.7 cm



b

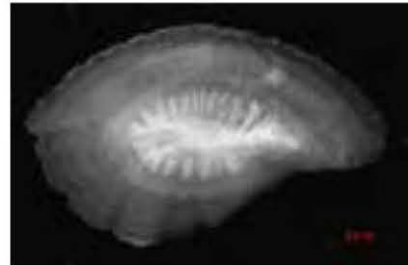
S. sprattus



МИНИСТЕРСТВО НА ЗЕМЕДЕЛИЕТО, ХРАНИТЕ И
ГОРИТЕ



Merlangius merlangus



Trachurus mediterraneus



E. encrasiculus



M. barbatus





МИНИСТЕРСТВО НА ЗЕМЕДЕЛИЕТО, ХРАНИТЕ И
ГОРИТЕ

P.salstarix

Figure 3.5.4.1. Sprat, anchovy, horse mackerel, red mullet, bluefish otoliths

3.5.5. Age reading protocol

1. Dissected otoliths rinsed and treated with 96% ethyl alcohol and stored dry.
2. Readings are carried out by inspecting the whole otolith in 96% ethyl alcohol in black colored convex glass bowl under reflected light against a dark background.
3. Magnification set considering the biggest otolith size which is totally fit the visual capacity of the lens. It is aimed not to change magnification rate which may enable false rings visible in bigger otoliths and permits to see true rings (hyalins) better by unchanging the color contrasts. That's why magnification rate X4 is selected for the sprat otoliths.
4. Otolith samples observed from distal surface as a whole, broken ones are not used.
5. Birthday of the sprat accepted as 1st of January as the common principle for the fish living in the Northern semisphere in line with the sub-tropic fish growth models.
6. Central point surrounded by the hyalin rings which is one in some cases or two for the others, is formed after the end of consumption of yolk sac and starting of the free feeding, and known as "stock rings". Next opaque accumulation is known as "first year growth ring". This ring keeps its circular form in the postrostrum region. Together with this ring and the next hyalin ring forming "V" shape in the rostrum, is accepted as first age rings.
7. Tiny and continuous consantric rings prolong close to real hyalin ringed are



МИНИСТЕРСТВО НА ЗЕМЕДЕЛИЕТО, ХРАНИТЕ И
ГОРИТЕ



counted together with the real one as one age. This ring may be either a very tiny and opaque inside the hyaline band or tiny hyaline ring near the outer edge of the opaque ring.

8. Sprat and some other short lived species has very fast growth rate especially in the first two years. Width of the growth bands after 2nd year ring has relatively getting narrower. This issue should be kept in mind in the older age ring readings. Number of tiny and weak hyaline rings, known as false rings, in the opaque region, is not so high and, their separation from age rings is rather easy. When they are so much and unseperable, these otoliths should not be used.

3.6. Sex and Maturity Estimation

3.6.1. Sprat

The European sprat (*Sprattus sprattus* L.) is a small short-lived pelagic species from the family Clupeidae. Sprat has a wide distribution including shelf areas of the Northeast Atlantic, the Mediterranean Sea and the Baltic Sea. Sprat is most abundant in relatively shallow waters and tolerates a wide range of salinities. Spawning is pelagic in coastal or offshore waters and occurs over a prolonged period of time that may range from early spring to the late autumn. Sprat is an important forage fish in the North Sea and Baltic Sea ecosystems. Commercial catches from pelagic fisheries are mainly used for fish meal and fish oil production. Three subspecies of sprat have been defined i.e. *Sprattus sprattus sprattus* L., distributed along the coasts of Norway, the North Sea, Irish Sea, Bay of Biscay, the western coast of the Iberian peninsula down to Morocco, *Sprattus sprattus phalericus*, R) in the northern parts of the Mediterranean and the Black Sea, and *Sprattus sprattus balticus* S. in the Baltic Sea. Knowledge about stock structure, migration of sprat and mixing of populations among areas is limited. Questions have been raised about the geographic distribution and separation of stocks and their



МИНИСТЕРСТВО НА ЗЕМЕДЕЛИЕТО, ХРАНИТЕ И
ГОРИТЕ



interaction with neighboring stocks (ICES 2011). The apparent overlap e.g. between North Sea sprat and English Channel sprat seems very strong, whereas the overlap between North Sea sprat and Kattegat sprat is not as strong and varies between years. A distribution wide phylo-geographic study showed that sprat in the Western Mediterranean is a subgroup of the Atlantic group and that these two populations are closer to each other than to sprat in the Eastern Mediterranean and Black Sea (Debes et al., 2008).

3.6.2. Maturity Stages of Sprat

It is very important to use standardized maturity scales for sprat (and all species) to evaluate sampling strategies and timing for accurate classification of maturity in order to provide reliable maturity determination for both sexes. For sprat, small gonad size and the batch spawnings by several cohorts of eggs over a long period of time are the main challenges for standardizing a maturity scale.

According to the ICES (2011), present standardized maturity scales of sprat include 6-stages for both sexes (Fig. 3.6.2.1, Table 3.6.2.1)



МИНИСТЕРСТВО НА ЗЕМЕДЕЛИЕТО, ХРАНИТЕ И
ГОРИТЕ

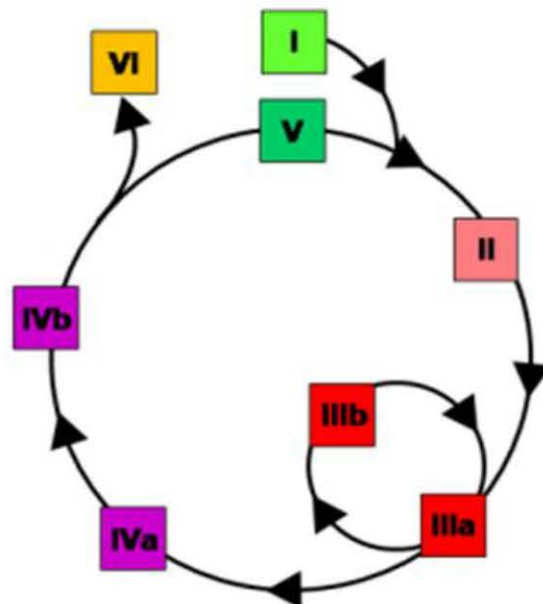


Figure 3.6.2.1. Scale with six maturity stages in sprat (Name of the stages are given in Table 3.6.2.1)

In particular, specimens without visible development have been combined into Immature and Preparation, whereas the spawning stage has been sub-divided into a non-active spawning stage (maturing and re-maturing characterized by visible development of gametes) and an active spawning stage indicated by hydrated eggs/running milt. The integration of maturing and re-maturing into the spawning stage allows an accurate determination of maturing and spawning specimens and reliable assessment of the spawning fraction of the population.

Table 3.6.2.1. Macroscopic and histological characteristics of gonadal development stages

Stages	<i>Macroscopic Characteristics</i>	<i>Histological characteristics</i>
--------	--	---



МИНИСТЕРСТВО НА ЗЕМЕДЕЛИЕТО, ХРАНИТЕ И
ГОРИТЕ

FEMALES (OG: Oogonia, PG1: Early previtellogenic oocytes, PG2: Late previtellogenic oocytes, CA: Cortil

alveoli oocytes, VT1: Early vitellogenic oocytes, VT2: Mid vitellogenic oocytes, VT3: Late

vitellogenic oocytes, HYD: Hydrated oocytes, POF: Postovulatory follicles, SSB: Spawning stock

biomass).

<i>I-Immature</i>	<i>Juvenile: ovaries threadlike and small; transparent to wine red and translucent in color; sex difficult to determine; distinguishable from testes by a more tubular shape; oocytes not visible to the naked eye</i>	OG+/-PGI
<i>II-Preparation</i>	<i>Transition from immature to early maturing; oocytes not visible to the naked eye; ovaries yellow-orange to bright red in color; ovaries occupy up to half of the abdominal cavity. This stage is not included in SSB.</i>	PG1, PG2, CA



<i>III. Spawning</i>		
a. Spawning(inactive)	<i>Maturing and re-maturing: yolked opaque oocytes visible to the naked eye; ovaries change from semi-transparent to opaque yellow-orange or reddish in color as more oocytes enter the yolk stage; ovaries occupy at least half of the body cavity; re-maturing ovaries may be red to grey-red or purple in color and less firm than an ovary maturing first batch, few hydrated oocytes may be left</i>	PG1, PG2, CA, VT1, VT2, VT3, +/- POF
b. Spawning (active)	<i>Spawning active. Hydrated eggs are visible among yolked opaque oocytes; hydrates oocytes may be running; ovaries fill the body cavity; overall color varies from yellowish to reddish.</i>	PG1, PG2, CA, VT1, VT2, VT3, HYD, POF



МИНИСТЕРСТВО НА ЗЕМЕДЕЛИЕТО, ХРАНИТЕ И
ГОРИТЕ

IV.a Cessation	<i>Baggy appearance; bloodshot; grey-red translucent in color; atretic oocytes appear as opaque irregular grains; few residual eggs may remain</i>	PG1, PG2, POF, atretic oocytes, residual HYD
IV.b. Recovery	<i>Ovaries appear firmer and membranes thicker than in sub-stage IV.a; these characteristics together with the slightly larger size distinguish this stage from the virgin stage; ovaries appear empty and there are no residual eggs; transparent to wine red translucent in color</i>	PG1, PG2, atretic VT oocytes
V. Resting	<i>Ovaries appear more tubular and firmer; oocytes not visible to the naked eye; transparent or grey-white to wine red in color with well-developed blood supply; this stage leads to stage II.</i>	PG1, PG2 +/- atretic oocytes
VI. Abnormal	<i>a) infection; b) intersex - both female and male tissues can be recognized; c) one lobe degenerated; d) stone roe (filled with connective tissue); e) other</i>	Abnormal tissue
<p>MALES (SG: Spermatogonia; PS: Primary spermatocytes; SS: Secondary spermatocytes; ST: Spermatids; SZ: Spermatozoa; SSB: Spawning stock biomass)</p>		



МИНИСТЕРСТВО НА ЗЕМЕДЕЛИЕТО, ХРАНИТЕ И
ГОРИТЕ

I. Immature	<i>Juvenile: Testes threadlike and small; white-grey to grey brown in color; difficult to determine sex, but distinguishable from ovaries by a more lanceolate shape (knife shaped edge of distal part of the lobe).</i>	SG, PS
II-Preparation	<i>Transition from immature to maturing: Testes easily distinguishable from ovaries by lanceolate shape; sperm development not clearly visible; reddish grey to creamy translucent in color; testes occupy up to ½ of the abdominal cavity; this stage is not included in SSB.</i>	SG, PS, SS, potentially few ST



МИНИСТЕРСТВО НА ЗЕМЕДЕЛИЕТО, ХРАНИТЕ И
ГОРИТЕ

III. Spawning	<i>Maturing and re-maturing: Testes occupy at least half of the body cavity and grow to almost the length of the body cavity; the empty sperm duct may be visible; color varies from reddish light grey, creamy to white; edges may still be translucent at the beginning of the stage, otherwise opaque; re-maturing testes may be irregularly colored with reddish or brownish blotches and grey at the lower edge with partly whitish remains of sperm</i>	SG, PS, SS, ST, SZ
a. Spawning(inactive)	<i>Spawning active: testes fill the body cavity; Sperm duct filled and distended throughout the entire length; sperm runs freely or will run from the sperm duct, if transected; color varies from light grey to white..</i>	SG, PS, SS, ST, SZ
c. Spawning (active)		



МИНИСТЕРСТВО НА ЗЕМЕДЕЛИЕТО, ХРАНИТЕ И
ГОРИТЕ

IV.a Cessation	<i>Baggy appearance (like an empty bag when cut open); bloodshot; grey to reddish brown translucent in color; residual sperm may be visible in sperm duct.</i>	SG, PS, atretic SS, ST and SZ
IV.b. Recovery	<i>Testes appear firmer and the testes membrane appear thicker than in stage IVa due to contraction of the testes membrane; these characteristics together with the slightly larger size distinguish this stage from the virgin stage; testes appear empty and no residual sperm is visible in the sperm duct; reddish grey to greyish translucent in color.</i>	SG, PS, potentially SS, atretic SZ
V. Resting	<i>Testes appear firmer, development of a new line of germ cells; grey in color; this stage leads to stage II.</i>	SG, PS, SS
VI. Abnormal	<i>a) infection; b) intersex - both female and male tissues can be recognized; c) one lobe degenerated; d) other.</i>	e.g. oocytes visible among spermatogenic tissues



МИНИСТЕРСТВО НА ЗЕМЕДЕЛИЕТО, ХРАНИТЕ И
ГОРИТЕ



3.6.3. Batch fecundity

All fish were measured to the nearest 1 mm in the Total Length (TL) and weighted to the nearest 1 g. Gonads of the fish were examined under a dissecting microscope for its external features such as turgidity and colour in order to determine a maturity stage. The sex ratio also calculated in this study (i.e., No. of males/No. of females (Simon et al., 2012). The female was determined by the macroscopic observation of matured ovary (Laevastu, 1965).

Batch fecundity can vary considerably during the short spawning season, low at the beginning, peaking during high spawning season and declining again towards the end.

Annual egg production is the product of the number of batches spawned per year and the average number of eggs spawned per batch.

Batch fecundity was determined as 'Hydrated Oocyte Method' (Hunter et al., 1985). Oily hydrated females were used. After sampling their body cavity was opened and they were preserved in a buffered formalin solution (Hunter et al., 1985). The ovary free female weight and the ovary weight were determined: Three tissue samples of - 50 mg were removed from different parts of the ovary and their exact weight were determined. Under binocular number of hydrated oocytes, in each of the three subsamples was determined.

Hydrated oocytes can easily be separated from all other types of oocytes because of their large size and their translucent appearance and their wrinkled surface which is due to formalin preservation. Batch fecundity was estimated based on the average number of hydrated oocytes per unit weight of the three subsamples.

Gonadosomatic Index (GSI) was determined monthly. GSI was calculated as:



МИНИСТЕРСТВО НА ЗЕМЕДЕЛИЕТО, ХРАНИТЕ И
ГОРИТЕ



$$GSI = \frac{GW}{SW} \times 100$$

where, GW is gonads weight and SW is somatic weight (represents the BW without GW)

For the estimation of sprat growth rate, the von Bertalanffy growth function (1938) is used, (according to Sparre, Venema, 1998):

$$(11) \quad L_t = L_\infty \left\{ 1 - \exp[-k(t - t_0)] \right\}$$

$$(12) \quad W_t = W_\infty \left\{ 1 - \exp[-k(t - t_0)] \right\}^n$$

where: Lt, Wt are the length or weight of the fish at age t years; L ∞ , W ∞ - asymptotic length or weight, k – curvature parameter, t₀ - the initial condition parameter.

The length – weight relationship is obtained by the following equation:

$$(13) \quad W_t = qL_t^n$$

where: q – condition factor, constant in length-weight relationship; n – constant in length-weight relationship.

Coefficient of natural mortality (M)

Pauly's empirical formula (1979, 1980) is applied:

$$(14) \quad \log M = -0.0066 - 0.279 * \log L_\infty + 0.6543 * \log k + 0.4634 * \log T^\circ C$$



МИНИСТЕРСТВО НА ЗЕМЕДЕЛИЕТО, ХРАНИТЕ И
ГОРИТЕ



$$(15) \log M = -0.2107 - 0.0824 \log W_\infty + 0.6757 \log K + 0.4627 \log T^\circ C$$

where: L_∞ , W_∞ and K – parameters in von Bertalanffy growth function; $T^\circ C$ – average annual temperature of water, ambient of the investigated species.

3.7. Feeding of sprat (*Sprattus sprattus*, L) in October – November 2019

The study includes analysis of stomach content composition of 110 sprat specimens, collected in front of the Bulgarian Black Sea coast during 28.X - 8.XI 2019, and it encompasses additional analyses of the zooplankton species composition and biomass in the marine environment (Mihneva et al., 2015).

The coordinates and information about the sampling sites were presented in Table 3.7.1.

Table 3.7.1. Investigated area in 28.X - 8.XI.2019

Date	Trawl №	Coordinates	Depth (m)	Temp °C	Zooplankton stations	Sprat food	Horse mackerel food
28.10.2019	2	42.91;28.15	45	18.2	Zoo1	S1	
29.10.2019	8	43.51;28.69	65	17.0	Zoo2	S2	
03.11.2019	22	42.69;27.82	21.5	16.2	Zoo3		T1
05.11.2019	27	42.37;27.97	45	16.6	Zoo4	S3	
06.11.2019	32	42.45;27.77	36	16.8	Zoo5	S4	
08.11.2019	38	42.59;27.74	30	16.8	Zoo6	S5	

Per trawl catch, about 10 fish specimens were separated and preserved in 10% formaldehyde: seawater solution. The absolute length (TL, to the nearest 0.1 cm) and weight (to the nearest 0.01 g) of fish specimens were measured. Under laboratory conditions, the stomachs of the selected animals were weighted with analytical balance (to the nearest 0.0001 g). The food mass of each individual has



МИНИСТЕРСТВО НА ЗЕМЕДЕЛИЕТО, ХРАНИТЕ И
ГОРИТЕ



been calculated as a difference between the weights of full and empty sprat stomach.

The stomach content was investigated under a microscope for the estimation of species composition and prey number. The prey biomass was estimated by multiplication of the number of consumed mesozooplankton species by their weights.

The following indices were calculated:

1. Stomach fullness index (ISF) as a per cent of body mass: (stomach content mass/fish mass) *100; and

2. Index of relative importance - IRI, Pinkas et al. (1971): $IRI = (N+M) \times FO$; where N - the proportion of prey taxa (species) in the diet by numbers (abundance); M - the percentage of prey taxa (species) in the diet by mass; FO - frequency of occurrence among fish.

The zooplankton samples in the marine environment were gathered from the whole water layer (bottom- surface) with a plankton set (opening diameter $d = 36$ cm; mesh size $150\text{ }\mu\text{m}$). The samples were fixed onboard ships with 4% formaldehyde: seawater solution (Korshenko and Aleksandrov, 2012). The mesozooplankton species composition has been identified by "Guides for the Black and Azov Seas" (Mordukhay-Boltovskoy et al., 1968; Alexandrov and Korshenko, 2006; Korshenko and Aleksandrov, 2013), and its quantity - by the method of Bogorov (Dimov, 1959; Korshenko & Aleksandrov, 2013).

3.8. Selectivity of the fishing gear

The change in mesh size of the codend is the basis of the analysis of the selectivity in the calculations. The mesh size (a , mm) of the trawl bag is shown in Fig. 3.8.1. The study of the variation in the trawl selectivity is based on calculations at the corresponding change in the size of the "eye" side.



МИНИСТЕРСТВО НА ЗЕМЕДЕЛИЕТО, ХРАНИТЕ И
ГОРИТЕ

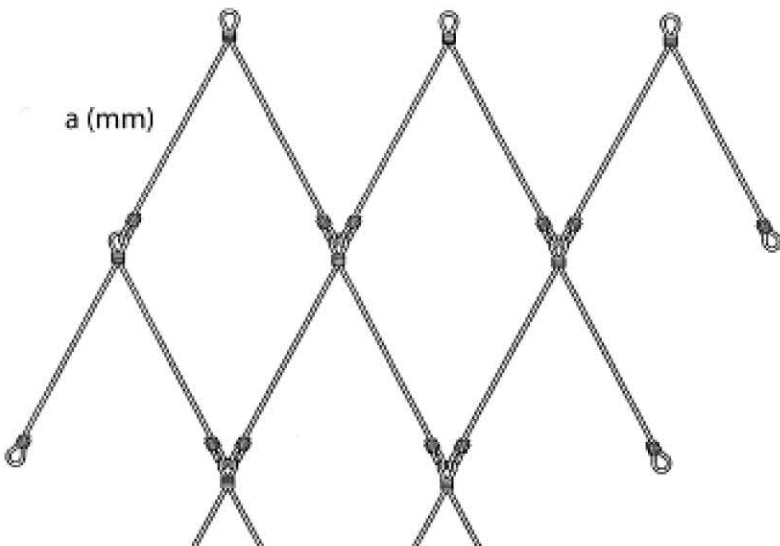


Figure 3.8.1. "Eye" of the codend and size a (mm)

Using the model of Treschev (1974), it was worked out to construct an additional trawl bag to experimentally study the change in selectivity (Fig. 3.8.2).



Figure 3.8.2. Codend bag scheme: 1 - main bag 2 - apron; 3 - connector, 4 - the main bag 5 - the trailer outer bag connection.



МИНИСТЕРСТВО НА ЗЕМЕДЕЛИЕТО, ХРАНИТЕ И
ГОРИТЕ



Linear size measurements were used to evaluate the following biological parameters:

L50, L25 and L75 the amount at which 50%, 25% and 75% of the individuals entered into the fishing gear are detained therein;

Selectivity factor;

(c) an extent of selectivity

The dimensional selectivity of the trawl bag is determined by the relationship between

the probability p, the fish entering the bag and its size l (Holden, 1971). This link is described by the logistic function (Fryer, 1996):

$$p = \frac{e^{(v_1 + v_2)l}}{(1 + e^{(v_1 + v_2)l})}$$

Where v1 represents the intersection of the abscissa, v2 is the slope of the curve following log-transformation. The L50, L25 and L75 function values can be estimated from the

following expressions:

$$L_{50\%} = \frac{v_1}{v_2} \quad L_{25\%} = \frac{(-\ln(3) - v_1)}{v_2} \quad L_{75\%} = \frac{(\ln(3) - v_1)}{v_2}$$



МИНИСТЕРСТВО НА ЗЕМЕДЕЛИЕТО, ХРАНИТЕ И
ГОРИТЕ

$$SR = L_{75} - L_{25} \quad SF = \frac{L_{50}}{\text{meshsize}}$$

Suppose that fish of size: I₁, I₂, . . . I_N enter the trawl bag. Small fish may loose through the mesh (ie, have a low probability of retention), but as they grow in length, the chance to get rid of the net decreases. At some point, because of their increased size, they can not get out of the net (their probability of retention equals 1).

4. Results

4.1. Selectivity of the fishing gear

The possibilities of holding individuals from sprat of mesh size a = 8 mm; 7.5 mm and 6.5 mm are presented (Table 4.1.1) in order to trace the change in the probability of retention of individuals when changing the mesh size of the network.

Table 4.1.1. Possibilities for holding individuals from a twine in a "mid-water otter trawl" of different mesh sizes; Selectivity factor (SF) and Selectivity Spectrum (SR)

	8		7,5		6,5	
"EYE" size	selectivity	mm	selectivity	mm	selectivity	mm
L25%	6,2cm	L25%	5,4cm	L25%	5,2cm	
Retention	L50%	7.0cm	L50%	6,2cm	L50%	5,7cm
capability	L75%	7,8cm	L75%	7,0cm	L75%	6,2cm
	SF	4,4		4,13		4,77
	SR	1,6		1,6		1



МИНИСТЕРСТВО НА ЗЕМЕДЕЛИЕТО, ХРАНИТЕ И
ГОРИТЕ

In the trawl bag of mesh size $a = 8.00$ mm, the probability is that 25% of the specimens retained in the bag should have a size of 6.2 cm ($L_{25} = 6.2$ cm). With 50% probability ($L_{50\%}$), individuals with a size of 7.00 cm and the largest will be retained probability of retention ($L_{75\%}$) were individuals with a linear size of 7.8 cm (Table 4.1.1, Fig. 4.1.1).

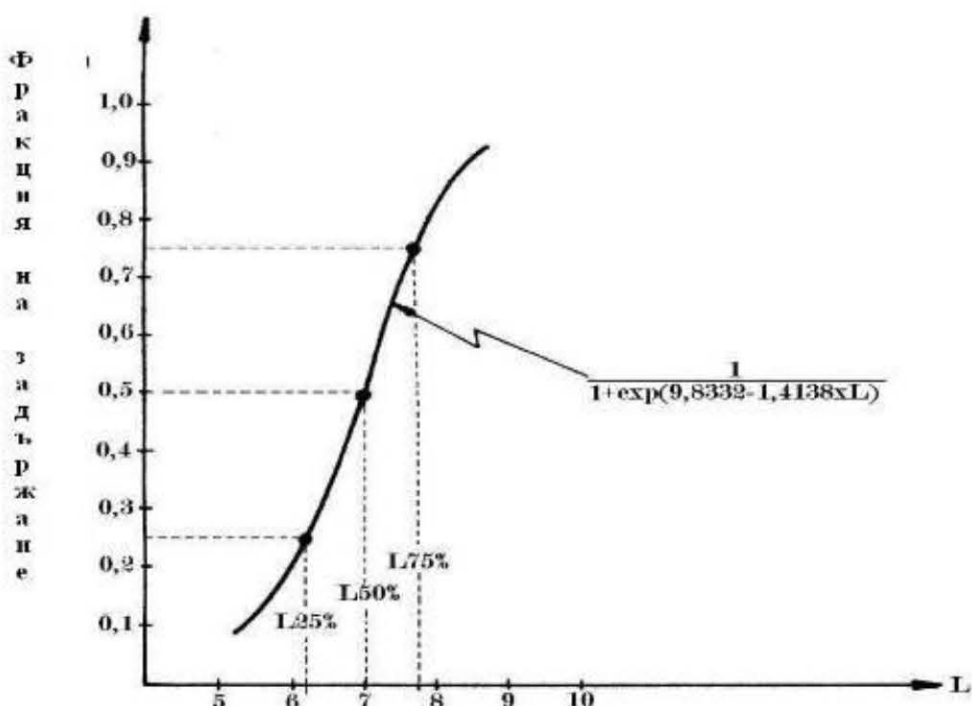


Figure 4.1.1. Graphical representation of $L_{25\%}$, $L_{50\%}$, $L_{75\%}$ at the mesh size of the "bag" $a = 8.00$ mm

The next scenario examined is to change the selectivity, with the mesh size being 0.5 mm smaller: 7.5 mm. In this case, 6.2 cm individuals will retain a probability of 50% in the trawl net ($L_{50\%} = 6.2$ cm, Table 4.1.1), which is 0.8 mm less than the case of mesh size $a = 8$ mm. In this case, it reduces the size of the specimens that would be retained in the trawl with a probability of 25%, namely $L_{25\%} = 5.4$ cm.



МИНИСТЕРСТВО НА ЗЕМЕДЕЛИЕТО, ХРАНИТЕ И
ГОРИТЕ



Reducing the network mesh from 8.00 to 7.5 cm results in a 75% retention probability of 7.00 cm specimens, which is 0.8mm less than the previous case. The selectivity factor for this particular case decreases to 4.13 and the SR selectivity range is maintained at the mesh size $a = 8.00$ cm. The proportion of the magnitude in both cases examined so far is the same, but with decreasing mesh size, the size of the retained specimens also diminishes. In the third case, the mesh size is $a = 6.5$ mm. Such a network will retain in a proportion of 50% individuals with TL = 5.7 cm, which is 1.3 cm less than in the case of mesh size of the net - $a = 7$ mm.

In this case, the difference between the individuals of the trickles of certain dimensions retained in the bag (inner) with an eye of 6.5 mm in the proportion of 25, 50 and 75% will be 0.5 cm.

A codend of mesh size $a = 6.5$ mm (the actual mesh size measured in the present research, and length distribution of sprat caught in such a codednd, Fig. 4.1.2) will hold fish in a proportion of 6.2 cm in a proportion of 75% and in a proportion of 25%, 5.2 cm in size, 5.1. The selectivity factor in this case increases to 4.77 (from 4.4 and 4.5) and the selectivity range is equal to one (SR = 1). It can be seen that in all cases with a mesh size of 6.5 mm, the change in the size of the detainees varies within a smaller range, but in all variants, the holdings are very much below the minimum allowable harvest size (2001) spatula, namely 7.00 cm. We should note the fact that active trawl-fishing gears are using nets with mesh sizes from 6.0 to 6.5 cm. This fact undoubtedly speaks of the fact that there are specimens that have not reached sexual maturity in different proportions. Not least, the fact that active fishing activity related to the use of trawls take place in the near coastal strip at a lower depth. It is well-known, from the biology of the species, which the large individuals, respectively the senior age groups, migrate to greater depths in search of favorable temperature and nutritional conditions. According to the calculations made on the selectivity of the trawl bag of different mesh size, it can be seen that at $a = 8$ mm,



МИНИСТЕРСТВО НА ЗЕМЕДЕЛИЕТО, ХРАНИТЕ И
ГОРИТЕ

50% of the TL = 7cm individuals have a chance of being trapped while the TL = 7.8 cm 75% retention capability. A further reduction in mesh size leads to a reduction in the selectivity of the trawl. In eye mesh $a = 7.0\text{cm}$, $L50\% = 6.2\text{cm}$ and $L75\% = 7\text{cm}$. For nets with a mesh size of 6.5mm, the size of the trait-retained individuals drops to 5.7cm at L50%. As the mesh of the bag grows, the number of small individuals that escape the trawl increases. At the same time, the average length of the fish caught, i.e. this is part of the breeding biomass that has already participated in the reproduction. The Regional Fisheries Commissions are aiming for maximum mesh sizes, which would allow maximum "extraction" of juvenile individuals.

The minimum allowable catch for sprat referred to in the Fisheries and Aquaculture Act (2001) is 7 cm. This fact is indicative that in order to comply with the measure of resource use referred to in the law, the mesh size of the trawl should be $a = 8\text{ mm}$, which would result in the proportion of individuals in the proportion of $L75\% = 7.8\text{cm}$. This measure is essential to protect the exploited resource from overloading and undermining stocks in the longer term.

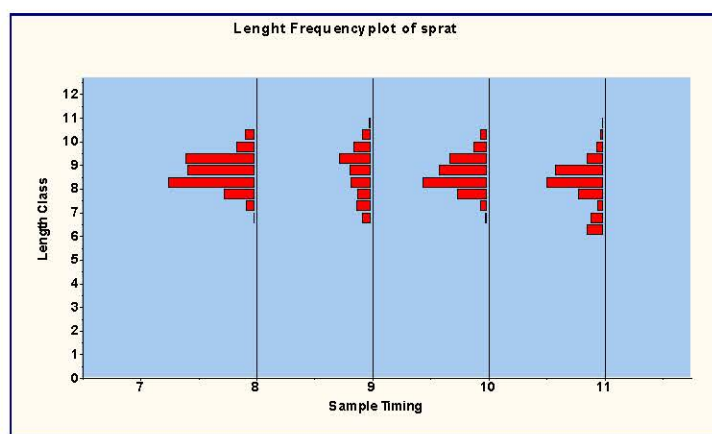


Figure 4.1.2. Linear dimensions of the sprat in the codend of the trawl



МИНИСТЕРСТВО НА ЗЕМЕДЕЛИЕТО, ХРАНИТЕ И
ГОРИТЕ



4.2. Abundance and biomass indices

A total of 38 trawls in the EEZ of the Republic of Bulgaria were carried out on the board of R/V "HaiHabu". The total number of the identified species is 34, of which 26 are fish, crustaceans - 2, molluscs - 2 and 4 macrozooplankton species. The most common species in total trawl operations (in terms of presence / absence) are (in descending order): in Oct - Nov 2019: *S. sprattus* (82.99%), *M. merlangius* (9.44%), and *M. barbatus* - 6.54%. Other species such as, *Tr. mediterraneus*, *A. immaculata*, *N. melanostomus*, *G. niger*, *N. melanostomus*, *M. batrachocephalus*, *At. boyeri*, *H. guttulatus*, *R. clavata*, *D. pastinaca*, *P. lascaris*, *Sc. umbra*, *U. scaber*, *Tr. draco*, *A. guldensaetii*, *A. stellatus*, *Sq. acanthias*, *Sc. maximus*, *B. gymnotrachelus*, *C. ocellatus*, *C. tinca*, *C. kessleri pontica*, *S. tenuirostris*, have insignificant catch presence as in June 2019. Single specimens from *A. stellatus*, *S. maximus Sparidae*, *Tr. draco*, *Scorpaena porcus*, *Pegusa lascaris* and others were caught.

In the Bulgarian Black Sea area 38 trawls were made in the period 28.10 - 8.11.2019. Trawling time is 30 and 40 min, between 15.8 m and 92 m deep, in the area between Kiten and Durankulak. The studied area (Fig. 4.2.1) in Bulgarian waters was 8010, 24 km². During the study period the largest number was the sprat, which dominated the pelagic society.



МИНИСТЕРСТВО НА ЗЕМЕДЕЛИЕТО, ХРАНИТЕ И
ГОРИТЕ

Locations of trawling stations



Figure 4.2.1. Location of trawl stations in the Oct-Nov 2019 survey

Global Comments on Fish and Other Species:

Sprat (*Sprattus sprattus*)

The species had the highest recorded biomass and catch per unit area in the studied areas in Oct-Nov 2019. At stratum 15-30 m CPUA = 11 537 kg.km⁻² and 23 825 t. In depth plots 30-50 m: 10 641 kg.km⁻² and biomass 19 311 t, for stratum (combined) 50-100 m the clusters were CPUA = 7 131 kg.km⁻² and 2945 t.



МИНИСТЕРСТВО НА ЗЕМЕДЕЛИЕТО, ХРАНИТЕ И
ГОРИТЕ

Whiting (*Merlangius merlangus*)

The whiting inhabits the layer near the bottom and feeds mainly on the sprat. The species is a predator on the sprat and is an important food component for the largest predators such as turbot and dolphins. In October-November 2019, whiting was most strongly represented in the deepest coastal zone zone 50-100 m with CPUA = 4803 kg.km⁻² and biomass of 19 839 t, followed by a depth strip of 30-50 m with catch (lowest) per unit area of 172 kg.km⁻² biomass 312 t, 496 kg.km⁻² for CPUA and 1023 t biomass at depths of 15-30 m.

Red mullet (*Mullus barbatus*)

In October-November 2019, the red mullet was best represented in the shallow coastal zone 15-30 m with a CPUA = 1016 kg.km⁻² and a biomass of 2099 t. The lowest CPUA values of 331 kg.km⁻² were detected in 50-100 m deep with 1366 t biomass, while the 914 kg.km⁻² values for CPUA and 1658 t biomass values were recorded in depth 30-50 m.

Other species:

Horse mackerel (*Tr. mediterraneus*)

The species is thermophilic and appear sporadically in several hauls.

Shad (*A. Immaculata*)

Only single specimen present during the 2019 Autumn survey.

Strongil (*N. melanostomus*)

The species is benthic, coastal. Single specimens were recorded in catches.

Other species

Pontic shad (*A. Immaculata*)

Only single catches are present during the 2019 Spring Survey.

Round goby (*N. melanostomus*)

The species is benthic, coastal. Single specimens were recorded in catches.



МИНИСТЕРСТВО НА ЗЕМЕДЕЛИЕТО, ХРАНИТЕ И
ГОРИТЕ



Comments on *Sprattus sprattus* biomass from different depth layers

The total biomass of sprat in October-November 2019 is 46 081,41t for the EEZ of the Republic of Bulgaria in the Black Sea (Table 4.2.1 and 4.2.2).

Table 4.2.1. Sprat. Area Method in X-XI 2019

CP UA mean	B (kg)	A x	No Fields
11536,8 15-30	23825	2065,1	33
10640,8 30-50	19311	1814,8	29
7130,8 50-100	2945,2	4130,3	66
	46081,41	8010,24	128

Table 4.2.2. Descriptive catch statistics for *Sprattus sprattus* X-XI 2019

	15-30m	30-50m	50-100m
Mean	11536,78	11079,19	7130,762
Standard Error	1504,147	1515,893	1354,206
Median	10579,09	10579,09	5289,545
Mode	7934,318	#N/A	#N/A
Standard Deviation	6556,427	5027,649	3582,893
Sample Variance	42986729	25277255	12837120
Kurtosis	1,739169	0,765473	-0,29889
Skewness	1,192791	0,31593	0,925681
Range	26976,68	18513,41	9962,321
Minimum	2115,818	2644,773	3261,543
Maximum	29092,5	21158,18	13223,86
Sum	219198,8	121871,1	49915,33
Count	19	11	7
Largest(1)	29092,5	21158,18	13223,86
Smallest(1)	2115,818	2644,773	3261,543
Confidence Level(95,0%)	3160,096	3377,621	3313,623



МИНИСТЕРСТВО НА ЗЕМЕДЕЛИЕТО, ХРАНИТЕ И
ГОРИТЕ



Comments on the biomass of *Mullus barbatus* from different depth layers

The total study area in the Bulgarian part is 8010.24 km.kg⁻² and the total biomass of the red mullet is 5122,056 t in October-November 2019 (Table 4.2.3 and 4.2.4).

Table 4.2.3. Red mullet. Area Method in X-XI 2019

CPUA mean	B (kg)	Ax	NºFields
1016,1 15-30	2098,5	2065,1	33
913,65 30-50	1658,1	1814,8	29
330,6 50-100	1365,5	4130,3	66
		5122,056	8010,24
			128

Table 4.2.4. Red mullet. Descriptive statistics of biomass indices (t) X - XI 2019

	15-30m	30-50m	50-100m
Mean	1016,15	793,4318	340,0422
Standard Error	324,1716	255,9238	73,78069
Median	528,9545	423,1636	317,3727
Mode	264,4773	476,0591	105,7909
Standard Deviation	1413,031	886,546	195,2054
Sample Variance	1996658	785963,7	38105,13
Kurtosis	12,25978	0,378341	-1,83577
Skewness	3,293862	1,394832	-0,08641
Range	6294,559	2591,877	476,0591
Minimum	52,89545	52,89545	105,7909
Maximum	6347,455	2644,773	581,85
Sum	19306,84	9521,182	2380,295
Count	19	12	7
Largest(1)	6347,455	2644,773	581,85
Smallest(1)	52,89545	52,89545	105,7909
Confidence Level(95,0%)	681,0594	563,2844	180,5348

Comments on the biomass of *M. merlangus* from different depth layers



МИНИСТЕРСТВО НА ЗЕМЕДЕЛИЕТО, ХРАНИТЕ И
ГОРИТЕ



Biomass was distributed unequally, as the bulk was in the strata 50-100m. The shallower coastal waters characterized by lower CPUA and whiting biomass (Table 4.2.5 and 4.2.6).

Table 4.2.5. Whiting. Area Method in X-XI 2019

CPUA mean	B (kg)	Ax	No Fields
495,55	15-30	1023,4	2065,1
171,91	30-50	311,99	1814,8
4803,4	50-100	19839	4130,3
		21174,59	8010,24
			128

Table 4.2.6. Whiting. Descriptive statistics of biomass indices in X-XI 2019

	15-30m	30-50m	50-100m
Mean	495,5469	171,9102	4803,362
Standard Error	184,002	74,84088	969,9527
Median	105,7909	0	5183,755
Mode	0	0	#N/A
Standard Deviation	802,0463	259,2564	2566,254
Sample Variance	643278,3	67213,89	6585658
Kurtosis	4,227399	1,956664	1,068786
Skewness	2,107151	1,575664	-0,92872
Range	2909,25	793,4318	7511,155
Minimum	0	0	105,7909
Maximum	2909,25	793,4318	7616,946
Sum	9415,391	2062,923	33623,53
Count	19	12	7
Largest(1)	2909,25	793,4318	7616,946
Smallest(1)	0	0	105,7909
Confidence Level(95,0%)	386,5739	164,7237	2373,389



МИНИСТЕРСТВО НА ЗЕМЕДЕЛИЕТО, ХРАНИТЕ И
ГОРИТЕ

4.3. Catch per unit area

The calculated area-by-catch (CPUA) for the Bulgarian Black Sea area of the deep layers is presented in Fig. 4.3.1.

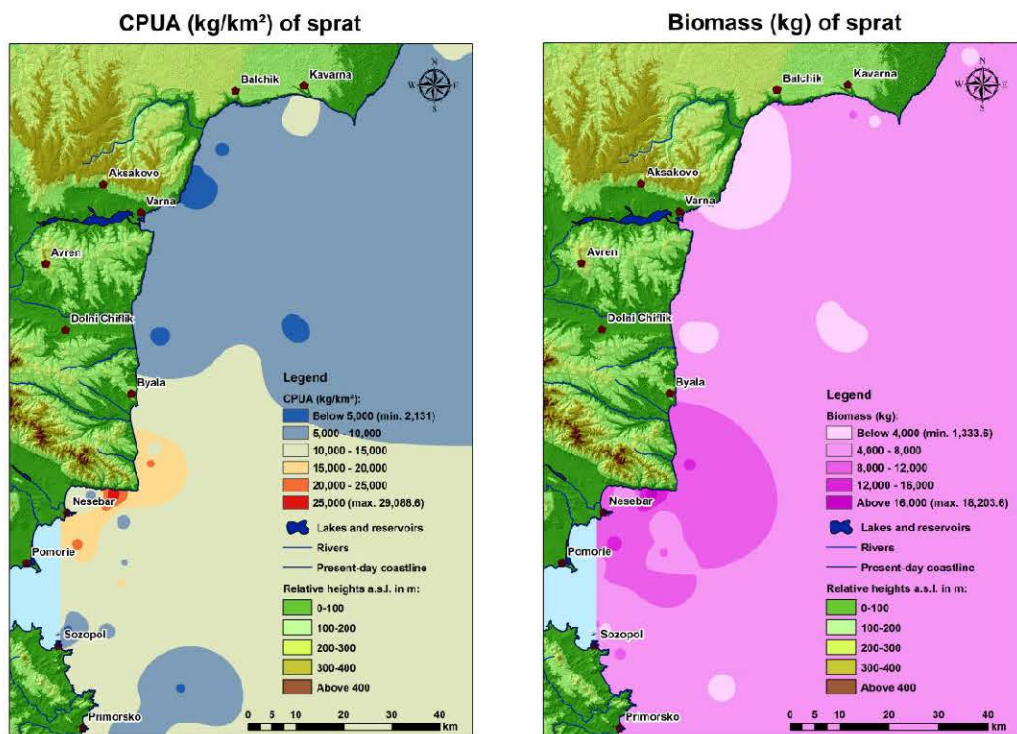


Figure 4.3.1. CPUA kg.km⁻² Biomass, kg of sprat for X-XI 2019 of the surveyed areas

Sprat, X-XI, CPUA kg.km⁻² and biomass (t)

The highest values of CPUA kg.km⁻² of the sawdust were recorded in a depth layer of 15-30 m (29 093 kg.km⁻²), followed by a strata 30-50 m (21 158 kg.km⁻²) in the southern part of the study area - in front of the town of Nessebar, in the area of Emine Cape and NW of Pomorie. Lower values were registered in front of the town of Sozopol, and the town of Kavarna. Relatively lower CPUA values were found at



МИНИСТЕРСТВО НА ЗЕМЕДЕЛИЕТО, ХРАНИТЕ И
ГОРИТЕ

shallow depths at the mouth of the Kamchia River, in the Aladja Bank District (<5000 kg.km⁻²).

Whiting, X-XI, CPUA kg.km⁻² and Biomass, kg

In October - November 2019, the highest values > 9 415 kg.km⁻² of CPUA of honeydew were regimented SW from Balchik and in front of Albena (Fig. 4.3.2.). In the 30-50 m strip, the highest catch per unit area was 2063 kg.km⁻², again in the described area during this study. At depths of 50-100 m, the average catch per unit area was significantly higher than 33 624 kg.km⁻², which clearly indicates concentrated clusters of the species in the deepest coastal zone during the described period.

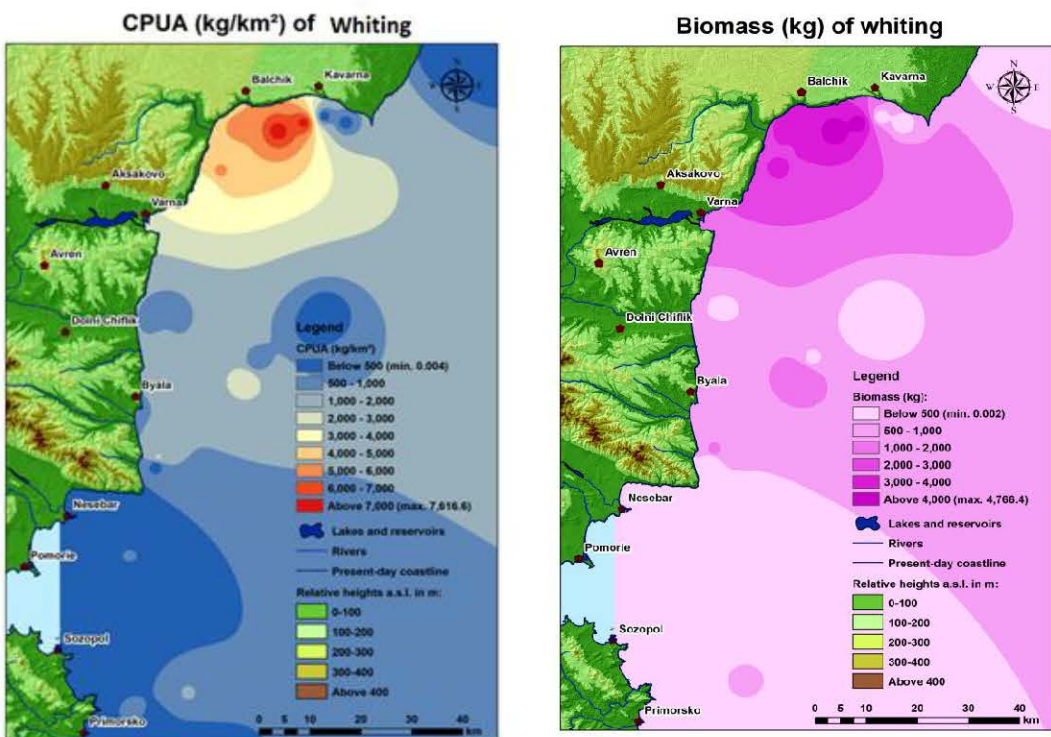


Figure 4.3.2. CPUA kg.km⁻² and Biomass, kg of whiting of the surveyed area



МИНИСТЕРСТВО НА ЗЕМЕДЕЛИЕТО, ХРАНИТЕ И
ГОРИТЕ

Red mullet X-XI, CPUA kg.km⁻² and Biomass, kg

The catch per unit area and perch during the October - November 2019 survey (Fig. 4.3.3.) indicates that CPUA in the 15-30 m depth band has the highest values (6348 kg.km⁻²). At greater depths of 50-100m the catch per unit area ranged from 106 to 476 kg.km⁻².

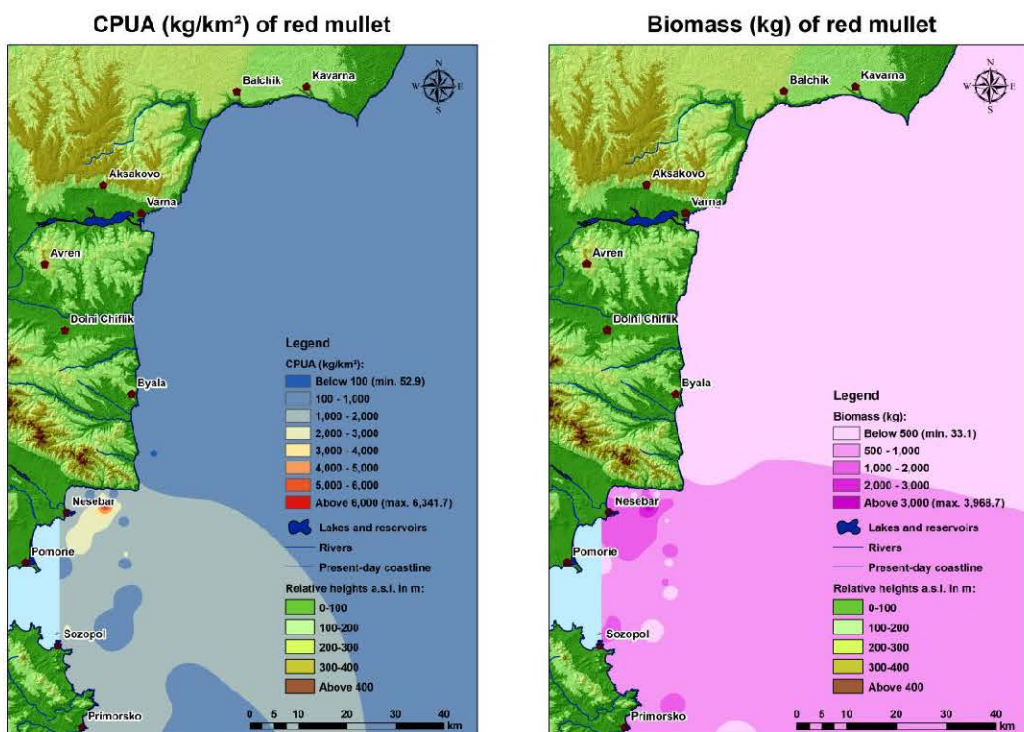


Figure 4.3.3. CPUA kg.km⁻² and Biomass,kg of whiting of the surveyed area

4.4. Catch per unit of effort

The catch per unit effort for identified species is presented graphically: $CPUE \text{ kg.h}^{-1}$ values for sprat, Oct 2019 - Pelagic trawl survey presented in Fig.4.4.1. Maximum



МИНИСТЕРСТВО НА ЗЕМЕДЕЛИЕТО, ХРАНИТЕ И
ГОРИТЕ

values of na CPUE values kg.h^{-1} for sprat were recorded at depths of 18-20 m ($\geq 2400 \text{ kg.h}^{-1}$), 30-36 m (.1200-1600 kg.h^{-1}).

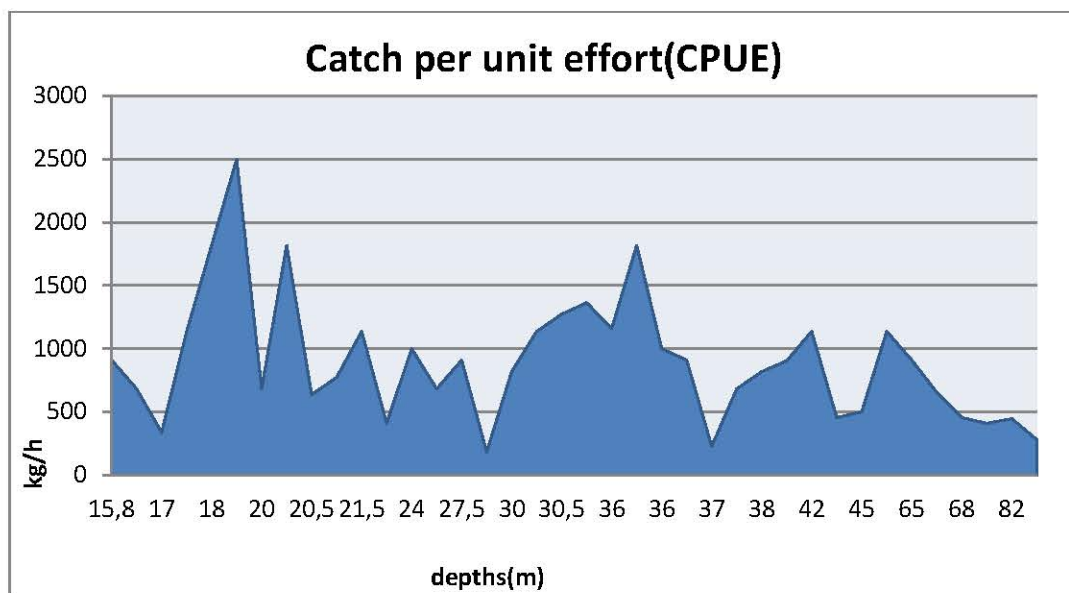


Figure 4.4.1. CPUE kg.h^{-1} values for sprat from X-XI 2019

CPUE kg.h^{-1} values for whiting from X-XI 2019 - pelagic trawl survey presented on Fig. 4.4.2.



МИНИСТЕРСТВО НА ЗЕМЕДЕЛИЕТО, ХРАНИТЕ И
ГОРИТЕ

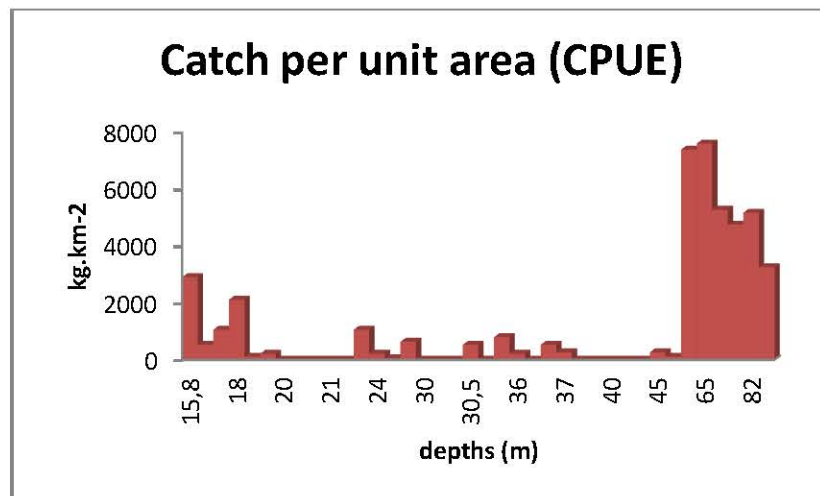


Figure 4.4.2. CPUE kg.h⁻¹ values for the whiting from X-XI 2019 - pelagic trawl survey

Red mullet CPUE show low levels in the investigated area, excluding, one maxima in the shallow waters (20m depths, >500 kg.h⁻¹). (fig.4.4.3.).

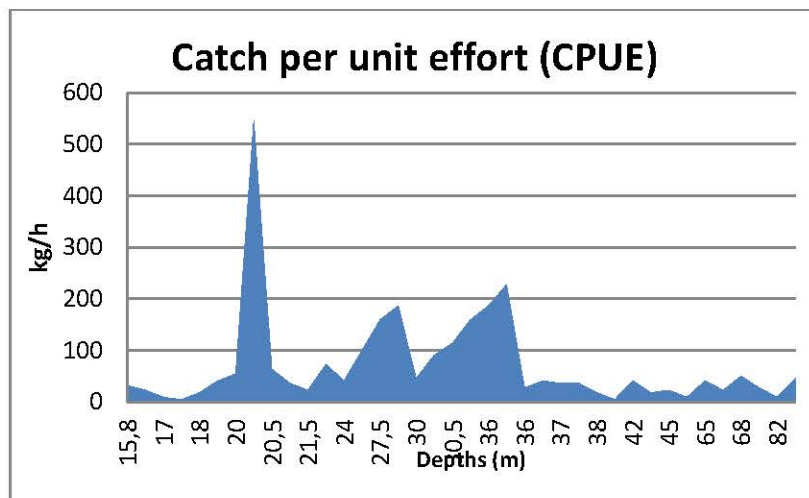


Figure 4.4.3. CPUE kg.h⁻¹ presentation of red mullet from X-XI 2019 - pelagic trawl survey



МИНИСТЕРСТВО НА ЗЕМЕДЕЛИЕТО, ХРАНИТЕ И
ГОРИТЕ

4.5. Size structure of *Sprattus sprattus*, Red mullet and Whiting

The linear distribution of the sprat during the study period is characterized by a peak of 7.5 cm in size group. The remaining size groups (from 8 to 11.5 cm) decrease in steps (Fig. 4.5.1 and 4.5.2).

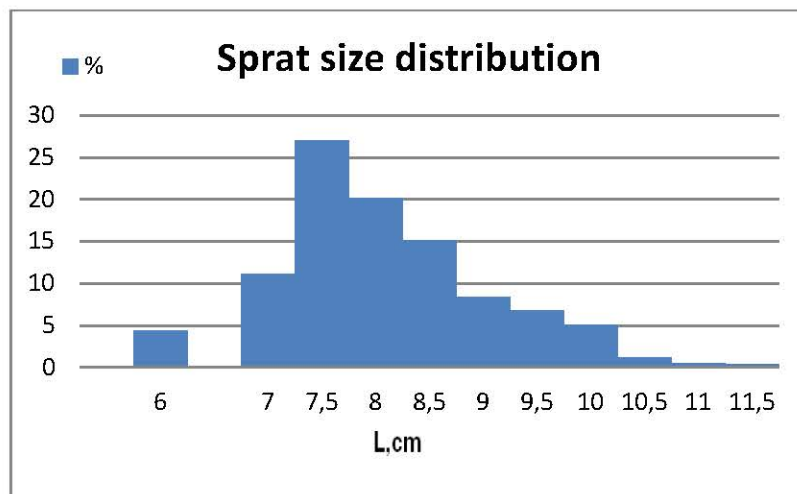


Figure 4.5.1. Size distribution of sprat, X-XI 2019

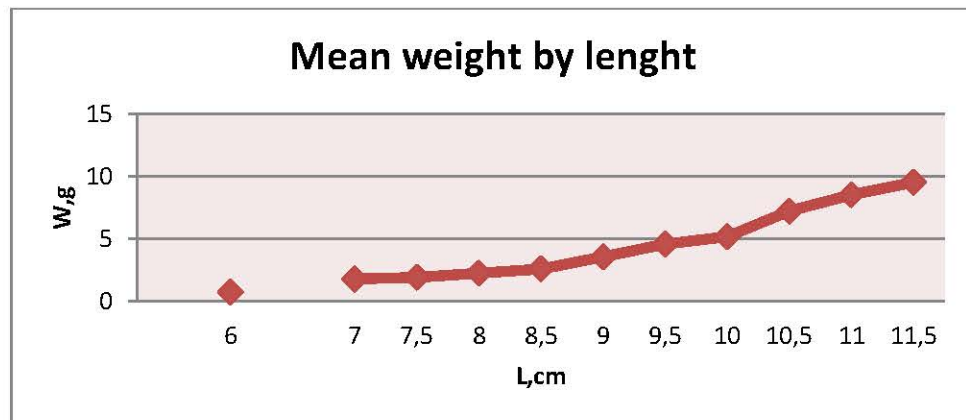


Figure 4.5.2. Length-weight distribution of sprat, X-XI 2019



МИНИСТЕРСТВО НА ЗЕМЕДЕЛИЕТО, ХРАНИТЕ И
ГОРИТЕ



Withing linear growth was characterized by a bimodal linear distribution for the bear (10.5 and 12cm). The other size groups had a subordinate presence in the catches in X-XI (Fig. 4.5.3).

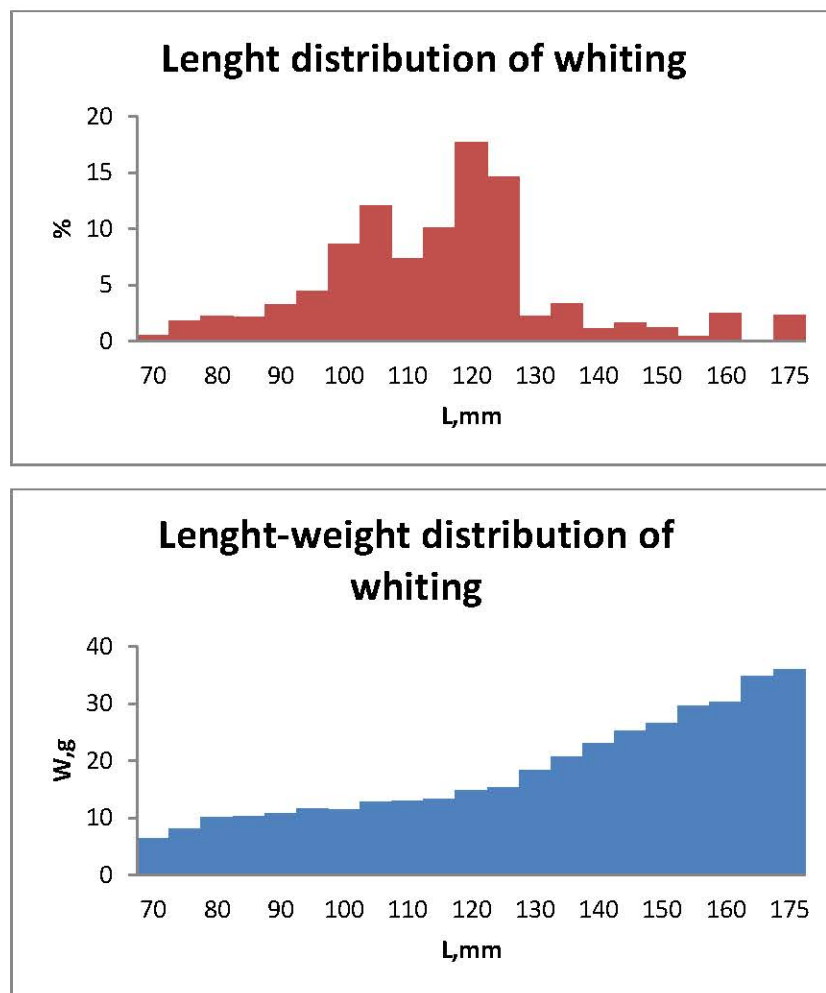


Figure 4.5.3. Length-weight distribution of whiting, X-XI 2019



МИНИСТЕРСТВО НА ЗЕМЕДЕЛИЕТО, ХРАНИТЕ И
ГОРИТЕ

The red mullet of this study was characterized by a uni-modal increase with a peak of 12 cm. There are no deviations in weight gain (Fig. 4.5.4).

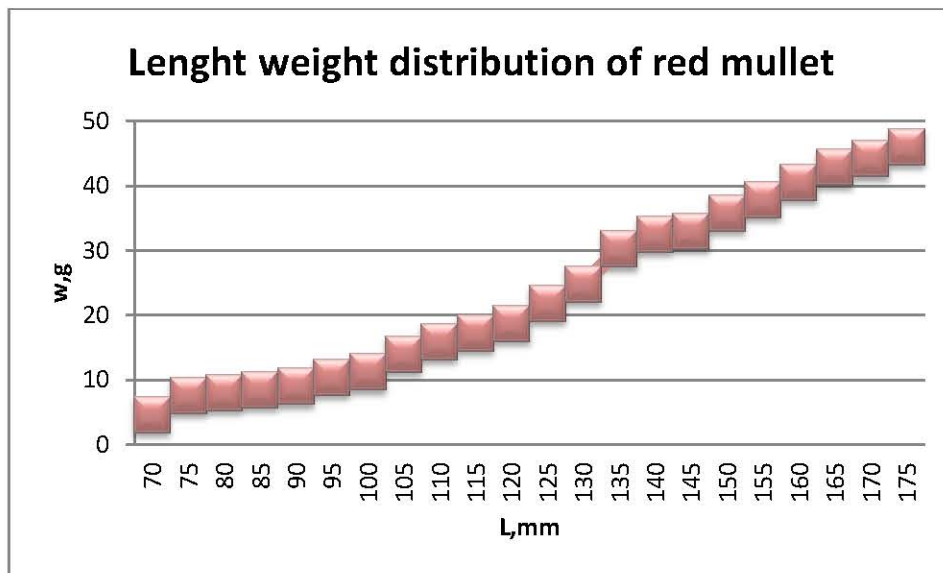
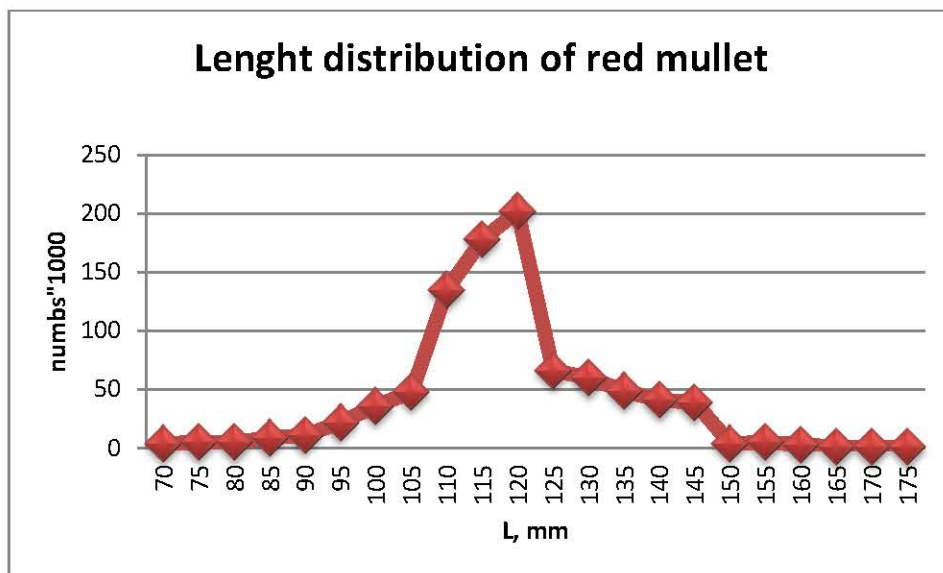


Figure 4.5.4 Length-weight distribution of red mullet, X-XI 2019



МИНИСТЕРСТВО НА ЗЕМЕДЕЛИЕТО, ХРАНИТЕ И
ГОРИТЕ



Data on by catch of horse mackerel and anchovy

The horse mackerel examined individuals from the present research were 294; anchovy-135 and spiny dogfish – 9.

Length structure by age of h.mackerel

Five age groups (0+ to 5+) have been estimated, as no deviations as regards length structure have been observed (9-15 cm length groups)

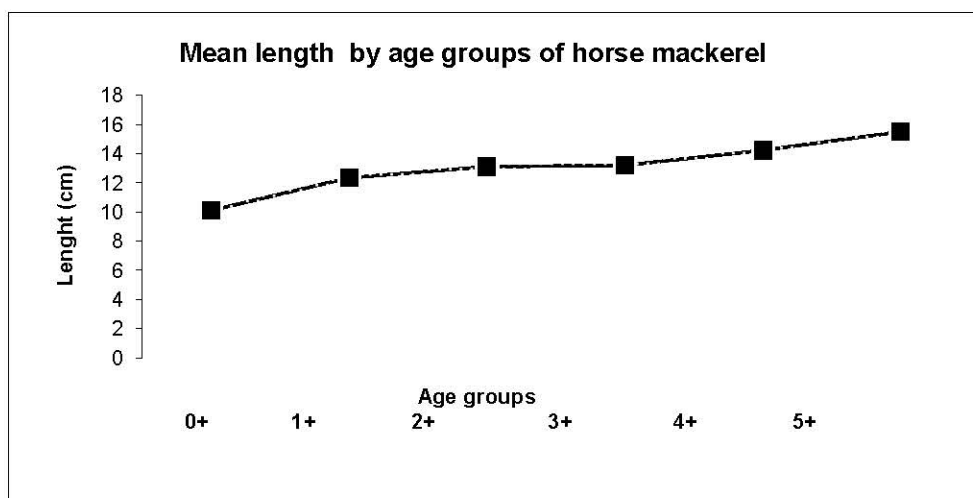


Fig.4.5.5. Length by age of horse mackerel

No recruitment of anchovy have been observed in autumn survey of 2019. The length structure comprised $L = 9.35 - 12.30$ cm, corresponding to the age groups of 1+ to 4+.



МИНИСТЕРСТВО НА ЗЕМЕДЕЛИЕТО, ХРАНИТЕ И
ГОРИТЕ

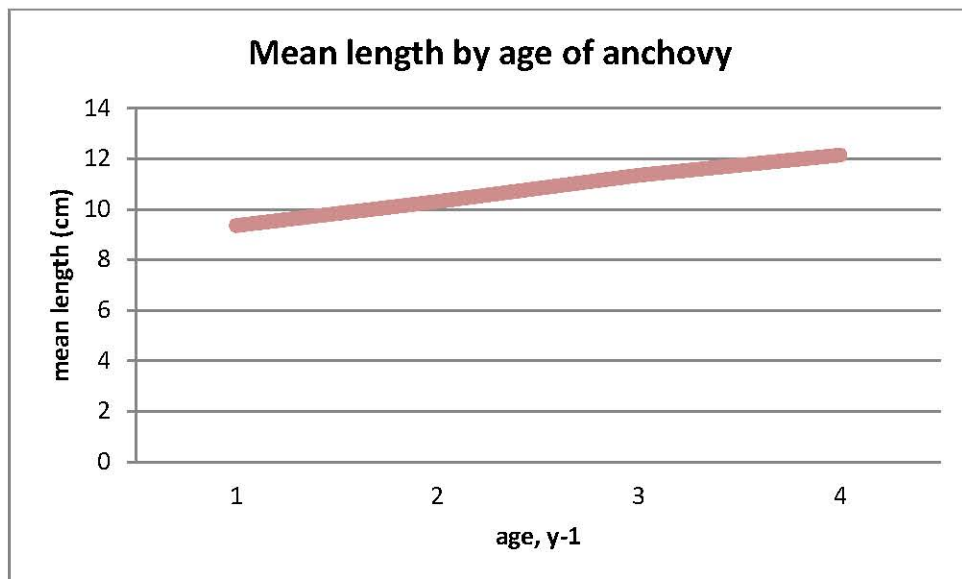


Fig.4.5.6. Length by age of anchovy

9 spiny dogfish specimen were caught in the OTM in autumn 2019 survey.

The length distribution comprised of 95.5-118 cm, and weight varied from 6.100 to 6.300 kg. all specimen were male.

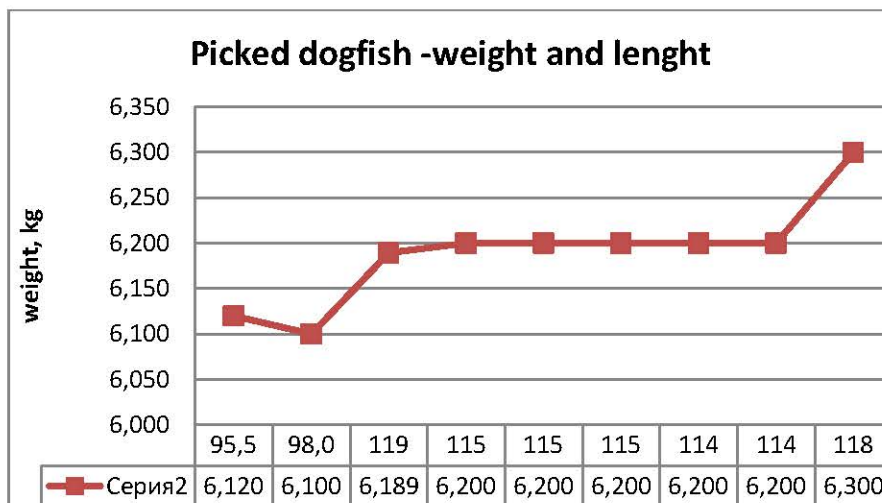


Fig.4.5.7. Length by weight of spiny dogfish



МИНИСТЕРСТВО НА ЗЕМЕДЕЛИЕТО, ХРАНИТЕ И
ГОРИТЕ



4.6. Age structure

The age structure is determined on the basis of direct reading of the otoliths with the binocular of the reflected light. The analysis shows that the percentage of annuals is the highest in the present study (Fig. 4.6.1.).

The prevalence of sprat in this study is 1-1 + (78%).

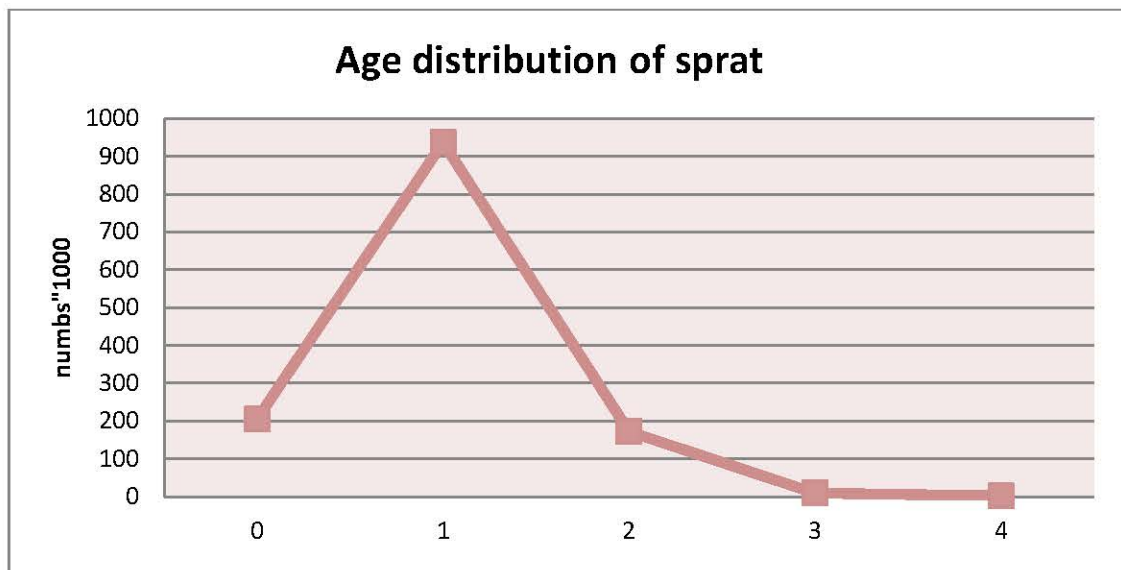


Figure 4.6.1. Sprat age distribution, October-November 2019

The prevailing age for whiting in this study was 2-2 + followed by ages 3-3 + (Fig. 4.6.2). There was no presence of recruits ($0 + y^{-1}$).



МИНИСТЕРСТВО НА ЗЕМЕДЕЛИЕТО, ХРАНИТЕ И
ГОРИТЕ

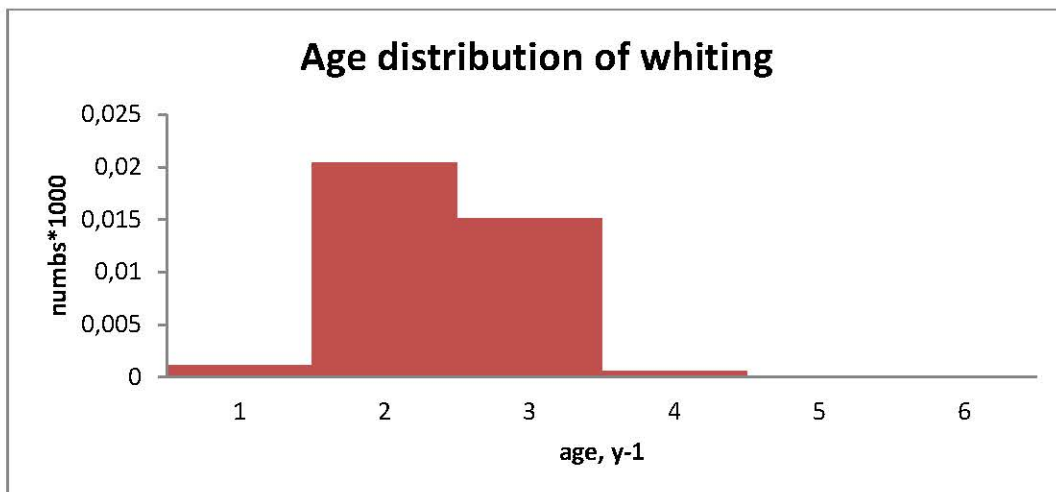


Figure 4.6.2. Age of the whiting from EEZ of the Republic of Bulgaria

The predominant age of the red mullet is 2-2 + (46%), 3-3 + (26.6%), The older age and juvenile forms were present with a low percentage (Fig. 4.6.3).

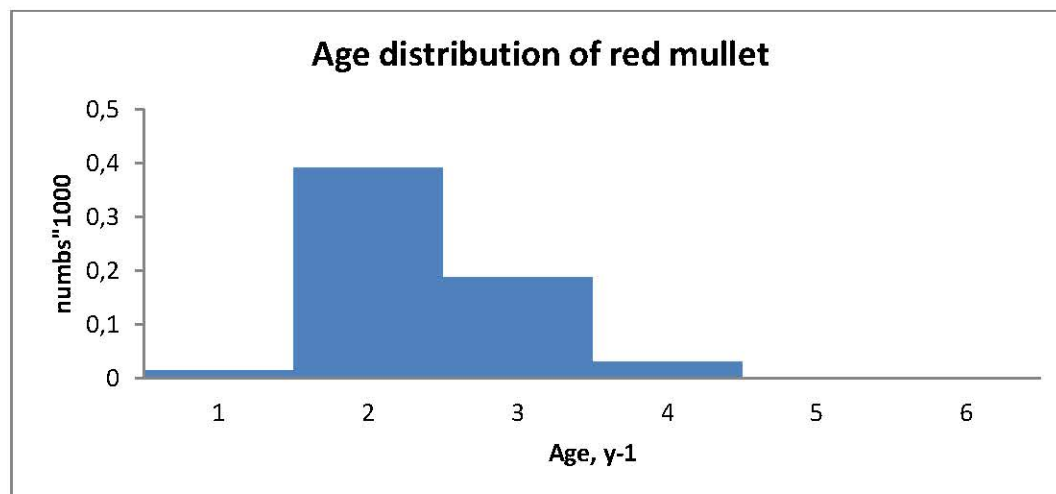


Figure 4.6.3. Age of the red mullet from the Bulgarian Sea Area

The predominant age of thered mullet is 2-2 + (46%), 3-3 + (26.6%). The older age and juvenile forms were present with a low percentage.



МИНИСТЕРСТВО НА ЗЕМЕДЕЛИЕТО, ХРАНИТЕ И
ГОРИТЕ

4.7. Growth

L growth

To calculate the growth rate and growth parameters from the Bulgarian area, we used the Von Bertalanfi equation, VBGF. The estimation of asymptotic length, growth rate and coefficients related to the coefficients is presented in Table 4.7.1.

Table 4.7.1. Parameters in the VBGF for sprat, whiting and red mullet

sprat	whiting	red mullet
$L_\infty = 12.2$	$L_\infty = 27.66$	$L_\infty = 19.33$
$k=0.44$	$k=0.25$	$k=0.24$
$t_0 = -1.115$	$t_0 = -2.0054$	$t_0 = -1.2111$
$q = 0.0008$	$q = 0.009$	$q = 0.009$
$n = 2.87$	$n = 3.002$	$n = 3.11$

The asymptotic length reaches 12.2 cm; 27.66 and 19.33 for red mullet respectively the rate of growth can be determined as being relatively high 0.45 y-1 for sprat; 0.25 and 0.24 – low for whiting and red mullet. The growth of sprat from the present study is negative allometric ($n = 2.87$), and positive allometric for whiting and red mullet (Fig. 4.7.1).



МИНИСТЕРСТВО НА ЗЕМЕДЕЛИЕТО, ХРАНИТЕ И
ГОРИТЕ

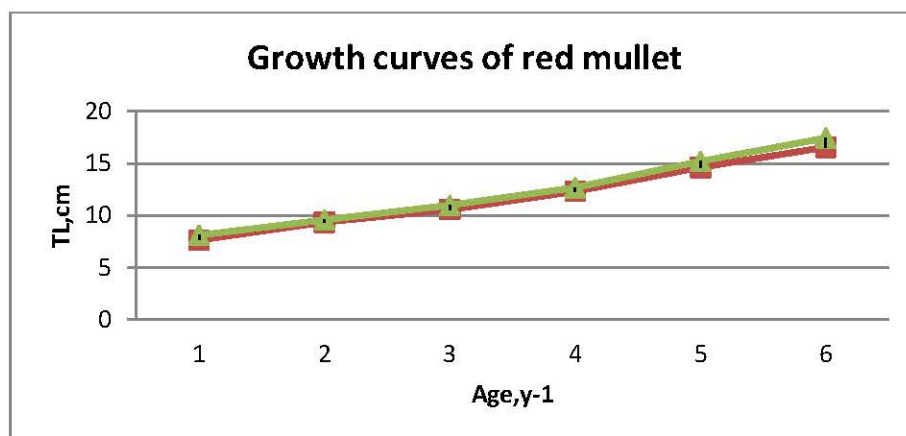
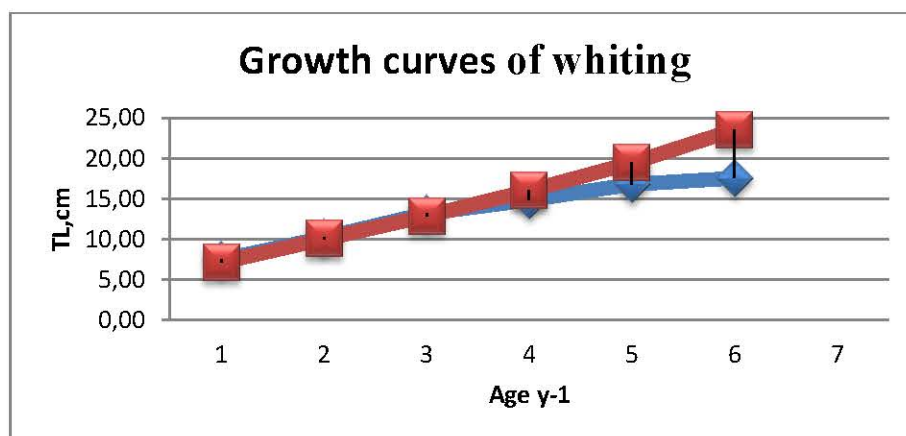
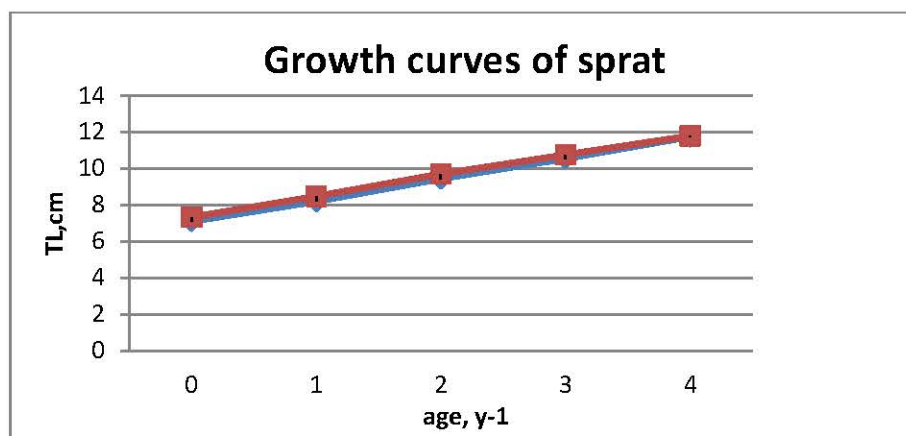


Figure 4.7.1. L asymptotic for sprat, whiting and red mullet



МИНИСТЕРСТВО НА ЗЕМЕДЕЛИЕТО, ХРАНИТЕ И
ГОРИТЕ



The most important note here is that because of the lack (or low share) of the oldest large age groups, the asymptotic size function shows a relatively low value. In this regard, the maximum or asymptotic length reaches this value, which is probably not fully consistent with the literature data on the size of the species and the marginal length and growth rates. Therefore, we can accept the growth analysis as this is what reflects in the current situation of absence (low presence) of large individuals.

4.8. Body growth

The average weights of sprat, mullet and whiting are expected to increase with age

The somatic growth of sprat from current research shows that the average weight corresponding to the oldest age group is 9.56 gr. The value corresponds to the marginal size of 11.75 cm measured in samples from the trawl survey in Bulgarian waters (Fig. 4.8.1).

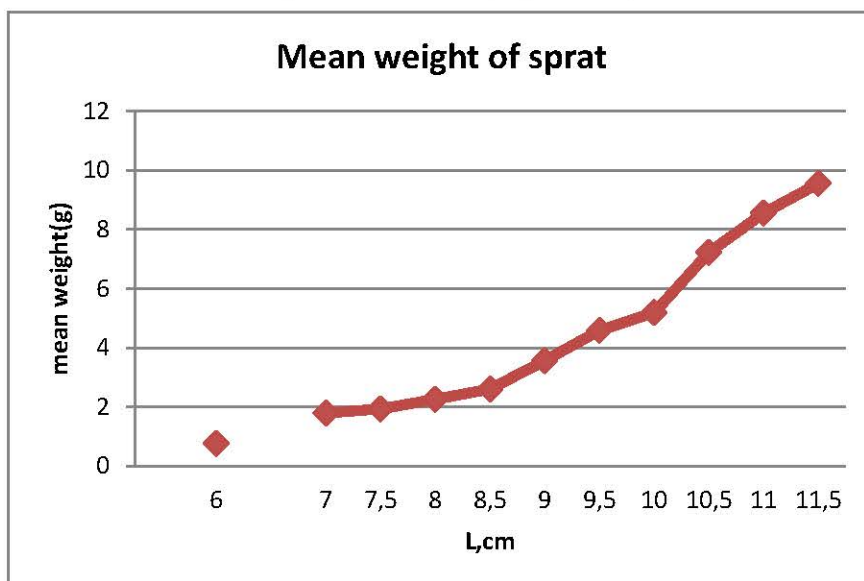


Figure 4.8.1. Somatic growth of sprat, X-XI, 2019



МИНИСТЕРСТВО НА ЗЕМЕДЕЛИЕТО, ХРАНИТЕ И
ГОРИТЕ

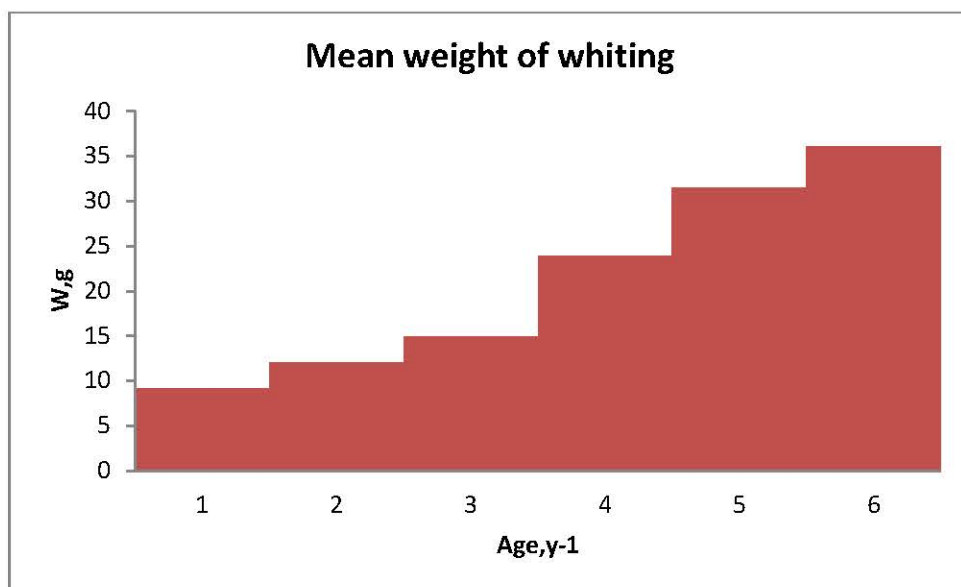


Figure 4.8.2. Somatic growth of whiting, X-XI 2019

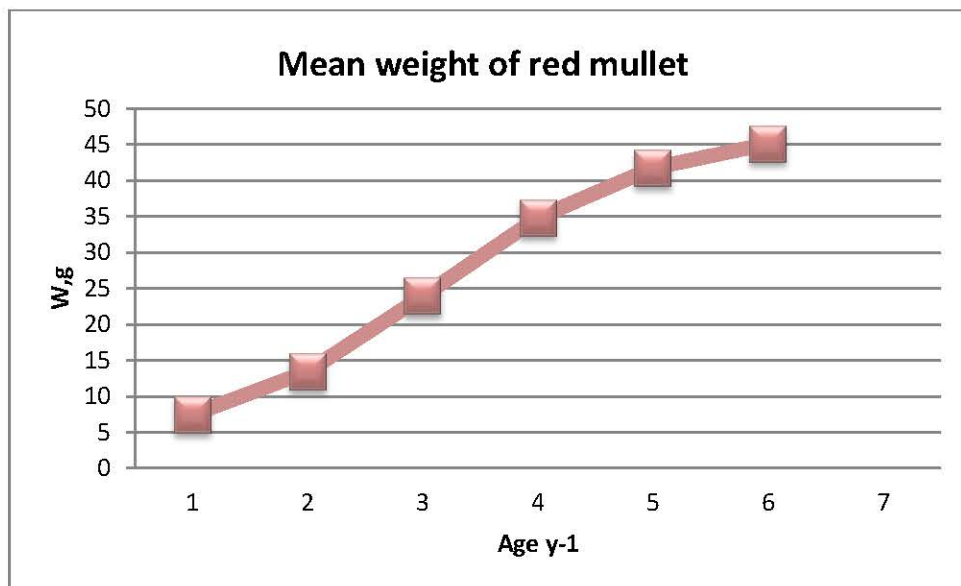


Figure 4.8.3. Somatic growth of red mullet

Mean weight by age of h.mackerel and anchovy



МИНИСТЕРСТВО НА ЗЕМЕДЕЛИЕТО, ХРАНИТЕ И
ГОРИТЕ

Mean weight of h.mackerel varied from 10.25g ($0+y^{-1}$) to 28g (age 5-5+). Mean weight of anchovy varied from 4.92g ($1-1+y^{-1}$) 10.51g ($4-4+y^{-1}$)

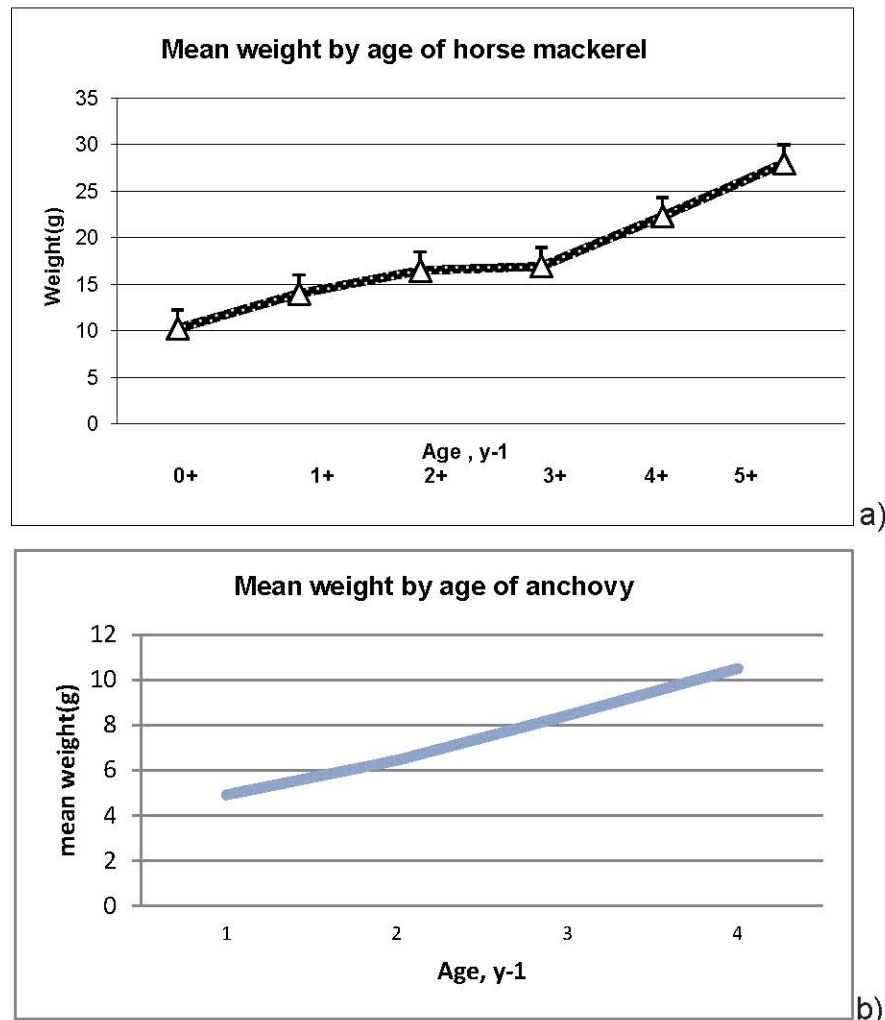


Fig.4.8.4. Somatic growth of a) h.mackerel and b) anchovy

The condition of the by caught h.mackerel show peak at 4-4+ age h.mackerel. Anchovy has a high condition at age 1-1+ age and lower at age of 3-3+y⁻¹.



МИНИСТЕРСТВО НА ЗЕМЕДЕЛИЕТО, ХРАНИТЕ И
ГОРИТЕ

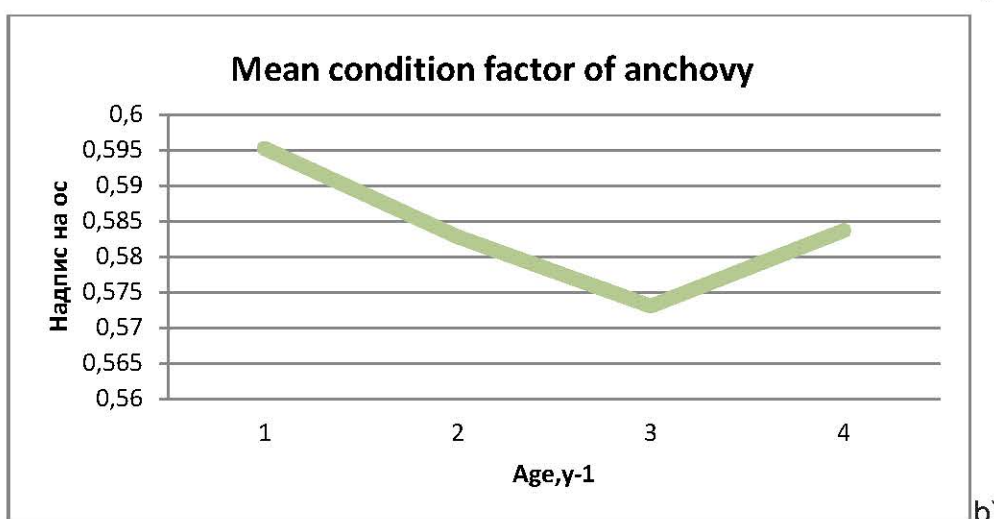
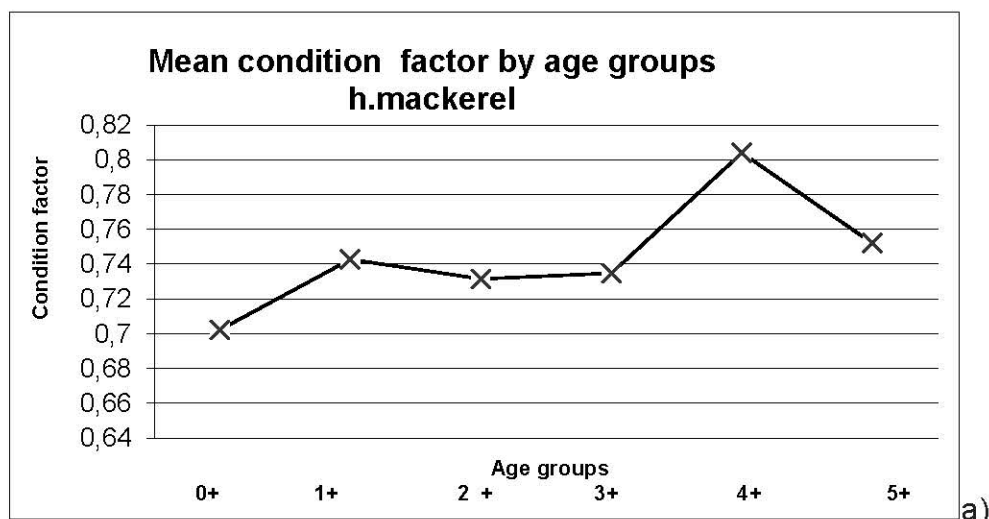


Fig.4.8.5. Mean condition factor of a) h.mackerel and b) anchovy

4.8.1. Sex Ratio

In sprat, females predominate by 51%, followed by males (45%). Juveniles were represented at a low percentage (4%). In the whiting, females predominate by 50%, followed by males (45%). Juveniles were represented at a low percentage (5%). In the red mullet, females predominate by 49%, followed by males (44%).



МИНИСТЕРСТВО НА ЗЕМЕДЕЛИЕТО, ХРАНИТЕ И
ГОРИТЕ

Juveniles were represented by (7%) (Fig. 4.8.1.1). Females predominate for h.mackerel and anchovy too (55 and 51 %) (Fig 4.8.1.2.).

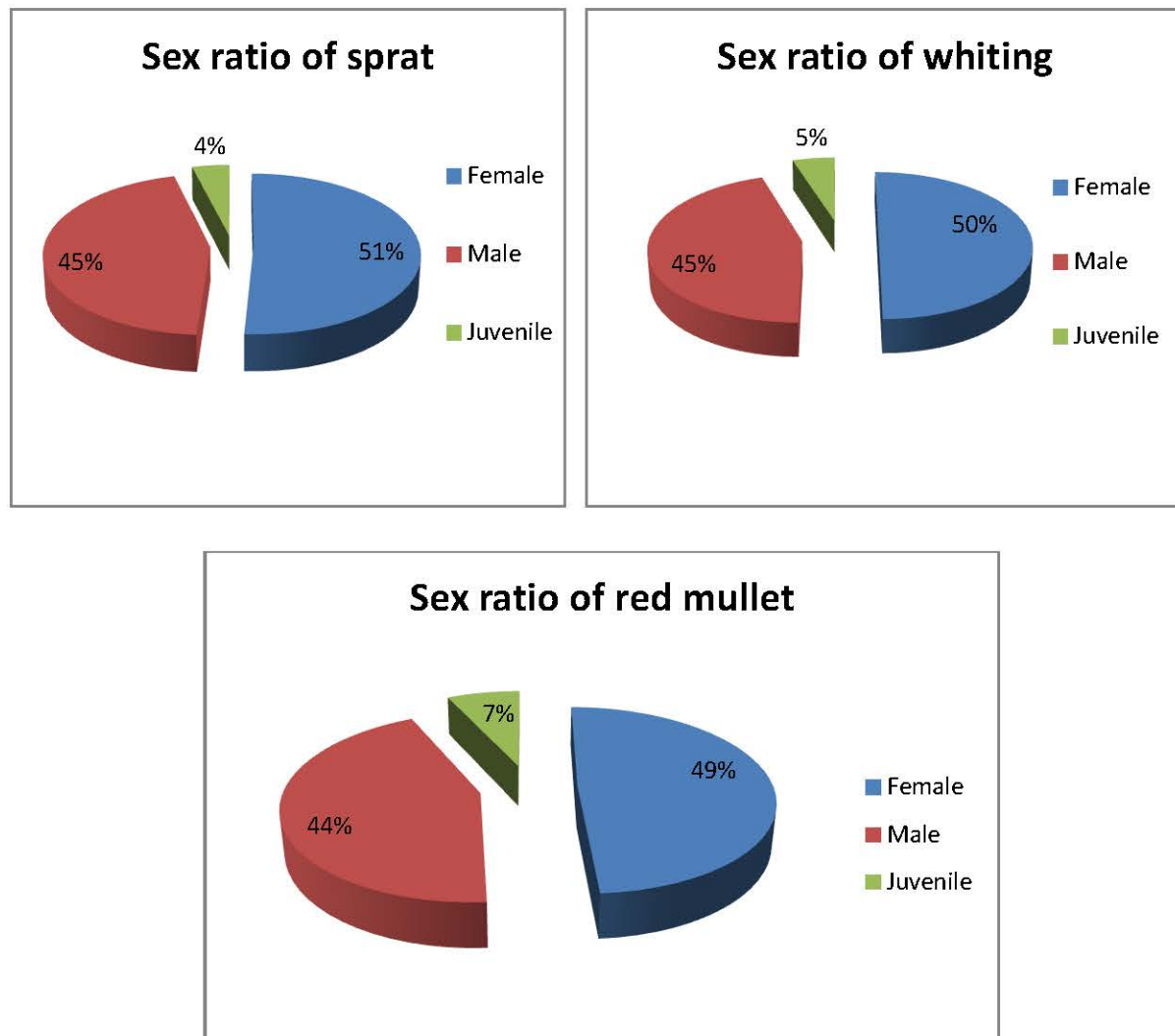


Figure 4.8.1.1. Sex ratio (1 - male; 2 - female; 3 – juvenile)



МИНИСТЕРСТВО НА ЗЕМЕДЕЛИЕТО, ХРАНИТЕ И
ГОРИТЕ

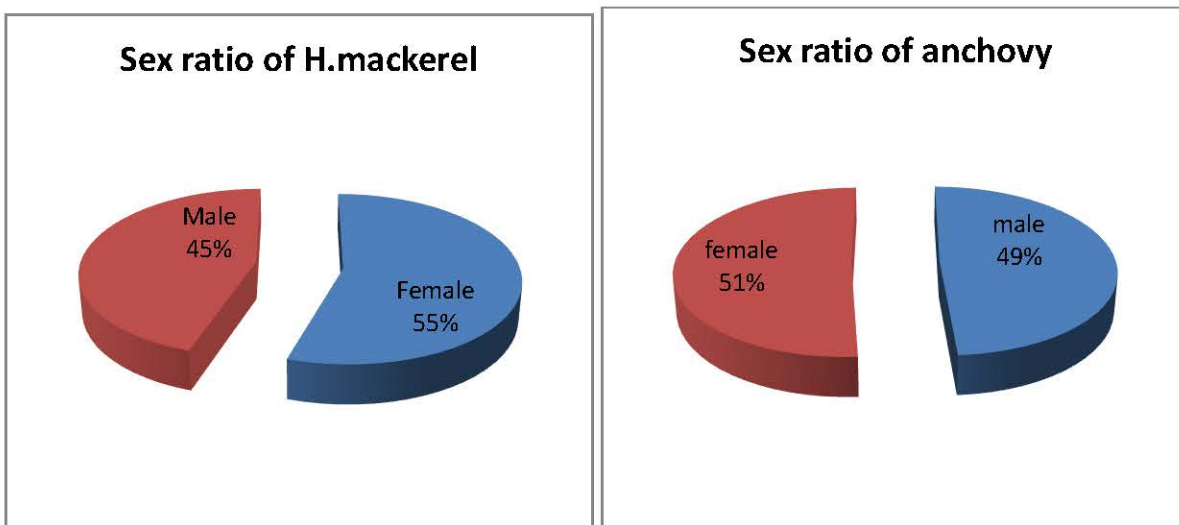


Figure 4.8.1.2. Sex ratio (1 - male; 2 – female)

4.9. Fertility and fecundity

In this October-November study, sprat was in the active phase of spawning. Most of the individuals have stage-IV-V-II of glands. The type does not show a high dependence of the linear ejection of the sexual products (Fig. 4.9.1).

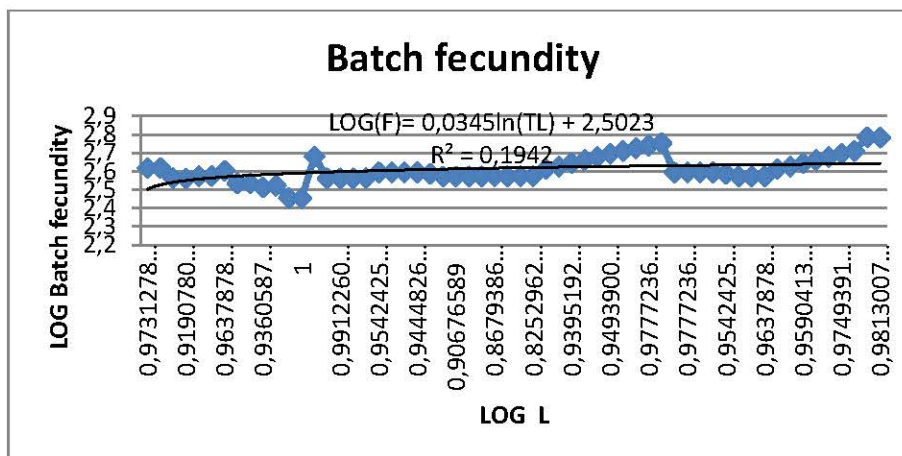


Figure 4.9.1. Fecundity Plot (LogF) in relation to the size (LogL) of the sprat from the X-XI 2019 study



МИНИСТЕРСТВО НА ЗЕМЕДЕЛИЕТО, ХРАНИТЕ И
ГОРИТЕ

Sprat fecundity correlates poorly with its length ($R^2 = 0.19$). The relationship between fecundity and total whiting size is linear, with a high degree of determination ($R^2 = 0.7855$) (Fig. 4.9.2.).

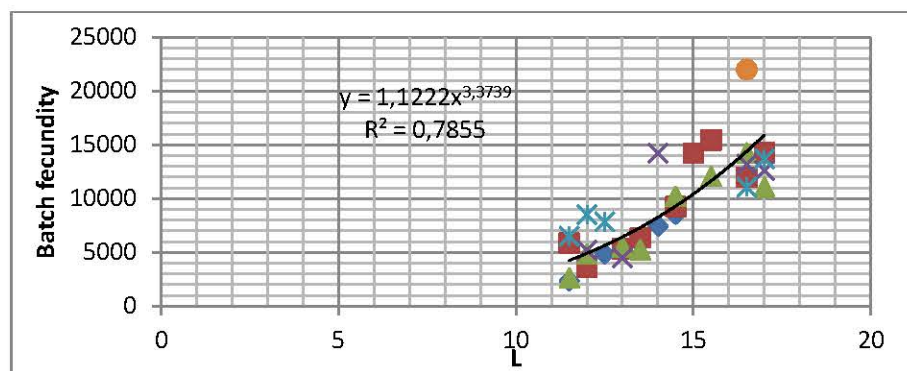


Figure 4.9.2. Batch fecundity of whiting

The relation between Log F (fecundity) and Log L (individual length) of horse mackerel from the present research show low level of correlation with weak determination ($R^2 = 0.2729$) (Fig. 4.9.3). This is related with the fact that the species is out of the active spawning period.

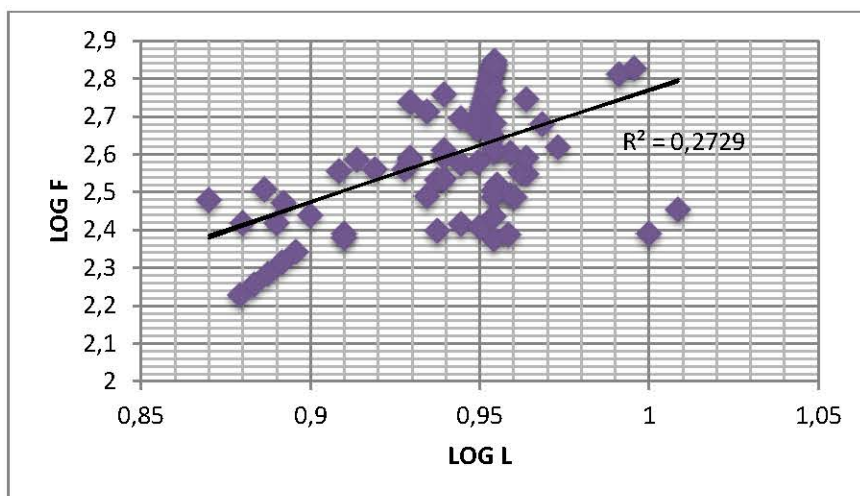


Figure 4.9.3. Batch fecundity of H.mackerel

Anchovy from the present research do not show strong dependence of individual
67 ----- www.eufunds.bg -----



МИНИСТЕРСТВО НА ЗЕМЕДЕЛИЕТО, ХРАНИТЕ И
ГОРИТЕ

length to the batch fecundity. This fact speak for that the species is already spawn and most probably the majority of population is not at active spawning phase at the time of research (fig.4.9.4).

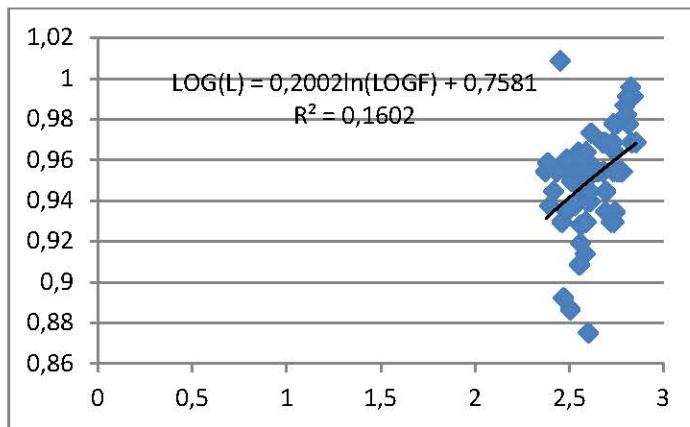


Figure 4.9.4. Batch fecundity of anchovy

4.10. Gonado-somatic index

The gonadomatic index of sprat varies widely over individual weight, and its values indicate to a greater extent that the mass reproduction of the species during the period under consideration has begun (Fig. 4.10.1).

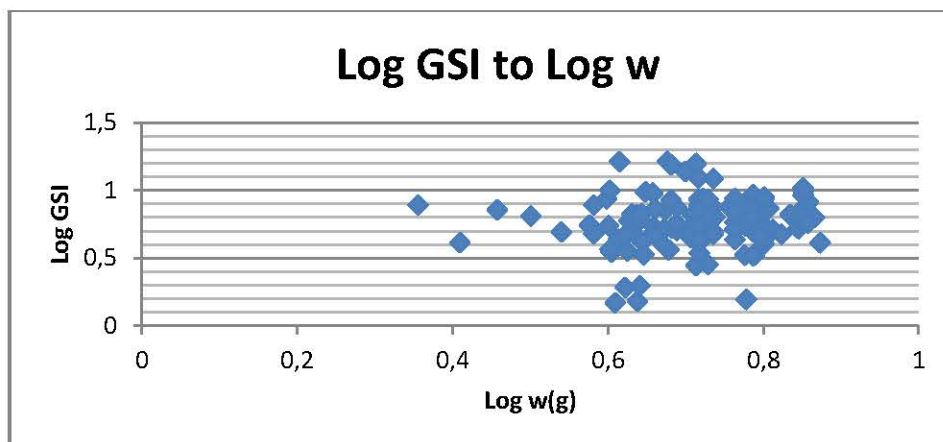


Figure 4.10.1. Gondo-somatic index of the sprat of this study (GSI, %)



МИНИСТЕРСТВО НА ЗЕМЕДЕЛИЕТО, ХРАНИТЕ И
ГОРИТЕ

The growing trend of the maturing females of whiting show very strong dependence between active glands weight and gonado-somatic index in X-XI 2019. The species is in active phase of maturing (Fig. 4.10.2). Strong dependence of GSI from weight of glandula was estimated for h.mackerel from the present study. Anchovy GSI has no such strong dependence for the same period.

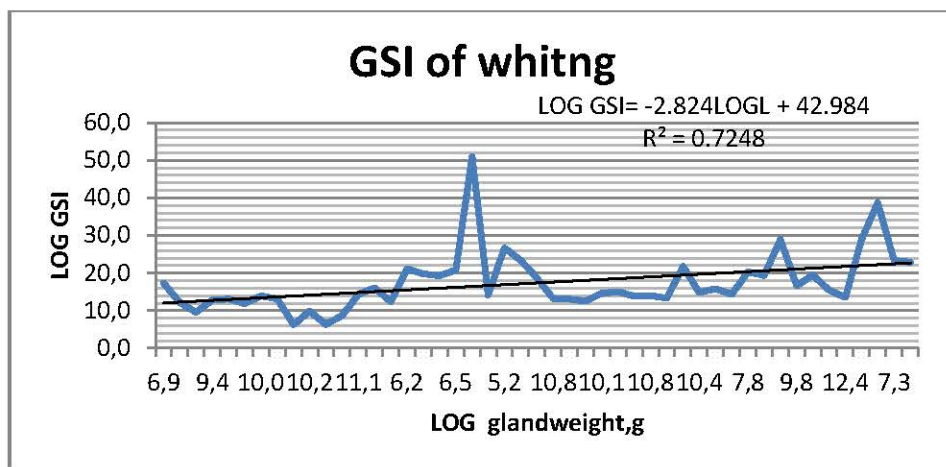


Figure 4.10.2. Gondo-somatic index of the whiting of this study (GSI,%)

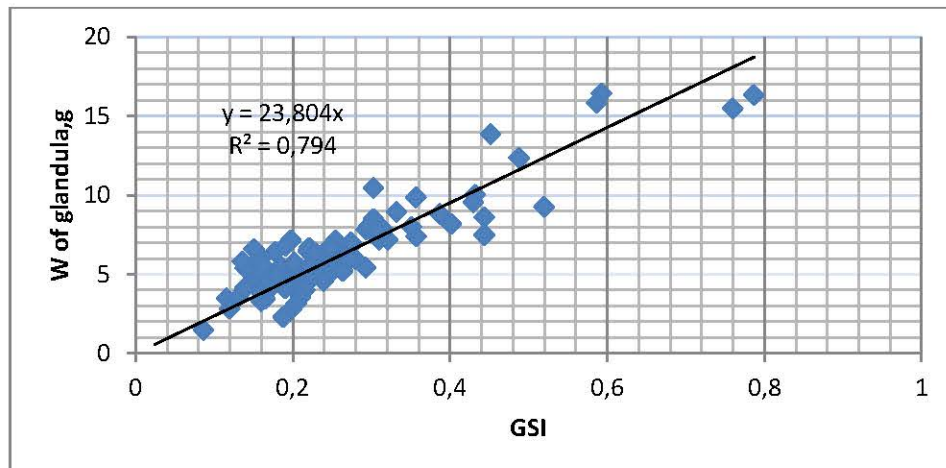


Figure 4.10.3. Gondo-somatic index of the h.mackerel of this study (GSI,%)



МИНИСТЕРСТВО НА ЗЕМЕДЕЛИЕТО, ХРАНИТЕ И
ГОРИТЕ

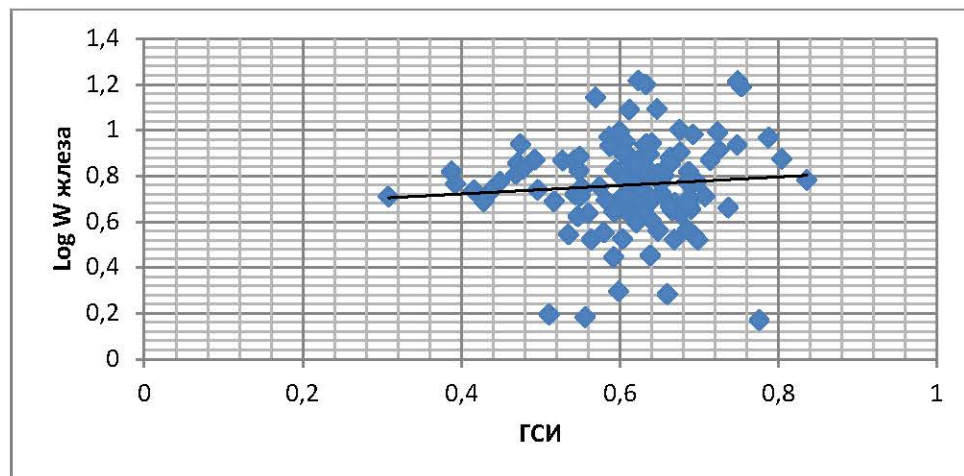


Figure 4.10.4. Gondo-somatic index of the anchovy of this study (GSI, %)

5. Length-weight dependence, Index of stomach fullness (ISF)

The mean absolute length of investigated sprat specimens reached $8.86 \text{ cm} \pm 0.98$ (SD), varying between 7 - 12 cm, correspondingly the mean weight was $4.11 \text{ g} \pm 1.39$ (SD), ranging from 2.09 g to 8.80 g (Table 5.1, Fig. 5.1).

Table 5.1. Summary statistics of sprat length (L, cm), weight (W, g) and ISF (% BW) analysed for stomach content composition during X-XI 2019

	L, cm	W, g	ISF, % BW
Mean	8.86	4.11	0.91
Standard Error	0.14	0.20	0.08
Median	8.75	3.80	0.78
Mode	8.50	#N/A	#N/A
Standard Deviation	0.98	1.39	0.60
Sample Variance	0.96	1.94	0.36
Kurtosis	1.00	1.44	-0.63



МИНИСТЕРСТВО НА ЗЕМЕДЕЛИЕТО, ХРАНИТЕ И
ГОРИТЕ

	0.66	1.07	0.53
Skewness	0.66	1.07	0.53
Range	5.00	6.71	2.39
Minimum	7.00	2.09	0.12
Maximum	12.00	8.80	2.50
Sum	443.10	205.62	45.30
Count	50.00	50.00	50.00
Confidence Level (95.0%)	0.28	0.40	0.17

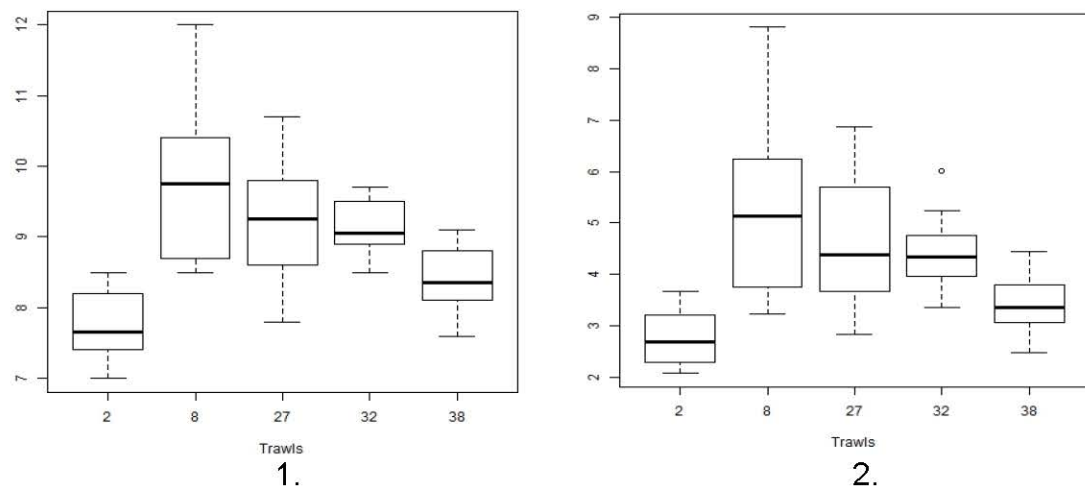


Figure 5.1. Box plot: sprat length (1, cm) and weight (2, g) per trawls during X-XI 2019 (median values, 25 – 75 % hinge, minimal and maximal values)

The weight-length dependence of sprat could be described by the following equation:

$$\text{Log WW (g)} = 2.9206 * \text{Log L (mm)} - 5.0891; (R^2 = 0.96, p < 0.001, \text{Fig. 5.2.})$$



МИНИСТЕРСТВО НА ЗЕМЕДЕЛИЕТО, ХРАНИТЕ И
ГОРИТЕ

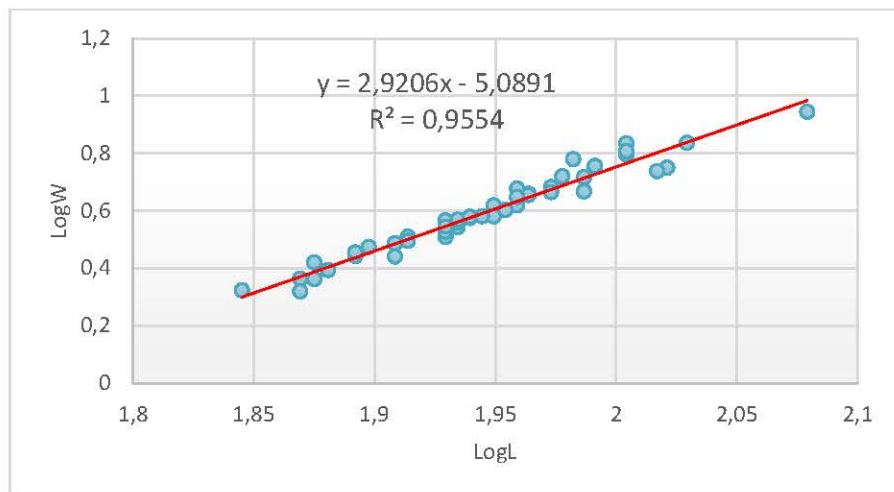


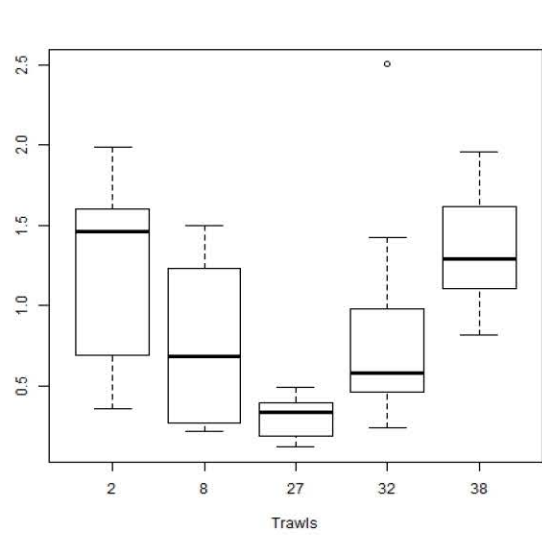
Figure 5.2. Sprat weight-length relationship in X-XI 2019

In October - November 2019, the average index of stomach fullness (ISF) has reached $0.91\% \pm 0.60$ (SD) of the sprat weight (Table 5.1). This value is with 13.75% higher than the level, estimated during the spring season.

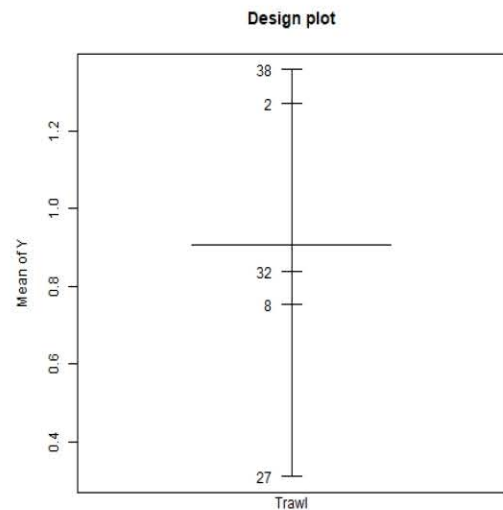
The highest average values of the ISF index - 1.36 - 1.3 % are established in the Bay of Burgas and in front of Kamchia river mouth (trawls 38 and 2, Fig. 5.3) at depths of 30 - 45 m (Fig. 5.4). The average ISF values are minimal ($\sim 0.3\%$ BW) in the Maslen nos region (Fig. 5.4).



МИНИСТЕРСТВО НА ЗЕМЕДЕЛИЕТО, ХРАНИТЕ И
ГОРИТЕ



1.



2.

Figure 5.3. (1) Boxplot: sprat index of stomach fullness (ISF, % BW) in X-XI 2019
(2) Design plot: distribution of mean ISF (% BW) by trawls

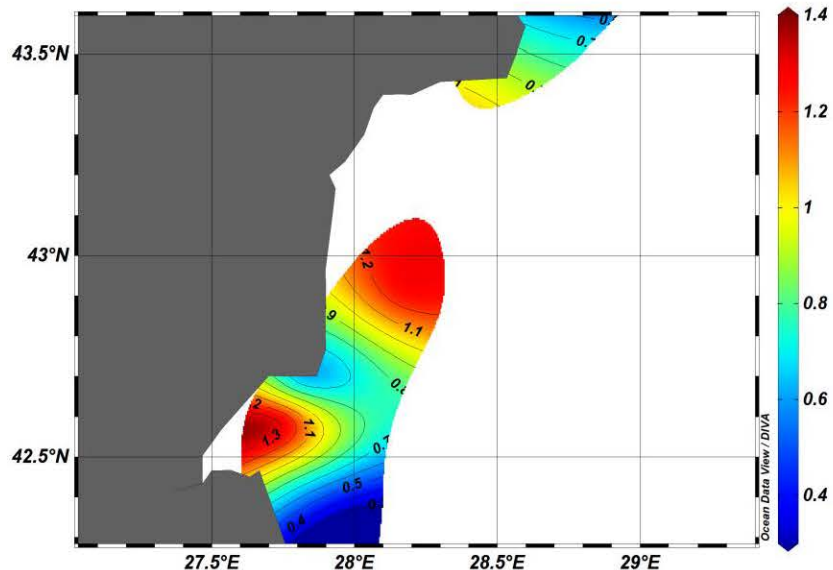


Figure 5.4. Spatial distribution of ISF (% BW) in X-XI.2019

A statistically significant inverse correlation ($R^2 = -0.30$, $p < 0.001$, Fig. 5.5) was found between the indices of stomach fullness and the sprat weight (ranging



МИНИСТЕРСТВО НА ЗЕМЕДЕЛИЕТО, ХРАНИТЕ И
ГОРИТЕ

between 2.09 – 8.80 g), with a small percentage of explained variability - 34.4%.

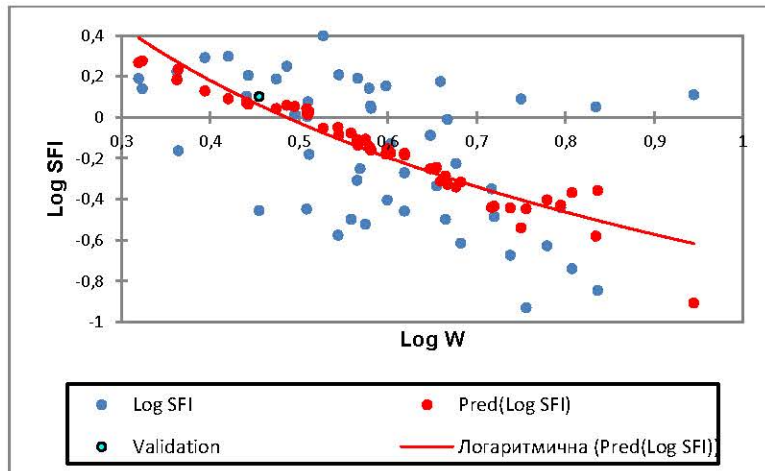


Figure 5.5. Relationship between the weights of sprat specimens (Log W, g) and fullness index - Log ISF (% BW) in X-XI 2019

The most significant ISF was found in the small-sized sprat with a weight of ~ 2.5 g (Figure 5.5). Due to the relatively low level of explained variability, other factors influence the sprat diet; e.g. such factors might be the concentration and species composition of food zooplankton, the importance of intraspecies and interspecies competitive relationships, etc.

Prey number (PN), species composition and index of relative importance (IRI) of mesozooplankton species in the sprat diet

In the surveyed area off the Bulgarian coast, the average PN in the sprat food is 230 ind/stomach \pm 321.64 SD. The maximal individual number of food organisms - 1340 ind/stomach was established in the Burgas Bay area (trawl 38, d = 30 m), where the average PN was 872 ind/stomach, corresponding to the maximal ISF index of 1.36% BW, due to intensive consumption of the zooplankton species *Paracalanus parvus* (Figure 5.6).



МИНИСТЕРСТВО НА ЗЕМЕДЕЛИЕТО, ХРАНИТЕ И
ГОРИТЕ

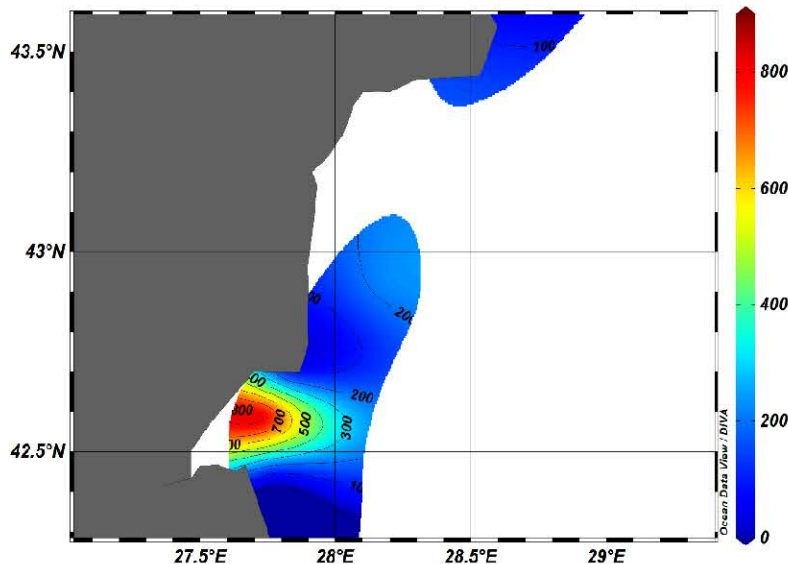


Figure 5.6. Spatial distribution of the average PN per trawls in X-XI 2019

In the zooplankton samples from the marine environment, 27 species/groups have been identified, of which 23 species/groups are presented as components in the sprat food. Copepoda are represented by *Calanus euxinus*, *Pseudocalanus elongatus*, *Paracalanus parvus*, *Acartia clausi*, *Centropages ponticus*, *Oithona similis*, *Oithona davisae* and *Harpacticocoida spp.*, cladocerans includes - *Pleopis polyphemoides*, *Penilia avirostris* and *Pseudoevadne tergestina*; five taxonomic groups are identified from the group of planktonic larvae of bottom organisms (meroplankton): *Lamellibranchia veliger*, *Gastropoda veliger*, *Cirripedia larvae*, *Decapoda larvae*, *Polychaeta larvae*; class *Chaetognatha* is represented by *Parasagitta setosa*, class *Appendicularia* - by *Oicopleura dioica*. Food objects were found in the stomachs of all studied sprat specimens, with fluctuations between 1-15 zooplankton species by separate sprat specimens. The indices of relative importance (IRI) of the main zooplankton species in sprat food spectrum (based on the percent shares from total abundance, biomass, and frequency of occurrence in samples) were represented in Table 5.2.

Table 5.2. The sprat food composition and IRI values in X-XI 2019



МИНИСТЕРСТВО НА ЗЕМЕДЕЛИЕТО, ХРАНИТЕ И
ГОРИТЕ

Sprat food composition	N (% , from abundance)	M (% , from biomass)	FO – frequency of occurrence	IRI – Index of relative importance
<i>Calanus euxinus</i>	12.02	62.18	84.0	6232.8
<i>Pseudocalanus elongatus</i>	6.21	1.33	62.0	467.48
<i>Paracalanus parvus</i>	40.17	20.39	62.0	3754.72
<i>Acartia clausi</i>	14.24	7.34	78.0	1683.24
<i>Centropages ponticus</i>	1.86	1.71	42.0	149.94
<i>Pleopis polyphemoides</i>	1.34	0.40	26	45.24
<i>Lamellibranchia veliger</i>	2.82	0.14	50	148
<i>Decapoda larvae</i>	1.91	2.95	26	126.36
<i>Cirripedia nauplii, cyparis</i>	1.42	0.20	56	90.72
<i>Parasagitta setosa</i>	13.38	2.98	30	490.8
<i>Oikopleura dioica</i>	3.28	0.19	42	145.74
other	1.35	0.19		
total	100%	100%		

Data on the number of species in the sprat food and some species diversity indices based on IRI values per different trawls are presented in Table 5.3.

Table 5.3. Number of species and species diversity indices (d, species richness, J'-Pielou's evenness, Brillouin, Fisher, Shannon) based on zooplankton species IRI values per different trawls

Sample	S	d	J'	Brillouin	Fisher	H'(loge)	1-Lambda'
T2	15	2.60	0.45	1.14	3.65	1.23	0.54
T8	11	2.17	0.68	1.50	3.15	1.63	0.77
T27	11	4.42	0.85	1.26	****	2.03	0.93
T32	14	2.97	0.64	1.49	4.92	1.69	0.75
T38	15	2.07	0.09	0.22	2.57	0.24	0.08



МИНИСТЕРСТВО НА ЗЕМЕДЕЛИЕТО, ХРАНИТЕ И
ГОРИТЕ



Considering the representation of the different zooplankton species in the sprat food, we found relatively high species evenness in the Maslen nos region (trawl 27) (Table 5.3), but it corresponded to the lowest ISF value.

Dominant positions in the sprat food have the copepods - *Calanus euxinus*, *Paracalanus parvus*, *Acartia clausi*, *Pseudocalanus elongatus* and *Centropages ponticus*, as well as the chaetognath *Parasagitta setosa* (Table 5.2 and 5.3, Fig. 5.7). The coldwater and eurytherm zooplankton species predominate in the sprat diet, both in frequency of occurrence and in numbers and biomass.

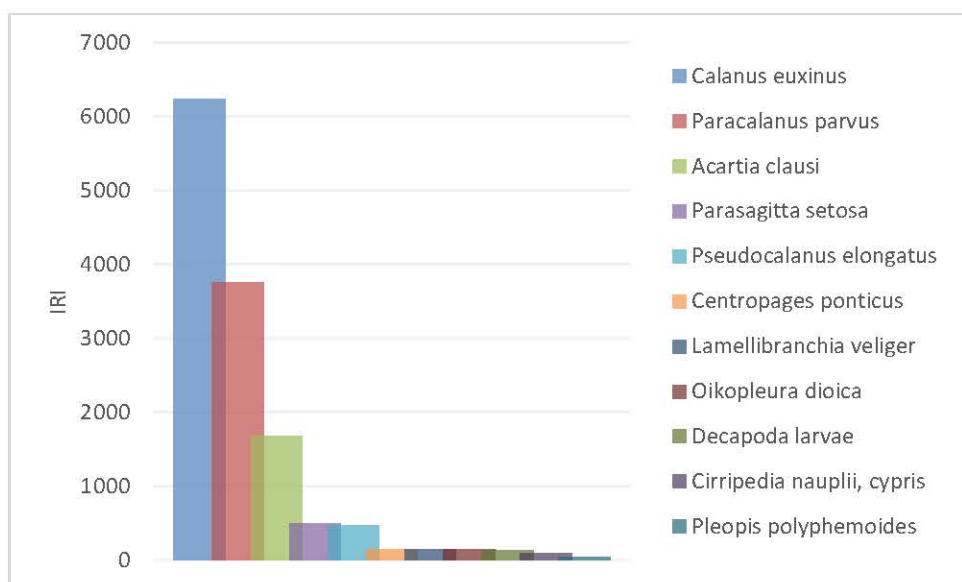


Figure 5.7. Mean IRI of mesozooplankton species in the sprat diet during X-XI 2019

The species *A. clausi* is found in the sprat food almost at all studied regions, while the cold-water copepod *C. euxinus* is mostly presented in the sprat diet around the Capes Kaliakra and Maslen nos, and the species *Paracalanus parvus* is found in the sprat diet in the Bourgas Bay and off the Cape Emine; *P. setosa* is observed in the sprat food off the southern part of the Bay of Burgas and Sozopol (Table 5.4,

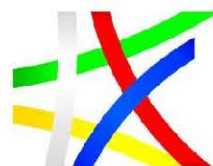


МИНИСТЕРСТВО НА ЗЕМЕДЕЛИЕТО, ХРАНИТЕ И
ГОРИТЕ

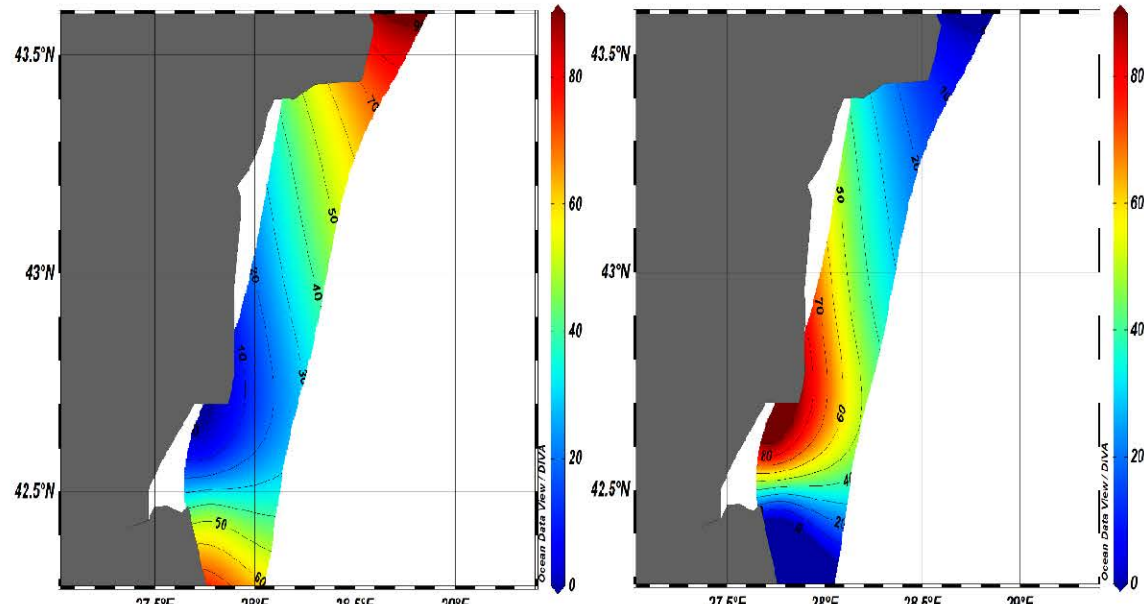
Figure 5.8).

Table 5.4. IRI(%) of different mesozooplankton species in sprat food per trawls in X-XI 2019

Sprat food composition	T2	T8	T27	T32	T38
<i>Calanus euxinus</i>	28.23	83.11	52.60	47.20	4.49
<i>Pseudocalanus elongatus</i>	0.91	4.95	11.06	0.21	0.66
<i>Paracalanus parvus</i>	47.87	3.35	1.04	4.26	88.21
<i>Acartia clausi</i>	14.77	0.17	24.90	25.50	1.01
<i>Centropages ponticus</i>	0.16	0.00	2.36	0.56	3.37
<i>Pleopis polyphemoides</i>	0.06	0.00	0.47	1.79	0.00
<i>Lamellibranchia veliger</i>	4.62	2.13	0.00	0.08	0.05
<i>Cirripedia nauplii/cypris</i>	0.46	0.21	1.25	0.45	0.15
<i>Decapoda larvae</i>	0.00	0.00	1.87	1.87	1.98
<i>Parasagitta setosa</i>	2.74	6.03	0.00	16.33	0.01
<i>Oikopleura dioica</i>	0.15	0.01	4.45	1.74	0.06
other	0.03	0.04	0.00	0.01	0.01
	100	100	100	100	100

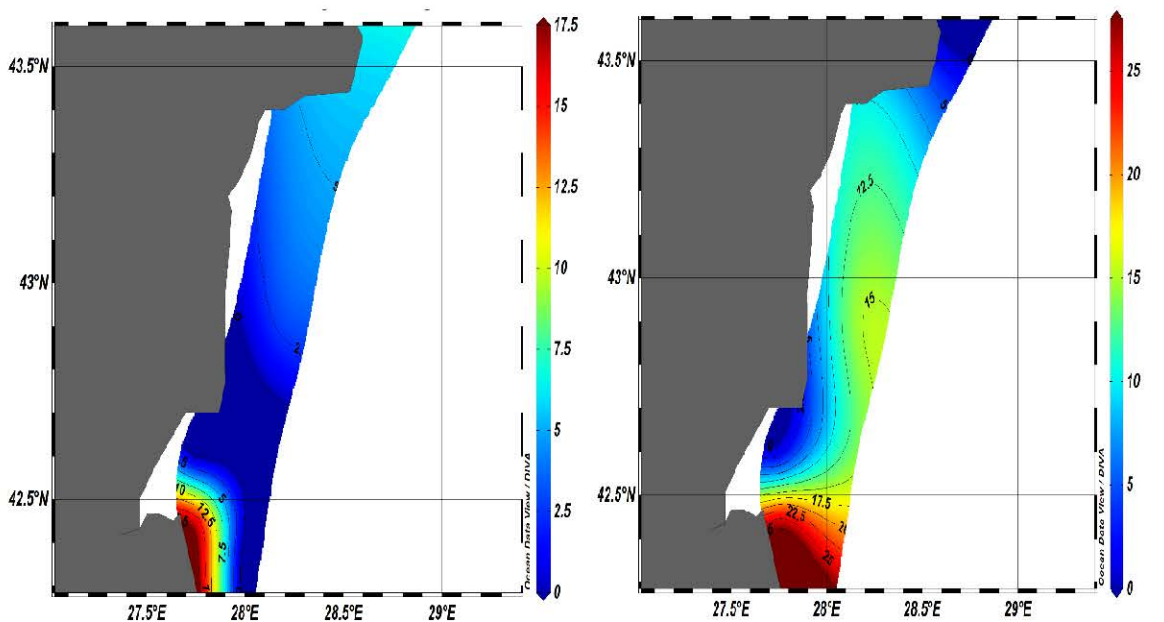


МИНИСТЕРСТВО НА ЗЕМЕДЕЛИЕТО, ХРАНИТЕ И
ГОРИТЕ



(1)

(3)



(2)

(4)

Figure 5.8. Spatial distribution of IRI (%) of zooplankton species in the sprat food:
(1) *C. euxinus*, (2) *Parasagitta setosa*, (3) *Paracalanus parvus*, (4) *A. clausi* in X-XI
2019



МИНИСТЕРСТВО НА ЗЕМЕДЕЛИЕТО, ХРАНИТЕ И
ГОРИТЕ



Horse mackerel: biological parameters and feeding

Ten specimens of horse mackerel were studied, with an average absolute length of $9.22 \text{ cm} \pm 0.65$ (SD) and an average weight of $6.60 \text{ g} \pm 1.61$ (SD) (Table 5.1, Figure 5.1.). The mean value of stomach fullness index of horse mackerel is $0.60\% \pm 0.27$ (SD) of body weight (Table 5.5, Figure 5.9).

Table 5.5. Summary data on the size (L, cm), weight (W, g) and ISF (% BW) of the horse mackerel determined in the analysis of stomach contents in XI 2019

	L, cm	W, g	ISF, % BW
Mean	9.22	6.60	0.60
Standard Error	0.21	0.51	0.09
Median	9.20	6.41	0.57
Mode	9.20	#N/A	#N/A
Standard Deviation	0.65	1.61	0.27
Sample Variance	0.43	2.58	0.07
Kurtosis	-1.24	3.38	-1.26
Skewness	-0.26	1.51	0.11
Range	1.80	5.78	0.81
Minimum	8.20	4.65	0.20
Maximum	10.00	10.43	1.01
Sum	92.20	66.00	5.98
Count	10.00	10.00	10.00
Confidence Level (95.0%)	0.47	1.15	0.19

The average prey number in a horse mackerel food is $97.9 \text{ ind/stomach} \pm 57.21$ SD, and the maximal individual number of food organisms is 178 ind/stomach.



МИНИСТЕРСТВО НА ЗЕМЕДЕЛИЕТО, ХРАНИТЕ И
ГОРИТЕ

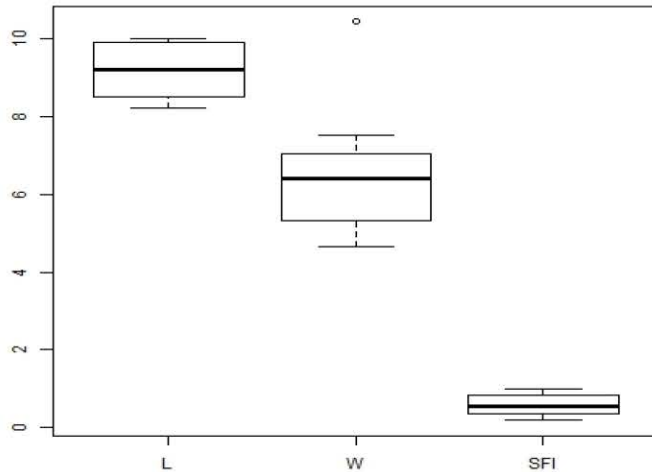


Figure 5.9. Size (L, cm), weight (W, g) and ISF index (% BW) of horse mackerel in XI 2019

Nineteen mesozooplankton species have been identified in horse mackerel food. The identified copepods include - *Calanus euxinus*, *Pseudocalanus elongatus*, *Paracalanus parvus*, *Acartia clausi*, *Centropages ponticus*, *Oithona davisae* and *Harpacticocoida spp.* Cladocera are represented by *Pleopis polyphemoides*, *Penilia avirostris*, *Pseudoevadne tergestina* и *Evdne spinifera*; four taxonomic groups are detected from the planktonic larvae of bottom organisms (meroplankton): *Lamellibranchia veliger*, *Gastropoda veliger*, *Cirripedia larvae*, *Decapoda larvae*; class *Chaetognatha* is presented by *Parasagitta setosa*, class *Appendicularia* - from *Oicopleura dioica*.

Food objects were found in all studied fish specimens, with an average number of zooplankton species consumed - 9 species, and fluctuations of 5-15 zooplankton species by the individually observed fish specimen. The indices of the relative importance of zooplankton organisms in the horse mackerel food, the percentages of abundance and biomass, as well as the frequency of occurrence among the studied horse mackerel specimens are presented in Table 5.6.



МИНИСТЕРСТВО НА ЗЕМЕДЕЛИЕТО, ХРАНИТЕ И
ГОРИТЕ

Table 5.6. Food composition of horse mackerel and IRI of main zooplankton species

<i>Food composition of horse mackerel</i>	<i>N (% from abundance)</i>	<i>M (% from biomass)</i>	<i>FO - frequency of occurrence</i>	<i>IRI – Index of relative importance</i>
<i>Acartia clausi</i>	30.64	24.75	100.00	5539.25
<i>Centropages ponticus</i>	11.03	11.89	90.00	2063.35
<i>Calanus euxinus</i>	2.66	44.20	40.00	1874.20
<i>Paracalanus parvus</i>	21.55	5.00	70.00	1858.71
<i>Cirripedia nauplii</i>	6.33	1.43	100.00	776.47
<i>Pleopis polyphemoides</i>	6.54	4.33	70.00	760.77
<i>Penilia avirostris</i>	2.86	2.27	80.00	410.70
<i>Oikopleura dioica</i>	3.78	0.49	40.00	170.69
<i>Lamellibranchia veliger</i>	4.60	0.23	30.00	144.75
<i>Decapoda larvae</i>	0.61	1.73	50.00	116.92
<i>other</i>	9.40	3.68		
<i>total</i>	100%	100%		

The copepods *Acartia clausi*, *Centropages ponticus*, *Calanus euxinus* and *Paracalanus parvus* play leading position in the horse mackerel diet (Table 5.6., Fig. 5.10.).



МИНИСТЕРСТВО НА ЗЕМЕДЕЛИЕТО, ХРАНИТЕ И
ГОРИТЕ

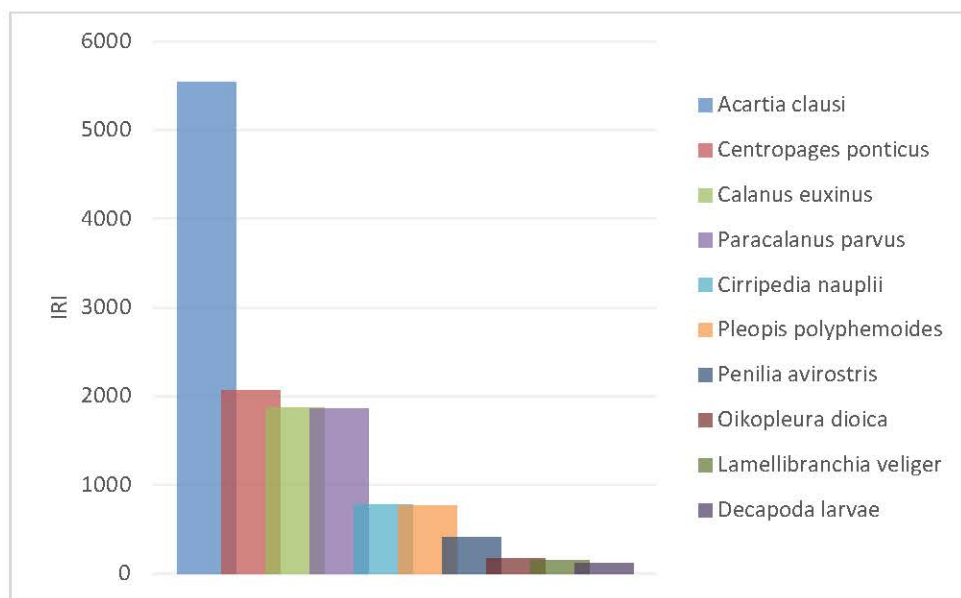


Figure 5.10. Average values of the relative importance indices (IRI) of the various mesozooplankton species/groups in the horse mackerel food off the Bulgarian coast in XI 2019

Zooplankton in the marine environment: species composition and biomass

The zooplankton biodiversity in the marine environment is formed by 27 species/groups of organisms (Table 5.7).



МИНИСТЕРСТВО НА ЗЕМЕДЕЛИЕТО, ХРАНИТЕ И
ГОРИТЕ

Table 5.7. Species diversity of zooplankton

X-XI.2019	
	<i>Noctiluca scintillans</i>
	<i>Ctenophora larvae</i>
	<i>Pleurobrachia pileus</i>
	<i>Aurelia aurita</i>
	<i>Beroe ovata</i>
	<i>Favella spp.</i>
	<i>Acartia clausi</i>
	<i>Acartia tonsa</i>
	<i>Pseudocalanus elongatus</i>
	<i>Calanus euxinus</i>
	<i>Paracalanus parvus</i>
	<i>Centropages ponticus</i>
	<i>Oithona daX-XIsae</i>
	<i>Oithona similis</i>
	<i>Harpacticoida spp.</i>
	<i>Pleopis polyphemoides</i>
	<i>Penilia aX-Xirostris</i>
	<i>Pseudoevadne tergestina</i>
	<i>Cirripedia nauplii/cypris</i>
	<i>Lamellibranchia veliger</i>
	<i>Polychaeta larvae</i>
	<i>Gastropoda veliger</i>
	<i>Bryozoa larvae</i>
	<i>Decapoda zoea/mysis</i>
	<i>Parasagitta setosa</i>
	<i>Oicopleura dioica</i>
	<i>Pisces ova</i>



МИНИСТЕРСТВО НА ЗЕМЕДЕЛИЕТО, ХРАНИТЕ И
ГОРИТЕ

The groups of *Copepoda* (36.07 %), water fleas (*Cladocera*, 25.19 %) and jellyplankton (24.02 %) have dominating positions in formation of the total zooplankton biomass (Fig. 5.11.A, Table 5.8). The representatives of crustaceans - *Copepoda* and *Cladocera* dominate in number (Fig. 5.11.B) and form significant proportions - 61.85 % and 14.54 % of the total zooplankton abundance.

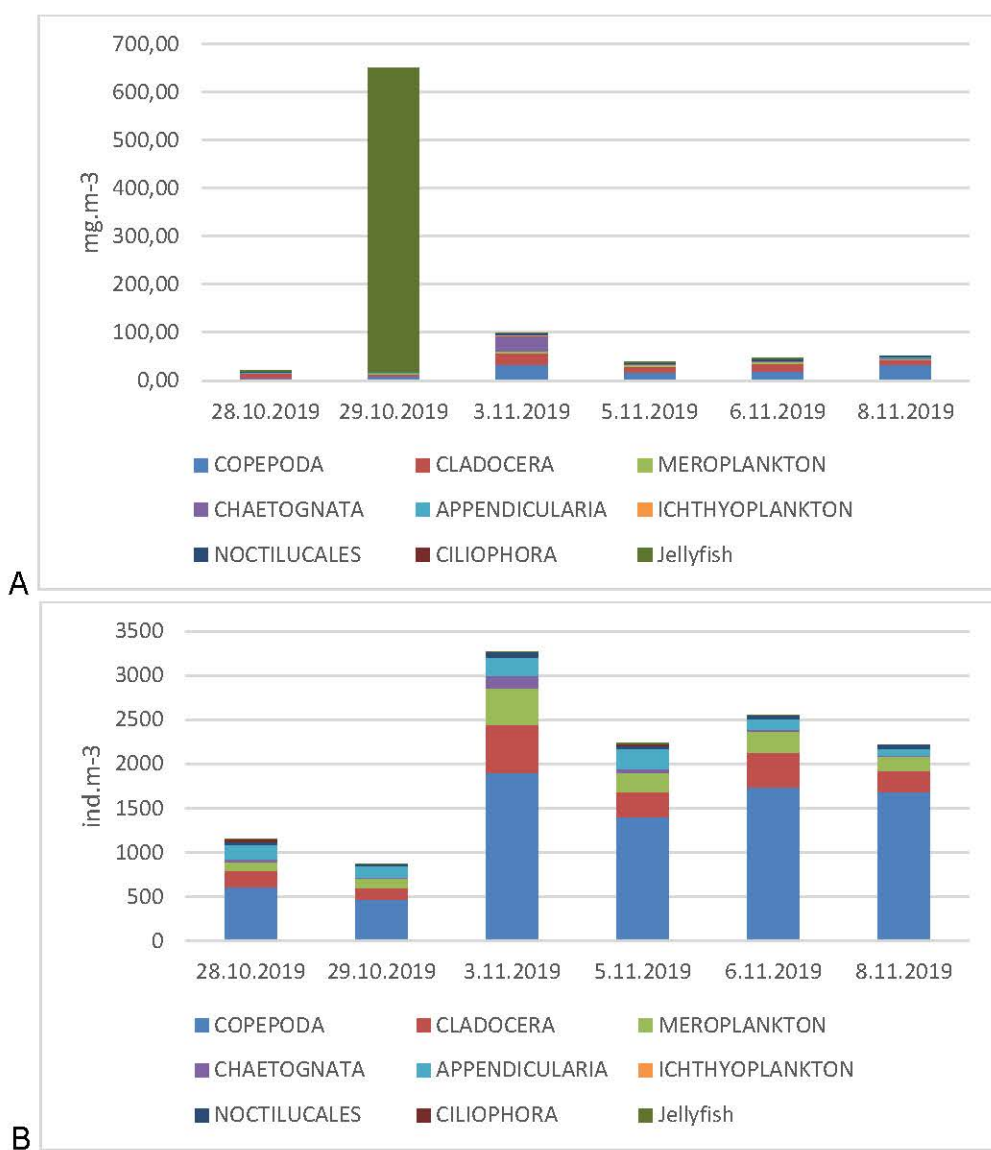


Figure 5.11. Distribution of the biomass (1. mg.m⁻³) and abundance (2, ind.m⁻³) of the main zooplankton groups (mg.m⁻³) during X-XI 2019



МИНИСТЕРСТВО НА ЗЕМЕДЕЛИЕТО, ХРАНИТЕ И
ГОРИТЕ

Table 5.8. Percentage distribution (% from total biomass) of main zooplankton groups during X-XI 2019

Date	COPEPODA	CLADOERA	MERO-PLANKTON	CHAETOGNATHA	APPENDICULARIA	ICHTHYO-PLANKTON	NOCTILUCES	JELLYFISH
28.10.2019	28.89	40.20	3.18	2.25	4.40	0.00	9.23	11.54
29.10.2019	1.26	0.89	0.17	0.05	0.13	0.00	0.20	97.29
3.11.2019	32.95	25.42	4.69	31.01	1.48	0.27	4.16	0.02
5.11.2019	46.15	30.65	6.71	4.95	3.31	0.00	4.96	3.10
6.11.2019	41.75	34.93	7.33	5.51	1.48	0.00	5.09	3.91
8.11.2019	65.39	19.06	4.93	4.32	1.19	0.53	4.59	0.00
<i>average</i>	36.07	25.19	4.50	8.01	2.00	0.13	4.71	19.31

During the autumn survey, the total zooplankton biomass is $150 \text{ mg.m}^{-3} \pm 100.52$ (SE), with the biomass of jellyplankton reaching $106.42 \text{ mg.m}^{-3} \pm 105.33$ (SE), and that of mesozooplankton - $42.14 \text{ mg.m}^{-3} \pm 11.69$ (SE). The biomass of food mesozooplankton is evaluated as relatively low for the season (Table 5.9).



МИНИСТЕРСТВО НА ЗЕМЕДЕЛИЕТО, ХРАНИТЕ И
ГОРИТЕ

Table 5.9. Statistical data about biomasses (mg.m^{-3}) of the main zooplankton groups in X-XI 2019

	<i>Mesozoo-plankton</i>	<i>Protozoa</i>	<i>Jellyfish</i>	<i>Total zooplankton biomass</i>
Mean	42.14	2.32	106.42	150.88
Standard Error	11.69	0.38	105.33	100.52
Median	38.73	2.13	1.50	48.49
Mode	#N/A	1.92	#N/A	#N/A
Standard Deviation	28.63	0.94	258.02	246.21
Sample Variance	819.64	0.88	66572.65	60620.80
Kurtosis	2.19	3.29	6.00	5.77
Skewness	1.34	1.56	2.45	2.39
Range	77.67	2.76	633.09	629.92
Minimum	16.30	1.32	0.00	20.80
Maximum	93.97	4.08	633.09	650.71
Sum	252.83	13.92	638.51	905.26
Count	6.00	6.00	6.00	6.00
Confidence Level (95.0%)	30.04	0.99	270.77	258.38

The highest mesozooplankton biomass is found off the Cape Emine region - up to 93.97 mg.m^{-3} (Fig. 5.12.A), while the jellyfish biomass increases to 650 mg.m^{-3} off the northern costs - in the Cape Kaliakra - Krapets strip (Fig. 5.12.B).



МИНИСТЕРСТВО НА ЗЕМЕДЕЛИЕТО, ХРАНИТЕ И
ГОРИТЕ

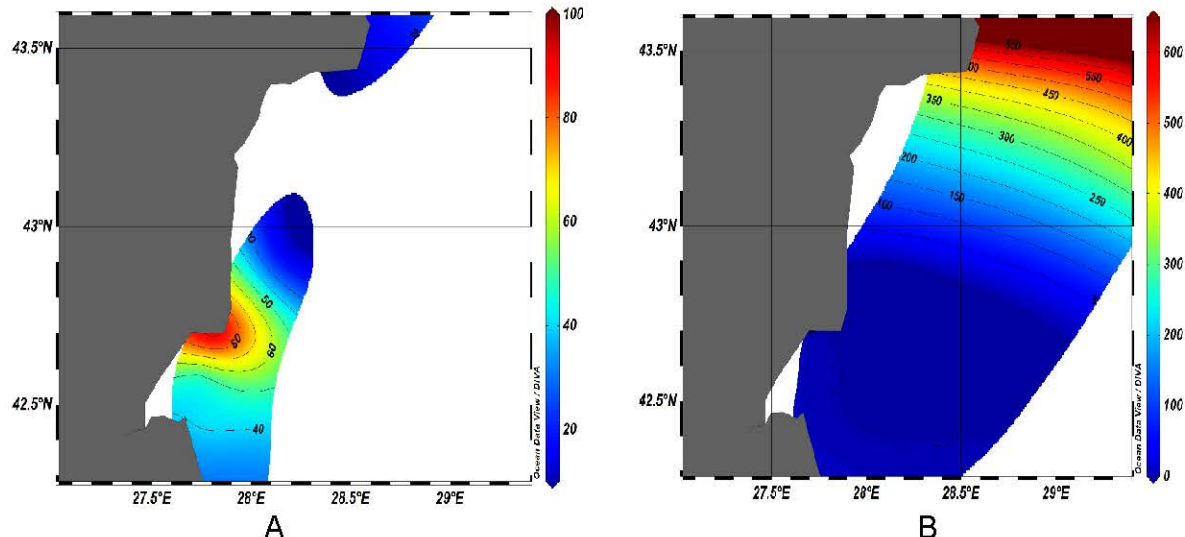


Figure 5.12. Spatial distribution of biomass ($\text{mg} \cdot \text{m}^{-3}$) of (A) mesozooplankton and jellyfish species (B) in X-XI 2019

6. Forecasts and Operational Opportunities

Steady state of sprat stock

Equilibrium and the associated biomass of sprat from Bulgarian Black Sea waters are presented graphically in Fig. 6.1. On the first graph, Equilibrium Yield with confidence intervals (showing very low Cimed and CI2.5%), Y / R with CI97.5% reaches its maximum and corresponds to fishing mortality at about 1.16 then follows the plateau the curve follows and the determination of Fmax becomes impossible.

Obviously, levels above $F = 0.8$ will result in stock collapse. Sustained fishing mortality rates are around $F = 0.5$, which will correspond to the level of the catch of 12.5 thousand tons of sprat in NW Black Sea.



МИНИСТЕРСТВО НА ЗЕМЕДЕЛИЕТО, ХРАНИТЕ И
ГОРИТЕ

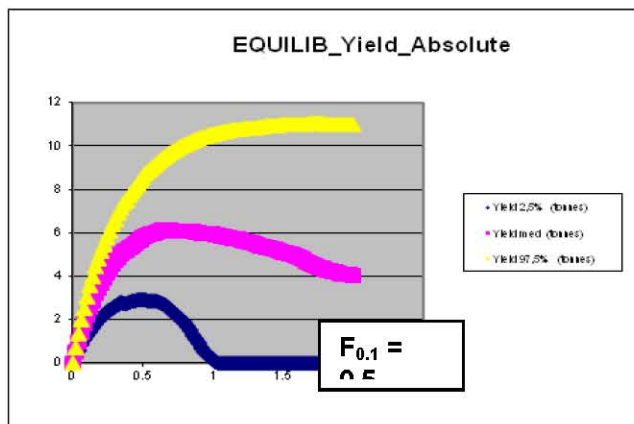


Figure 6.1. Equilibrium level with CI. Optimal level of fishing mortality and corresponding catches of sprat from Bulgarian waters

Biomass of the reproductive stock, vulnerable to fishing biomass and total biomass follow a similar downward trend since only CI values of 97.5% have relatively high levels of the lowest fishing mortality. Therefore, with increasing fishing mortality of all biomass tested (Fig. 6.2, Fig. 6.3, and Fig. 6.4), A decreasing trend follows, following $F = 0.8$ (at CI2.5%) and after 1.16 (with Cimed), the stocks of trinkant will fall below unsustainable levels (Fig. 6.1).

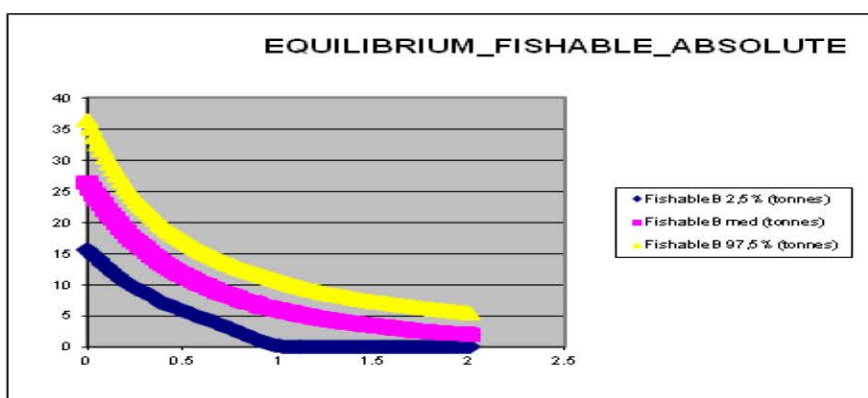


Figure 6.2. Balance state of biomass vulnerable to fishing



МИНИСТЕРСТВО НА ЗЕМЕДЕЛИЕТО, ХРАНИТЕ И
ГОРИТЕ

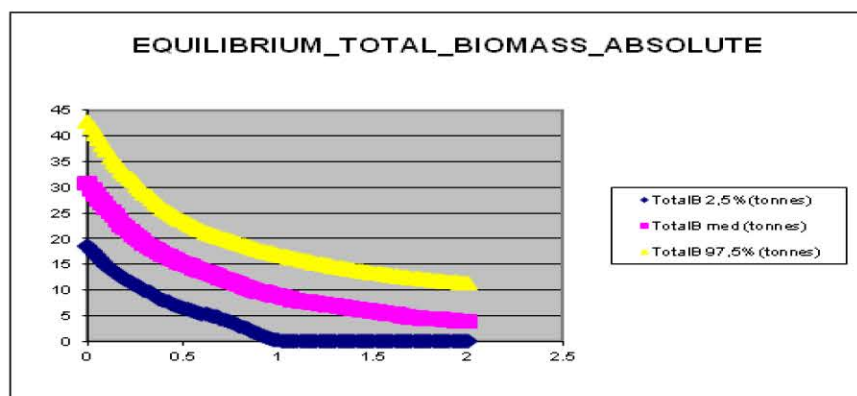


Figure 6.3. Balanced state of total biomass

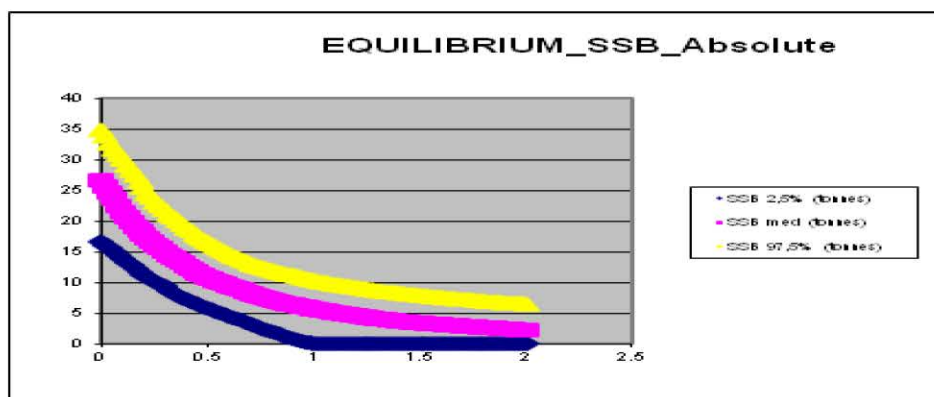


Figure 6.4. Sustainable propagation biomass

Filling is heavily affected by fishing mortality and after $F = 0.5$ falls very steeply (Fig. 6.5).



МИНИСТЕРСТВО НА ЗЕМЕДЕЛИЕТО, ХРАНИТЕ И
ГОРИТЕ

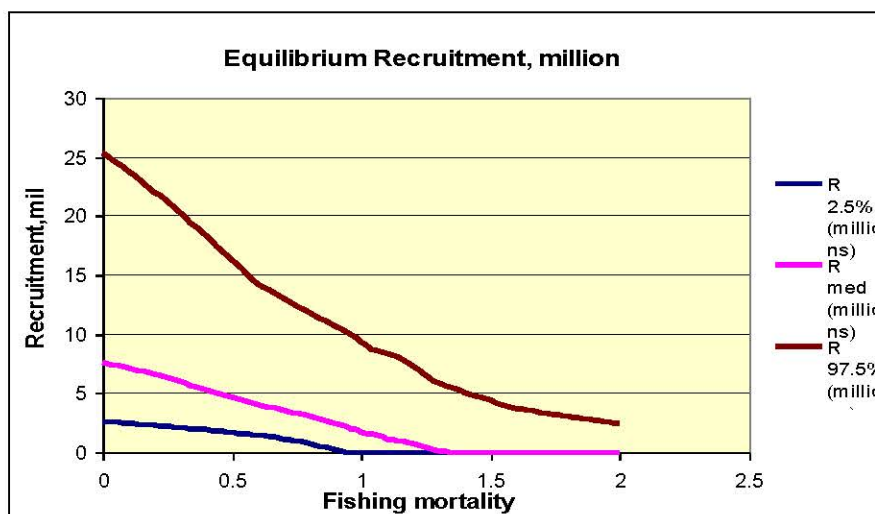


Figure 6.5. Balance equilibrium

From Figure 6.6. it is clear that the number of individuals in the catch in December marks a peak for 1-1++ year olds. From Figure 6. 6. it can be seen that the maximum of catch numbers belongs to individuals aged 1-1 + years. What is noteworthy is the high proportion of recruits 2-2 + aged, were significantly less and the older age groups were in a subordinate position.

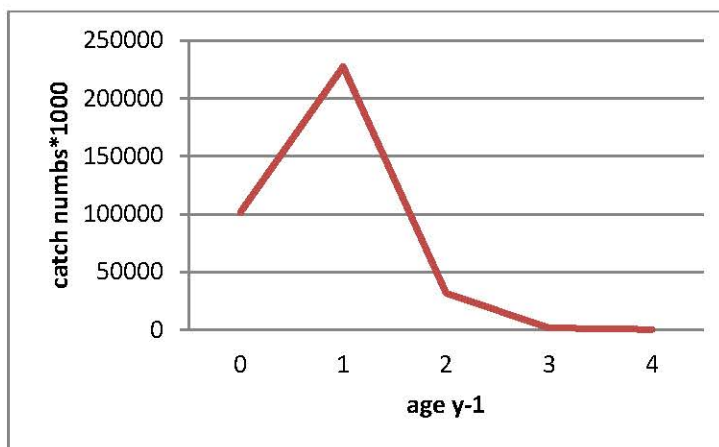


Figure 6.6. Catch numbers X-XI2019 by age for sprat



МИНИСТЕРСТВО НА ЗЕМЕДЕЛИЕТО, ХРАНИТЕ И
ГОРИТЕ



7. Maximum sustainable yield

Maximum sustainable yield (MSY), in accordance with the Gulland method (1970), is calculated for the exploited biomass from the studied area. In this study, we used the natural mortality rate $M = 0.82$, calculated by the method of Gislason et al., (2010). The results obtained are given in Table 7.1.

Table 7.1. Biomass (t) and MSY

Държава България	Биомаса (t)	MSY (t)		2/3MSY
		Gulland	BH steepness, $F_{0.1}$	
Окт-Ное	46 081,41	18893,38 t	11750 t	7833,33t

Expected MSYs are the maximum potential catches, including quota-based catch, as well as false or unreported catches and by-catches in other fisheries. Calculated exploitation biomass and equilibrium levels (MSYs) should not be considered as an absolute value for possible future yields given the fact that the methods have some ambiguities and the share of IUU catches is still unknown. In such cases, special approaches have been used, such as 2/3 MSY (Caddy and Mahon, 1995).

The recommended value of the catches in the Bulgarian Black Sea Basin, according to the current condition, should not exceed 7833,333 tonnes.



МИНИСТЕРСТВО НА ЗЕМЕДЕЛИЕТО, ХРАНИТЕ И
ГОРИТЕ



8. Conclusions

1. The total number of identified species is 34, of which 26 are fish, crustaceans 2, molluscs - 2 and 4 macrozooplankton species. The most common species in general trawl operations (in terms of presence / absence) are (in descending order): in June 2019 they are: *S.sprattus* (82.99%), *M. merlangius* (9.44%), and *M.barbatus* - 6.54%). The other species were in small quantities or as separate individuals in the catches.
2. Sprat (*Sprattus sprattus*). The species had the highest recorded biomass and catch per unit area in the study areas during the period X-XI 2019. At a layer of 15-30m $CPUA = 11\ 536 \text{ kg.km}^{-2}$ and 23 825 t., followed by a strip depth of 30-50 m with a catch per unit area of 10 640 kg.km^{-2} biomass 19 311 t, 7 130 kg.km^{-2} for $CPUA$ and 2945,2t biomass at a depth of 50-100m. In X-XI 2019, the highest $CPUA$ values of the red mullet of $1016.1 \text{ kg.km}^{-2}$ were established in a layer of depth 15-30m, with biomass of 2098.5t, followed by a depth of 15-30m with catch per unit area of 496 kg.km^{-2} biomass 1023.4 t, 172 kg.km^{-2} for $CPUA$ and 312 t biomass at a depth of 30-50m.
3. The whiting was well presented in the 50-100m layer during the reporting period. with a $CPUA = 4\ 803,4 \text{ km}^{-2}$ and a biomass of 19 839 tonnes, followed by a layer depth of 30-50 m with a catch per unit area of 218 kg.km^{-2} biomass of 396 t, 115 kg.km^{-2} for $CPUA$ and 473 t of biomass at a depth of 50-100m.
4. The total biomass of sprat in X-XI 2019 is 46 081,4 t for the Bulgarian Black Sea;
5. The total area of the survey in the Bulgarian part is $8010,24 \text{ km} \cdot \text{kg}^{-2}$ and the total identified biomass of the red mullet is 5122.056 t in X-XI 2019;
6. The total surveyed area is 8010, 24 km^2 . The total biomass of whiting in X-XI in



МИНИСТЕРСТВО НА ЗЕМЕДЕЛИЕТО, ХРАНИТЕ И
ГОРИТЕ

2019 is 21 174.59 t in the Bulgarian Black Sea area.

7. Sprat size frequencies indicate a maximum in the class distribution (7.5 cm), with a columnar decrease in the direction of the maximum established sample sizes.

8. The prevalence of sprat in this study was 1-1 + (78%);

9. The predominant age of whiting in this study is 2-2 + (32%), 3-3 + (24%)

10. The predominant age of the red mullet was 2-2 + (46%), followed by the age of 3-3 + (26,6%).

11. H.mackerel length groupd were 9-15 cm, age clasess 0+ to 5+;anchovy: L = 9.35 -12.30 cm, corresponding to the age groups of 1 to 4; spiny dogfish – 95.5-118 cm;

12. Sprat was in the active phase of spawning in October-November. Most of the individuals had gonads in stage IV-V-II. and. active reproduction has commenced;

13. GSI (%) indicates that a big percentage of females are actively breeding. Most individuals were in the late stages of maturation, so we can conclude that in X-XI 2019, active reproduction begun.

14. During the autumn survey, the sprat food spectrum was constituted by 23 zooplankton species/groups, including several copepods - *Calanus euxinus*, *Pseudocalanus elongatus*, *Paracalanus parvus*, *Acartia clausi*, *Centropages ponticus*, *Oithona similis*, *Oithona davisae*, *Harpacticocoida spp*; cladocerans (water fleas) are presented by *Pleopis polyphemoides*, *Penilia avirostris* and *Pseudoevadne tergestina*; the group of planktonic larvae of bottom organisms includes five taxonomic groups - *Lamellibranchia veliger*, *Gastropoda veliger*, *Cirripedia larvae*, *Decapoda larvae* and *Polychaeta larvae*; class *Chaetognatha* is represented by *Parasagitta setosa*, class *Appendicularia* - by *Oicopleura dioica*.

15.The average value of sprat ISF is $0.91\% \pm 0.60$ (SD) (SD) and it is with 13.75% higher than the measured level during the spring survey. The highest average ISF = 1.36 - 1.3 % are established in the Bay of Burgas and in front of Kamchia river mouth at depths of 30 - 45 m, while the minimal ISF (~ 0.3% BW) are registered in the area



МИНИСТЕРСТВО НА ЗЕМЕДЕЛИЕТО, ХРАНИТЕ И
ГОРИТЕ



of the Cape Maslen nos.

16. The average prey number (PN) in the sprat diet is 230 ind/stomach \pm 321.64 SD. The maximal individual number of food organisms - 1340 ind/stomach is established in the open part of the Burgas Bay ($d = \sim 30$ m), related to intensive consumption of the copepod *Paracalanus parvus*.

17. Nineteen mesozooplankton species have been identified in horse mackerel food: copepods - *Calanus euxinus*, *Pseudocalanus elongatus*, *Paracalanus parvus*, *Acartia clausi*, *Centropages ponticus*, *Oithona davisae* and *Harpacticocoida spp.*, cladocerans - *Pleopis polyphemoides*, *Penilia avirostris*, *Pseudoevadne tergestina* and *Evdadne spinifera*; four taxonomic groups are found from the meroplankton group: *Lamellibranchia veliger*, *Gastropoda veliger*, *Cirripedia larvae* and *Decapoda larvae*; the class *Chaetognatha* is represented by *Parasagitta setosa*, the class *Appendicularia* - from *Oicopleura dioica*.

18. The average stomach fullness index of horse mackerel is 0.60% BW \pm 0.27 (SD) and the average PN is 98 ind/stom. \pm 57.21 SD, with the maximal individual number of food organisms - 178 ind / stom.

19. In October-November 2019, the total zooplankton biomass amounts to $150 \text{ mg.m}^{-3} \pm 100.52$ (SE), the biomass of jelly-plankton is $106.42 \text{ mg.m}^{-3} \pm 105.33$ (SE) and of mesozooplankton - $42.14 \text{ mg.m}^{-3} \pm 11.69$ (SE). Fodder mesozooplankton biomass is evaluated as low for the season.

20. The maximum sustainable yield (MSY), in accordance with the Gulland method (1970), is estimated at 18 893, 38 t; t; BH steepness, F0.1 = 11 750 t.

21. The calculated exploitation biomass and equilibrium levels (MSYs) should not be considered as an absolute value for possible future yields, given the fact that the methods have some uncertainties and the proportion of IUU catches is still unknown. In such cases, special approaches such as using 2/3 MSY were used (Caddy and Mahon, 1995).

22. The recommended value of catches in the Bulgarian Black Sea waters,



МИНИСТЕРСТВО НА ЗЕМЕДЕЛИЕТО, ХРАНИТЕ И
ГОРИТЕ



according to the current situation, should not exceed 7333 tonn.



МИНИСТЕРСТВО НА ЗЕМЕДЕЛИЕТО, ХРАНИТЕ И
ГОРИТЕ



9. References

- Alexandrov B. and Korshenko A., 2006. Manual for zooplankton sampling and analysis in the Black Sea Region.
- Bertalanffy L. von, 1938. A quantitative theory of organic growth (Inquiries on growth laws. II). Human Biol. 10: 181-213.
- Beveton, R.J. and S.J. Holt, 1957. On the dynamics of exploited fish populations. Fish. Invest. Ser. 2, Vol 19.
- Caddy, J.F., and R. Mahon, 1995. Reference points for fisheries management Rome: Food and Agriculture Organization of the United Nations. ,Vol. 374.
- Debes, P.V., F.E. Zachos and R. Hanel, 2008. Mitochondrial phylogeography of the European sprat (*Sprattus sprattus* L., Clupeidae) reveals isolated climatically vulnerable populations in the Mediterranean Sea and range expansion in the northeast Atlantic. Molecular Ecology 17: 3873-3888.
- Dimov I., 1959. Improved quantitative method for zooplankton calculation. Rep. BAS, 12, 5, 427 429. (in Russian)
- FAO, 1995. Precautionary approach to fisheries. FAO Fish. Tech. Paper N. 350 (1), 1995.
- Foote, K.G., 1996. Quantitative fisheries research surveys, with special reference to computers. In: B.A. Megrey & E. Moksness. Computers in fisheries research. Chapman & Hall. 254 pp. 80-112.
- Fryer, R.J., & Shepherd, J.G., 1996. Models of codend size selection. Journal of Northwest Atlantic Fishery Science, 19, 51-58.
- Gislason, H., Daan, N., Rice, J. C., & Pope, J. G., 2010. Size, growth, temperature and the natural mortality of marine fish. Fish and Fisheries, 11(2), 149-158.
- Godø, O. R., Pennington, M., & Vølstad, J.H., 1990. Effect of tow duration on length composition of trawl catches. Fisheries Research, 9(2), 165-179.



МИНИСТЕРСТВО НА ЗЕМЕДЕЛИЕТО, ХРАНИТЕ И
ГОРИТЕ



Gulland J.A., 1966. Manual of sampling and statistical methods for fisheries biology. Part I: Sampling methods. FAO Manuals in Fisheries Science No. 3, Rome.

Gulland J.A., 1970. The fish resources of the ocean. FAO Fish. Techn. Pap. No. 97, 1-425, Rome.

Holden, C., 1971. "Fish flour: protein supplement has yet to fulfill expectations.". 410-412.

Hunter, J.R., Lo, N.C. and Leong, R.J., 1985. Batch fecundity in multiple spawning fishes. NOAA Technical Report NMFS, 36, pp.67-77.

ICES, 2012. Report of the Workshop on Sexual Maturity Staging of Turbot and Brill (WKMSTB 2012), 5–9 March 2012, Ijmuiden, Netherlands. ICES 2012/ACOM: 56-48 pp

ICES, 2011. Report of the Workshop on Sexual Maturity Staging of Herring and Sprat (WKMSHS), 20-23 June 2011, Charlottenlund, Denmark. ICES CM 2011/ACOM:46. 143pp.

Jearld, A., 1983. Age determination. In In: Nielsen LA and Johnson DL (eds) Fisheries Techniques.

Kasapoglu, N., Duzgunes, E. 2014. Otolith Atlas for the Black Sea. Journal of Environmental Protection and Ecology 16, No 1, 133–144

Korshenko, A. and Alexandrov B., 2012. Manual for mesozooplankton sampling and analysis in the Black Sea monitoring (Black Sea Zooplankton Manual) Online: <http://bsc.ath.cx/documents/ExpertNetwork/default.asp?I=/Expert%20Network%20-%20Zooplankton>

Laevastu, T., 1965. Manual methods in fisheries biology. Observations on the chemical and physical environment. Chemical analysis of water FAO. Marine Physiological Sci., 6: 86-86.

Mihneva V., Raykov V., Grishin A., Stefanova K., 2015. Sprat feeding in front of the Bulgarian Black Sea Coast, MEDCOAST conference 2015, vol.1, 431- 443

Mordukhay-Boltovskoy, F.D. (Ed.). 1968. The identification book of the Black Sea and the Sea of Azov Fauna.- Kiev: Naukova Dumka Publ., T. 1 (Protozoa, Porifera, Coelenterata, Ctenophora, Nemertini, Nemathelminthes, Annelida, Tentaculata), 423 pp. (in Russian).

Mordukhay-Boltovskoy, F.D. (Ed.). 1969. The identification book of the Black Sea



МИНИСТЕРСТВО НА ЗЕМЕДЕЛИЕТО, ХРАНИТЕ И
ГОРИТЕ



and the Sea of Azov Fauna.- Kiev: Naukova Dumka Publ., T. 2 (Arthropoda: Cladocera, Calanoida, Cyclopoida, Monstrilloida, Harpacticoida, Ostracoda, Cirripedia, Malacostraca, Decapoda), 536 pp. (in Russian).

Mordukhay-Boltovskoy, F.D. (Ed.). 1972. The identification book of the Black Sea and the Sea of Azov Fauna.-Kiev: Naukova Dumka Publ., T. 3 (Arthropoda, Mollusca, Echinodermata, Chaetognatha, Chordata: Tunicata, Ascidiacea, Appendicularia), 340 pp. (in Russian).

Panfili, J., De Pontual, H., Troadec, H. and Wrigg, P.J., 2002. Manual of fish sclerochronology.

Pinkas L., Oliver M.S, Iverson I.L.K., 1971. Food habits of albacore, bluefin tuna and bonito in Californian waters. California Fish Game 152:1-105.

Pisil, Y., 2006. Karadeniz'de Yaşayan Çaça Balığı (*Sprattus sprattus* (L., 1758))'nda Kemiksi Yapıları ve Uzunluk-Frekans Metodu ile Yaşı Tayini. 19 Mayıs Üniversitesi, Fen Bilimleri Enstitüsü, Y. Lisans Tezi, 32 s.

Polat, N., & Beamish, R. J., 1992. Annulus formation on anatomical structures of Siraz (*Capoeta capoeta*) in Altınkaya Dam Lake. Ondokuz Mayıs Uni J Sci, 4(1), 70-88.

Prodanov, K., Mikhailov K., Daskalov G., Maxim C., Chashchin A., Arkhipov A., Shlyakhov V., Ozdamar E., 1997. Environmental management of fish resources in the Black Sea and their rational exploitation. Studies and Reviews. GFCM. No. 68. FAO, Rome.

Raykov, V., 2007. Primary management objectives for sustainable Sprat (*Sprattus sprattus* L.) stock exploitation at the Bulgarian Black Sea coast - preliminary results J.Environmental Protection and Ecology, 8 (2),302-318.

Raykov V.S, V.V.Mihneva, G, Daskalov, 2007. Investigations on sprat (*Sprattus sprattus* L.) population dynamics related to its trophic base and climate change over the period 1996-2004 in Bulgarian waters of the Black Sea. J.Environmental Protection and Ecology, 8 (2), 319-332.

Raykov V., Panayotova M., Stefanova K., Stefanova E., Radu G., Maximov V., Anton E., 2011. Statement to the Deputy Minister of Ministry of environment and waters in order to annual workshop of Black Sea commission National Report to GFCM 35 - Annual Assembly; Scientific report from international pelagic trawl survey in the Bulgarian and in the Romanian Black Sea area, June 2010 to National Agencies of Fisheries and Aquaculture of Bulgaria and Romania in



МИНИСТЕРСТВО НА ЗЕМЕДЕЛИЕТО, ХРАНИТЕ И
ГОРИТЕ



relation to National Data Collection programs for 2010, 71 pp.

Simon, K.D., Y. Bakar, A.G. Mazlan, C.C. Zaidi and A. Samat et al., 2012. Aspects of the reproductive biology of two archer fishes *Toxotes chatareus*, (Hamilton, 1822) and *Toxotes jaculatrix* (Pallas, 1767). Environ. Biol. Fish., 93: 491-503.

Somerton, D. A., Otto, R. S., & Syrjala, S. E., 2002. Can changes in tow duration on bottom trawl surveys lead to changes in CPUE and mean size?. Fisheries Research, 55(1-3), 63-70.

Sparre, P., & Venema, S.C., 1998. Introduction to tropical fish stock assessment, Vol. 1. FAO Fisheries Technical Paper, Rome.

Treschev, AI (1974). Scientific bases of selective fisheries. M.: Pisht prom, 443, 3 (in Russian)

Wassenberg, T.J., Dews,G., and Cook, S.D., 2002. The impact of fish trawls on megabenthos (sponges) on the north-west shelf of Australia. Fisheries Research, 58(2), 141-151.



МИНИСТЕРСТВО НА ЗЕМЕДЕЛИЕТО, ХРАНИТЕ И
ГОРИТЕ

ANNEXES

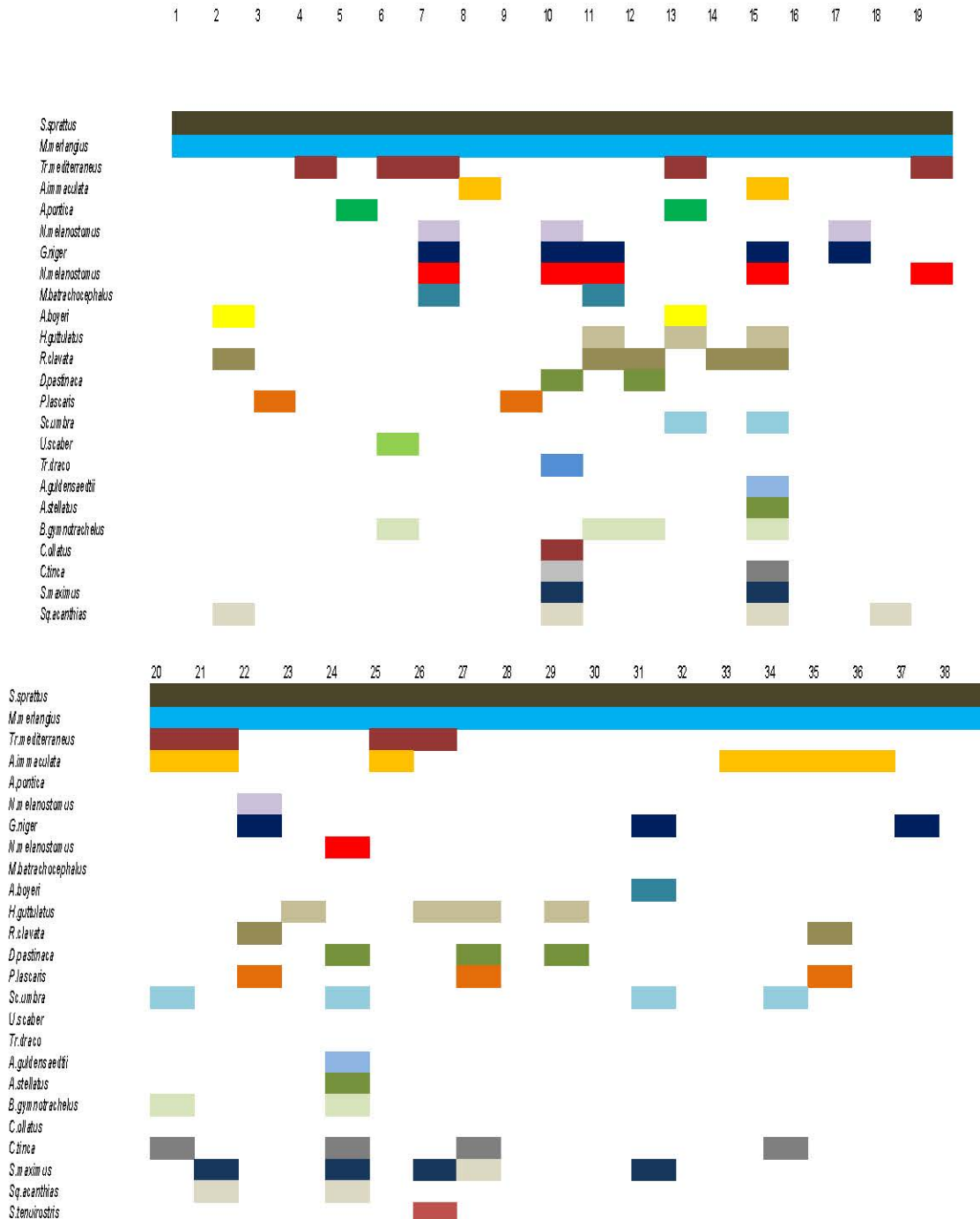
ANNEX I CPUE kg.h-1 and CPUAkg.km-2 in the Bulgarian part of the Black Sea - sprat, whiting and red mullet

CPUEkg/h	CPUAkg/k	CPUEkg/h	CPUAkg/k	CPUEkg/h	CPUAkg/k
909,0909	10579,09	31,81818	370,2682	250	2909,25
681,8182	7934,318	22,72727	264,4773	45,45455	528,9545
336,3636	3914,264	9,090909	105,7909	90,90909	1057,909
1136,364	13223,86	4,545455	52,89545	181,8182	2115,818
1818,182	21158,18	18,18182	211,5818	9,090909	105,7909
2500	29092,5	40,90909	476,0591	18,18182	211,5818
681,8182	7934,318	54,54545	634,7455	0	0
1818,182	21158,18	545,4545	6347,455	0	0
636,3636	7405,364	63,63636	740,5364	0	0
772,7273	8992,227	36,36364	423,1636	0	0
1136,364	13223,86	22,72727	264,4773	0	0
409,0909	4760,591	72,72727	846,3273	90,90909	1057,909
1000	11637	40,90909	476,0591	18,18182	211,5818
681,8182	7934,318	100	1163,7	4,545455	52,89545
909,0909	10579,09	159,0909	1851,341	54,54545	634,7455
181,8182	2115,818	186,3636	2168,714	0	0
818,1818	9521,182	45,45455	528,9545	0	0
1136,364	13223,86	90,90909	1057,909	0	0
1272,727	14810,73	113,6364	1322,386	45,45455	528,9545
1363,636	15868,64	159,0909	1851,341	0	0
1159,091	13488,34	186,3636	2168,714	68,18182	793,4318
1818,182	21158,18	227,2727	2644,773	18,18182	211,5818
1000	11637	27,27273	317,3727	0	0
909,0909	10579,09	40,90909	476,0591	45,45455	528,9545
227,2727	2644,773	36,36364	423,1636	22,72727	264,4773
681,8182	7934,318	36,36364	423,1636	0	0
818,1818	9521,182	18,18182	211,5818	0	0
904,5455	10526,2	4,545455	52,89545	0	0
1136,364	13223,86	40,90909	476,0591	0	0
454,5455	5289,545	18,18182	211,5818	0	0
500	5818,5	22,72727	264,4773	22,72727	264,4773
1136,364	13223,86	9,090909	105,7909	9,090909	105,7909
909,0909	10579,09	40,90909	476,0591	636,3636	7405,364
654,5455	7616,946	22,72727	264,4773	654,5455	7616,946
454,5455	5289,545	50	581,85	454,5455	5289,545
409,0909	4760,591	27,27273	317,3727	409,0909	4760,591
445,4545	5183,755	9,090909	105,7909	445,4545	5183,755
a) 280,2735	3261,543	45,45455	528,9545	c) 280,2735	3261,543
b)					



МИНИСТЕРСТВО НА ЗЕМЕДЕЛИЕТО, ХРАНИТЕ И
ГОРИТЕ

ANNEX II Species composition in the Bulgarian Black Sea





МИНИСТЕРСТВО НА ЗЕМЕДЕЛИЕТО, ХРАНИТЕ И
ГОРИТЕ

ANNEX III. Surveys indicator targets and results in 2019 June (Bulgarian part)

Black Sea	Length @age	market, discards, surveys	2,50%	Survey: 1326 1250
Black Sea	Weight @length	market, discards, surveys	2,50%	Survey: 2565 5000
Black Sea	Weight @age	market, discards, surveys	2,50%	Market: Discard: - Survey: 1326 1250
Black Sea	Maturity @length	surveys	2,50%	5000 140
Black Sea	Maturity @age	surveys	2,50%	5000 140
Black Sea	Sex-ratio @length	market, surveys	2,50%	Market: 250 Survey: 250 125
Black Sea	Sex-ratio @age	market, surveys	2,50%	Market: Survey: 250 250



МИНИСТЕРСТВО НА ЗЕМЕДЕЛИЕТО, ХРАНИТЕ И
ГОРИТЕ

Navigation, bathymetry and hydroacoustics

For more sensitivity interpretation of the results of trawl picture was used navigation software **OpenCPN 4.8.0 [1]** and GPS "HOLLUX" (Fig. 1, 2)

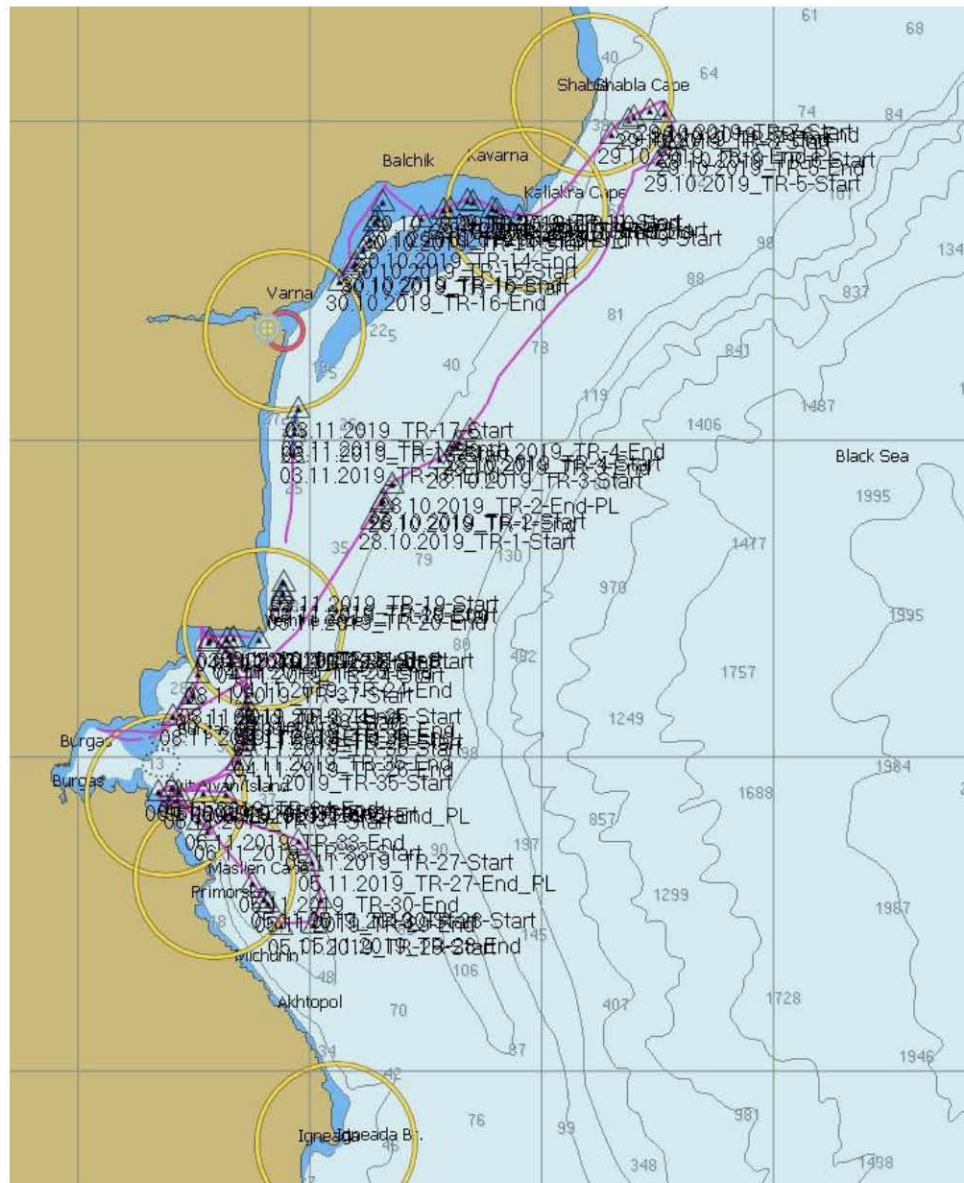


Figure 1. Navigation map of the expedition in October-November 2019 (OpenCPN 4.8.0) [1]



МИНИСТЕРСТВО НА ЗЕМЕДЕЛИЕТО, ХРАНИТЕ И
ГОРИТЕ



For the more detailed depth measurement, determination of the fish species and determination of the marine sediments type, was used Hydrographic Survey Echo Sounder “LituGraph 4F” (Fig. 2 - 5).

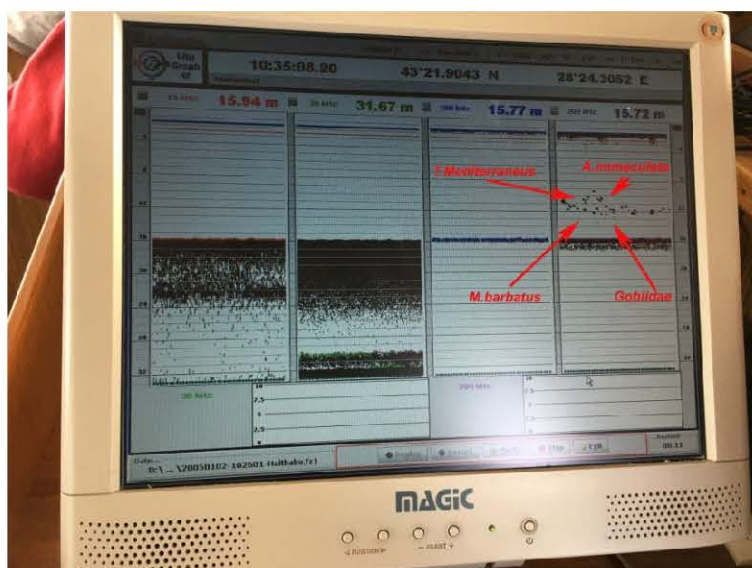


Figure 2. Hydrographic Survey Echo Sounder “LituGraph 4F”

Trawl 10, fish schools of *T.Mediterraneus*, *M.barbatus*, *Gobiidae*, *A.immaculata*



МИНИСТЕРСТВО НА ЗЕМЕДЕЛИЕТО, ХРАНИТЕ И
ГОРИТЕ



Figure 3. Trawl 10, catch – 2,5 kg,

T.Mediterraneus, M.barbatus, Gobiidae, A.immaculata and Psetta maxima – 3,6 kg

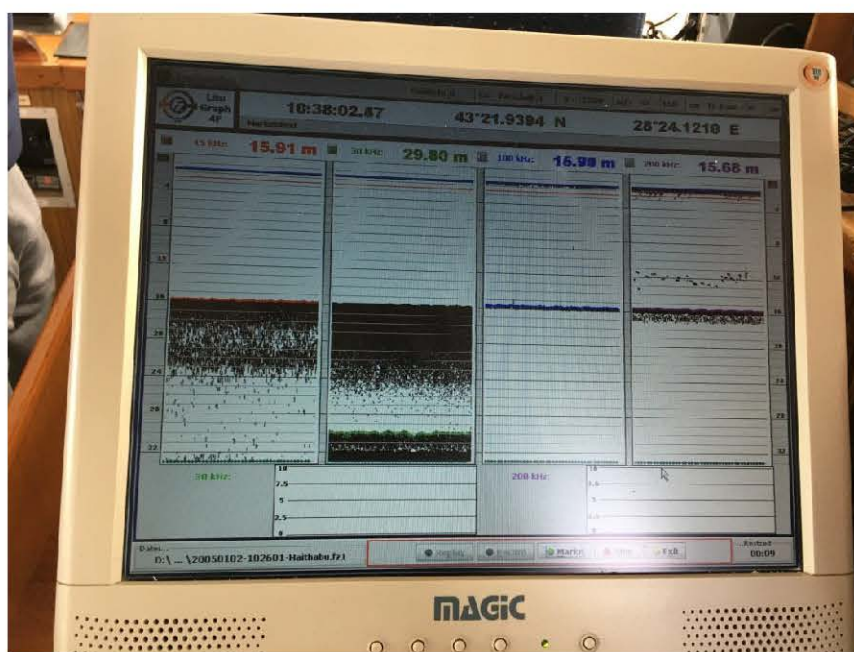


Figure 4. Hydrographic Survey Echo Sounder “LituGraph 4F”.

Trawl 12, **fish schools** of *T.Mediterraneus, M.barbatus, Gobiidae, A.immaculata*.



МИНИСТЕРСТВО НА ЗЕМЕДЕЛИЕТО, ХРАНИТЕ И
ГОРИТЕ



Figure 5. Trawl 12, catch – 4,5 kg,
T.Mediterraneus, M.barbatus, Gobiidae, A.immaculata

For the purposes and tasks of the present study, the hydro-acoustic equipment SIMRAD - NSO evo3 / HDS Carbon / LOWRANCE (Fig. 6, 7, 8), [2, 3] was used.



Figure 6. SIMRAD - NSO evo3 / HDS Carbon / LOWRANCE



МИНИСТЕРСТВО НА ЗЕМЕДЕЛИЕТО, ХРАНИТЕ И
ГОРИТЕ



Figure 7. Probe of "SIMRAD - NSO evo3"

The hydroacoustic profiles make it possible to determine the quantitative and qualitative characteristics of the fish schools in combination with the macroscopic description of the trawl picture taken.

NSO evo3 delivers the ultimate view with an ultra-bright display, available in 16, 19, or 24-inch widescreen sizes. Wide viewing angles keep the screen in view from anywhere in sight, even if you're wearing polarized sunglasses. See more than ever with Full HD resolution, and the option to combine up to six panels in a split-screen layout. Intuitively navigate charts, define waypoints, and take control of connected systems such as autopilot, radar, and sonar with a touch.

The Carbon HDS Series combines side imaging, downscan imaging, dual-channel CHIRP sonar, real-time underwater 3D mapping capabilities and ultra-bright displays to deliver the most advanced and easy-to-use fish finder/chart plotter on the market. The units' touch-screen interface works much like a smartphone with pinch-to-zoom and touch-and-move abilities for fast and intuitive control.

HDS Carbon units also feature the ability to create custom maps using recorded sonar logs. Anglers can add custom color layers, vegetation and bottom-hardness overlays. Each unit supports the most advanced marine technology and is easily updated to the most current software for optimal performance.



МИНИСТЕРСТВО НА ЗЕМЕДЕЛИЕТО, ХРАНИТЕ И
ГОРИТЕ



Featuring a powerful dual-core, high-performance processor, the HDS Carbon delivers accurate and definitive images with superior target separation. HDS Carbon multi-touch, super bright displays offer a wider viewing angle and feature an advanced anti-reflective coating for ultimate viewing in bright sunlight and while wearing polarized sunglasses.

HDS Carbon units remove the hassle of constantly monitoring and repositioning the boat with connectivity to certain autopilot trolling motors and shallow water anchors, freeing up anglers to concentrate on fishing. Both bow-mounted and console sonar can be displayed side-by-side with different zoom levels for a clear and precise view of schools or individual fish.

"SIMRAD - NSO evo3" provides the following data processing capabilities: navigation map, sonar and radar.

The Sonar feature provides an underwater view of the area, under and around the ship, allowing easy visualization of fish passages and geological - geomorphologic exploration of the sea floor. The format of the files is <*.sl3>, which includes the Sonar and StructureScan3D options. StructureScan HD provides a 328-meter wide-screen coverage with SideScan, while DownScan™ provides a detailed view of the bottom structure and fish passages directly below the boat up to 92 m. StructureScan 3D is a multi-beam sonar technology that allows you to observe the structure and geomorphological features of the bottom in 3D.



МИНИСТЕРСТВО НА ЗЕМЕДЕЛИЕТО, ХРАНИТЕ И
ГОРИТЕ

The "ReefMaster2.0.38.0" software was used to process and interpret hydroacoustic profile data (Fig. 8) [4].

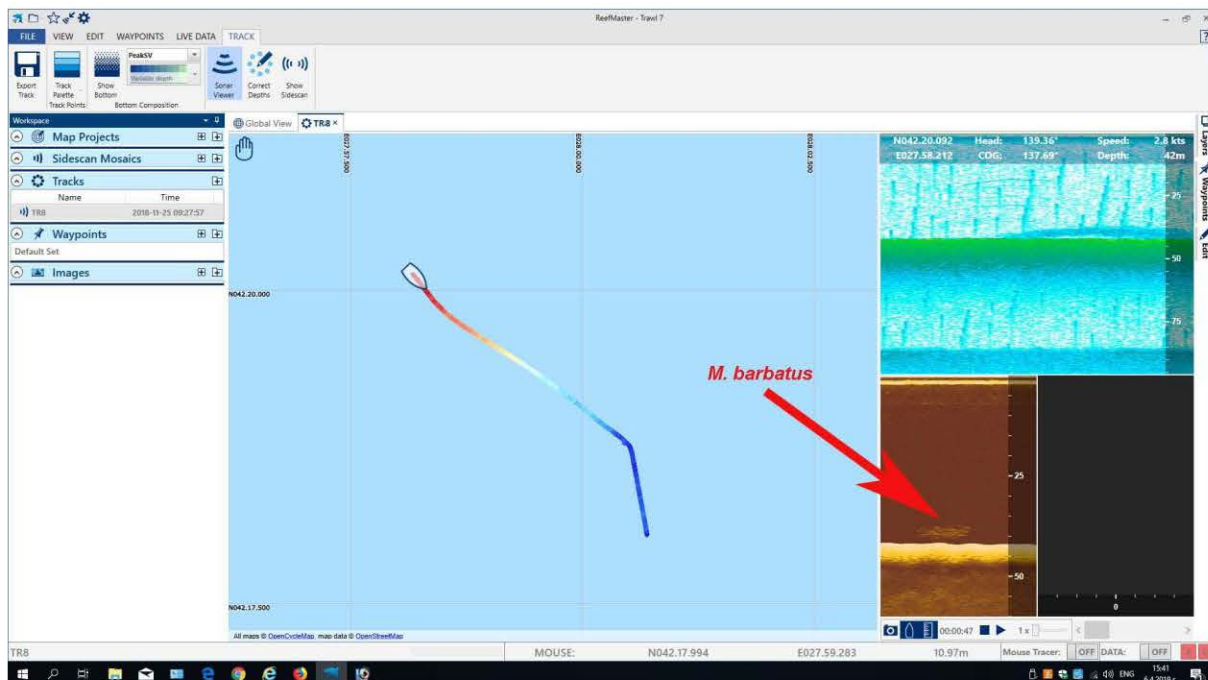


Figure 8. Processing and interpretation of hydroacoustic profile data
(ReefMaster2.0.38.0)



МИНИСТЕРСТВО НА ЗЕМЕДЕЛИЕТО, ХРАНИТЕ И
ГОРИТЕ

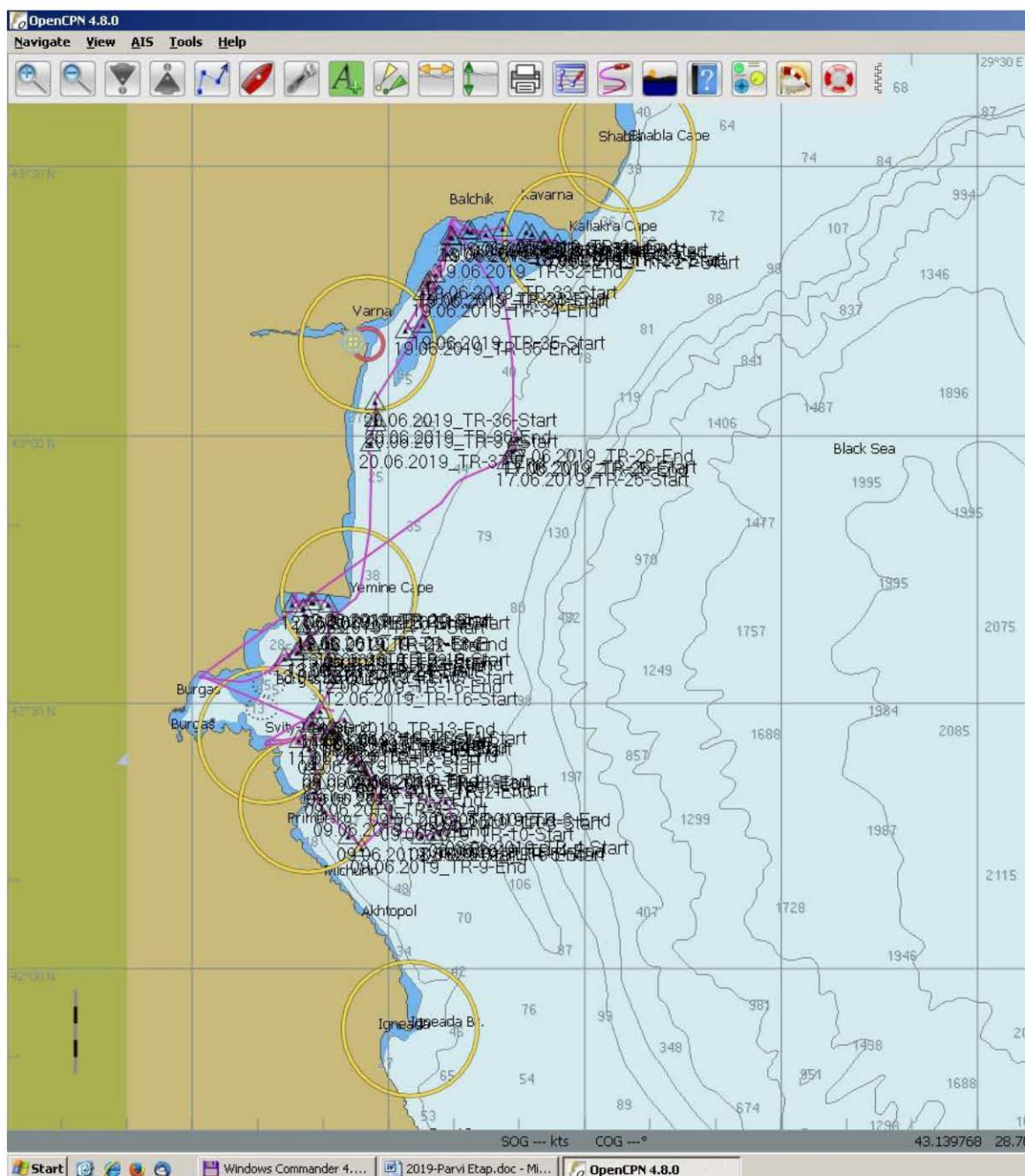


Figure 9. Navigation map of the expedition in June 2019 (OpenCPN 4.8.0) [1]



МИНИСТЕРСТВО НА ЗЕМЕДЕЛИЕТО, ХРАНИТЕ И
ГОРИТЕ

For more detailed depth measurement, determination of the fish species and determination of the bottom sediments type, was used Hydrographic Survey Echo Sounder "LituGraph 4F" (Fig. 10 - 15).

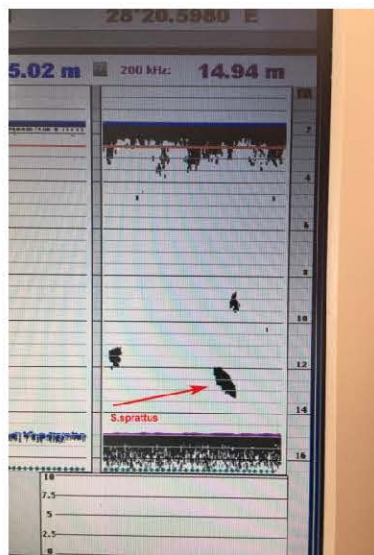


Figure 10. Hydrographic Survey Echo Sounder "LituGraph 4F"

Trawl 27, fish schools of *S.sprattus*



Figure 11. Trawl 27, catch - 150 kg *S.sprattus*, 5 kg *E.encrasiculus*, 10 kg *M.merlangus*, 10 kg *M.barbatus*, 2 ind. *A.immaculata*, 20 kg Gobiidae, 5 kg *A.aurita*, 5 ind. *T. mediterraneus*, 3 ind. *A.stellatus*, 3 ind. *S.maximus*



МИНИСТЕРСТВО НА ЗЕМЕДЕЛИЕТО, ХРАНИТЕ И
ГОРИТЕ

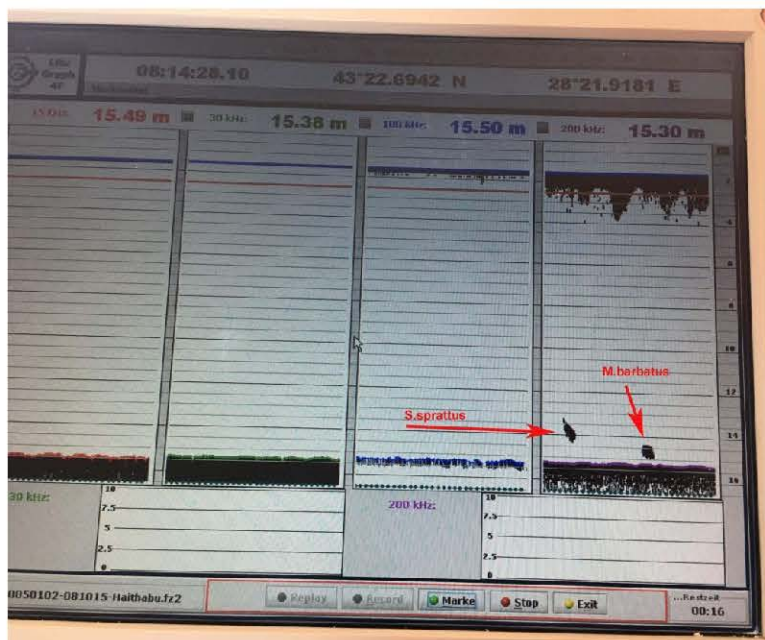


Figure 12. Hydrographic Survey Echo Sounder "LituGraph 4F"

Trawl 31, fish schools of *S.sprattus*, *M.barbatus*, Gobiidae.



Figure 13. Trawl 31, catch - 90 kg *S.sprattus*, 20 kg *M.barbatus*, 3 ind. *A.immaculata*, 20 kg Gobiidae, 70 kg *A.aurita*, 7 бр. *T. Mediterraneus*, 2 ind. *S.maximus*, 1 ind. *U.scaber*, 5 ind. *E.encrasiculus*



МИНИСТЕРСТВО НА ЗЕМЕДЕЛИЕТО, ХРАНИТЕ И
ГОРИТЕ

For the purposes and tasks of the present study, the hydro-acoustic equipment SIMRAD - NSO evo3 / HDS Carbon / LOWRANCE (Fig. 6, 7, 8), [2, 3] was used.



Figure 14. SIMRAD - NSO evo3 / HDS Carbon / LOWRANCE



Figure 15. Probe of "SIMRAD - NSO evo3"

The hydroacoustic profiles make it possible to determine the quantitative and qualitative characteristics of the fish schools in combination with the macroscopic description of the trawl picture taken.

NSO evo3 delivers the ultimate view with an ultra-bright display, available in 16, 19, or 24-inch widescreen sizes. Wide viewing angles keep the screen in view from anywhere in sight, even if you're wearing polarized sunglasses. See more than ever



МИНИСТЕРСТВО НА ЗЕМЕДЕЛИЕТО, ХРАНИТЕ И
ГОРИТЕ



with Full HD resolution, and the option to combine up to six panels in a split-screen layout. Intuitively navigate charts, define waypoints, and take control of connected systems such as autopilot, radar, and sonar with a touch.

The Carbon HDS Series combines side imaging, downscan imaging, dual-channel CHIRP sonar, real-time underwater 3D mapping capabilities and ultra-bright displays to deliver the most advanced and easy-to-use fish finder/chart plotter on the market. The units' touch-screen interface works much like a smartphone with pinch-to-zoom and touch-and-move abilities for fast and intuitive control.

HDS Carbon units also feature the ability to create custom maps using recorded sonar logs. Anglers can add custom color layers, vegetation and bottom-hardness overlays. Each unit supports the most advanced marine technology and is easily updated to the most current software for optimal performance.

Featuring a powerful dual-core, high-performance processor, the HDS Carbon delivers accurate and definitive images with superior target separation. HDS Carbon multi-touch, super bright displays offer a wider viewing angle and feature an advanced anti-reflective coating for ultimate viewing in bright sunlight and while wearing polarized sunglasses.

HDS Carbon units remove the hassle of constantly monitoring and repositioning the boat with connectivity to certain autopilot trolling motors and shallow water anchors, freeing up anglers to concentrate on fishing. Both bow-mounted and console sonar can be displayed side-by-side with different zoom levels for a clear and precise view of schools or individual fish.

"SIMRAD - NSO evo3" provides the following data processing capabilities: navigation map, sonar and radar.

The Sonar feature provides an underwater view of the area, under and around the ship, allowing easy visualization of fish passages and geological - geomorphologic exploration of the sea floor. The format of the files is <*.sl3>, which includes the Sonar and StructureScan3D options. StructureScan HD provides a 328-meter wide-screen coverage with SideScan, while DownScan™ provides a detailed view of the bottom structure and fish passages directly below the boat up to 92 m. StructureScan 3D is a multi-beam sonar technology that allows you to observe the structure and geomorphological features of the bottom in 3D.



МИНИСТЕРСТВО НА ЗЕМЕДЕЛИЕТО, ХРАНИТЕ И
ГОРИТЕ

The "ReefMaster2.0.38.0" software was used to process and interpret hydroacoustic profile data (Fig. 16.) [4].

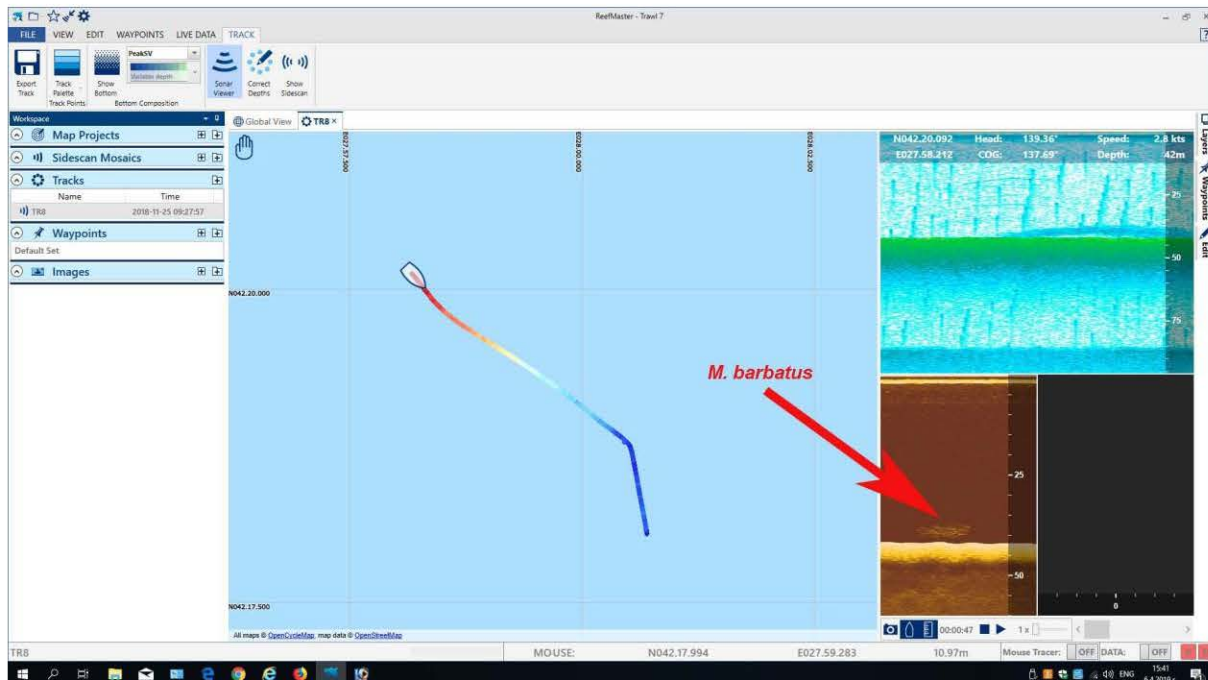


Figure 16. Processing and interpretation of hydroacoustic profile data
(ReefMaster2.0.38.0)



ЕВРОПЕЙСКИ СЪЮЗ
ЕВРОПЕЙСКИ ФОНД ЗА
МОРСКО ДЕЛО И РИБАРСТВО



МИНИСТЕРСТВО НА ЗЕМЕДЕЛИЕТО, ХРАНИТЕ И
ГОРИТЕ



ANNEX III Surveys indicator targets and results in 2018 (Bulgarian part)

Black Sea		market, discards, surveys	2,50%	Survey: 1326 1250
Black Sea	Length @age	market, discards, surveys	2,50%	Survey: 1326 5000
Black Sea	Weight @length	market, discards, surveys	2,50%	Market: Discard: - Survey: 1326
Black Sea	Weight @age	market, discards, surveys	2,50%	1250
Black Sea	Maturity @length	surveys	2,50%	5000 140
Black Sea	Maturity @age	surveys	2,50%	5000 140
Black Sea		market, surveys	2,50%	Market: 250 Survey: 250
Black Sea	Sex-ratio @length			125
Black Sea	Sex-ratio @age	market, surveys	2,50%	Market: 250 250 survey



ЕВРОПЕЙСКИ СЪЮЗ
ЕВРОПЕЙСКИ ФОНД ЗА
МОРСКО ДЕЛО И РИБАРСТВО



МИНИСТЕРСТВО НА ЗЕМЕДЕЛИЕТО, ХРАНИТЕ И
ГОРИТЕ



ANNEX IV Navigation, bathymetry and hydroacoustics

For more sensitivity interpretation of the results of trawl picture was used navigation software OpenCPN 4.8.0 [1] and GPS "HOLLUX" (Fig. I, II)

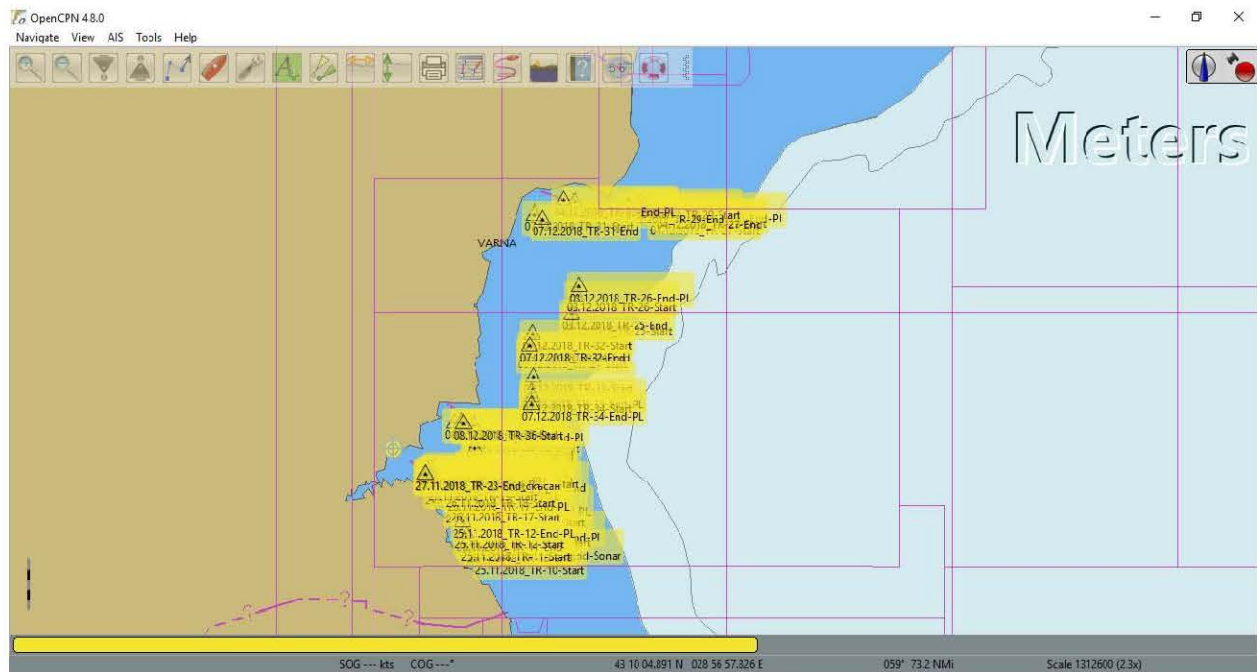


Figure I. Navigation map of the first expedition 2018 (OpenCPN 4.8.0) [1]



ЕВРОПЕЙСКИ СЪЮЗ
ЕВРОПЕЙСКИ ФОНД ЗА
МОРСКО ДЕЛО И РИБАРСТВО



МИНИСТЕРСТВО НА ЗЕМЕДЕЛИЕТО, ХРАНИТЕ И
ГОРИТЕ

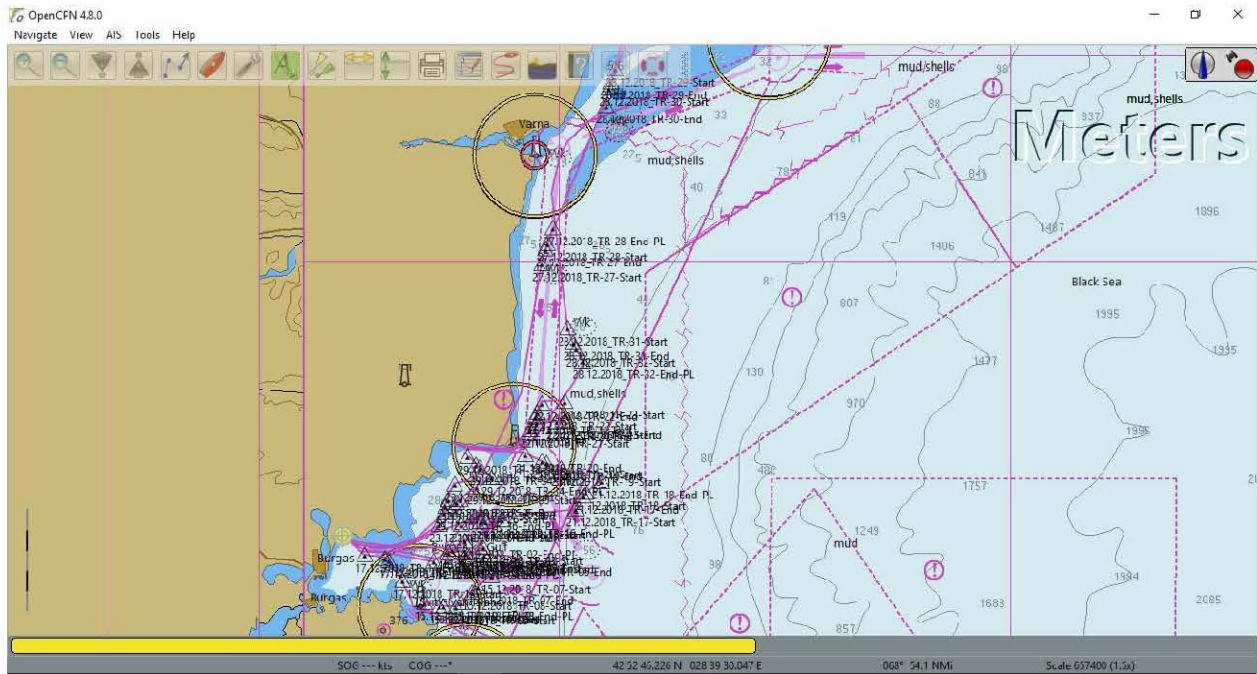


Figure II. Navigation map of the second expedition 2018 (OpenCPN 4.8.0) [1]

For the more detailed depth measurement and determination of the bottom sediments type, was used Hydrographic Survey Echo Sounder "LituGraph 4F" (Fig. III)

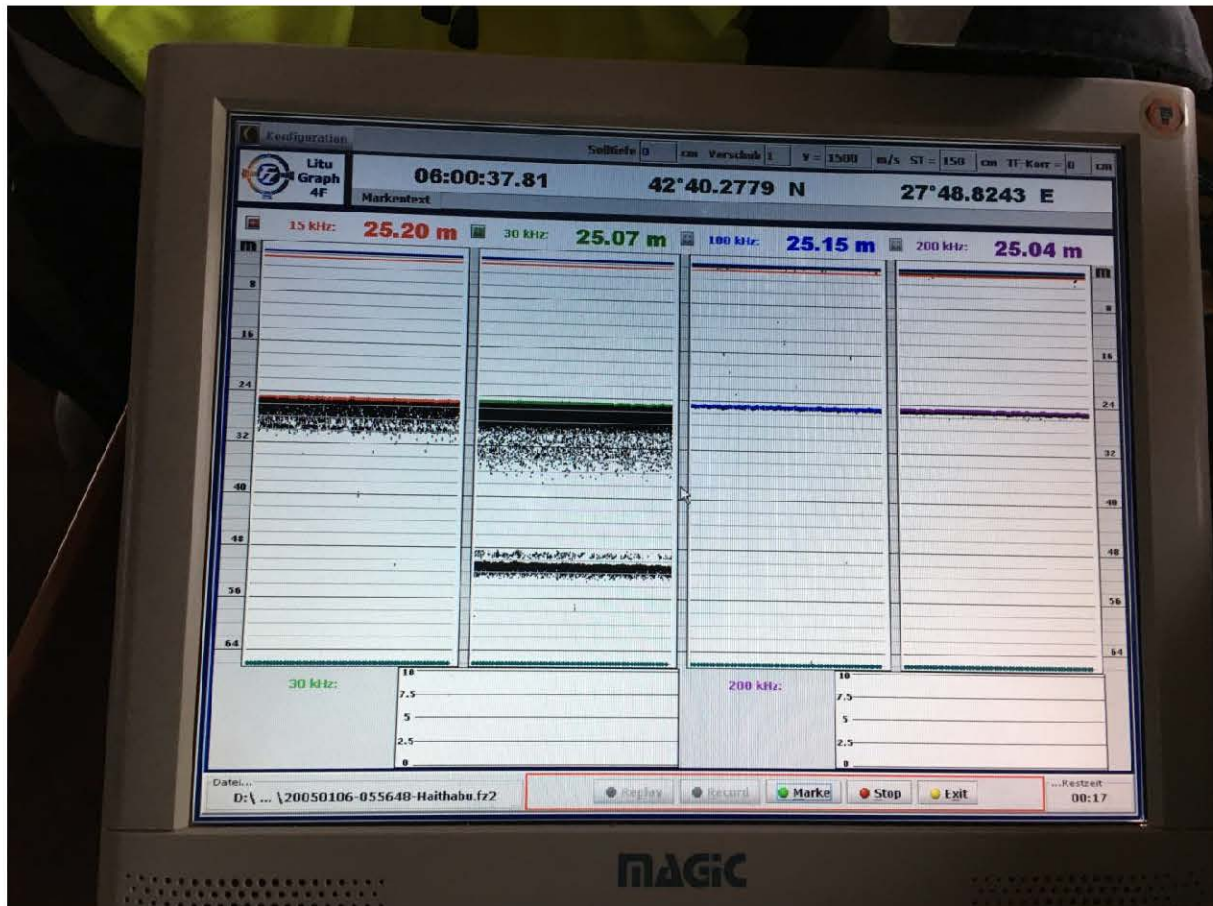


Figure III. Hydrographic Survey Echo Sounder "LituGraph 4F"

For the purposes and tasks of the present study, the hydro-acoustic equipment SIMRAD
- NSO evo3 / HDS Carbon / LOWRANCE (Fig. IV, V) was used.



Figure IV. "SIMRAD - NSO evo3"



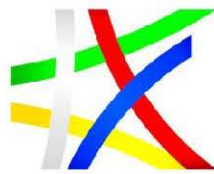
Figure V. Probe of "SIMRAD - NSO evo3"



ЕВРОПЕЙСКИ СЪЮЗ
ЕВРОПЕЙСКИ ФОНД ЗА
МОРСКО ДЕЛО И РИБАРСТВО



МИНИСТЕРСТВО НА ЗЕМЕДЕЛИЕТО, ХРАНИТЕ И
ГОРИТЕ



ПРОГРАМА ЗА
МОРСКО ДЕЛО И
РИБАРСТВО

The hydroacoustic profiles make it possible to determine the quantitative and qualitative characteristics of the fish schools in combination with the macroscopic description of the trawl picture taken. Due to the unfavorable autumn-winter weather conditions (strong wind, excitement over 4 balls and low temperatures), 3 profiles were made during the first stage of the expedition. Excitement over 4 bales may cause a sonar probe to break or damage and also is danger for live of crew.

NSO evo3 delivers the ultimate view with an ultra-bright display, available in 16, 19, or 24-inch widescreen sizes. Wide viewing angles keep the screen in view from anywhere in sight, even if you're wearing polarized sunglasses. See more than ever with Full HD resolution, and the option to combine up to six panels in a split-screen layout. Intuitively navigate charts, define waypoints, and take control of connected systems such as autopilot, radar, and sonar with a touch.

The Carbon HDS Series combines side imaging, downscan imaging, dual-channel CHIRP sonar, real-time underwater 3D mapping capabilities and ultra-bright displays to deliver the most advanced and easy-to-use fish finder/chart plotter on the market. The units' touch-screen interface works much like a smartphone with pinch-to-zoom and touch-and-move abilities for fast and intuitive control.

HDS Carbon units also feature the ability to create custom maps using recorded sonar logs. Anglers can add custom color layers, vegetation and bottom-hardness overlays. Each unit supports the most advanced marine technology and is easily updated to the most current software for optimal performance.

Featuring a powerful dual-core, high-performance processor, the HDS Carbon delivers



ЕВРОПЕЙСКИ СЪЮЗ
ЕВРОПЕЙСКИ ФОНД ЗА
МОРСКО ДЕЛО И РИБАРСТВО



МИНИСТЕРСТВО НА ЗЕМЕДЕЛИЕТО, ХРАНИТЕ И
ГОРИТЕ



ПРОГРАМА ЗА
МОРСКО ДЕЛО И
РИБАРСТВО

accurate and definitive images with superior target separation. HDS Carbon multi-touch, super bright displays offer a wider viewing angle and feature an advanced anti-reflective coating for ultimate viewing in bright sunlight and while wearing polarized sunglasses.

HDS Carbon units remove the hassle of constantly monitoring and repositioning the boat with connectivity to certain autopilot trolling motors and shallow water anchors, freeing up anglers to concentrate on fishing. Both bow-mounted and console sonar can be displayed side-by-side with different zoom levels for a clear and precise view of schools or individual fish.

"SIMRAD - NSO evo3" provides the following data processing capabilities: navigation, map, sonar, radar.

The Sonar feature provides an underwater view of the area, under and around the ship, allowing easy visualization of fish passages and geological - geomorphologic exploration of the sea floor. The format of the files is <*.sl3>, which includes the Sonar and StructureScan3D options. StructureScan HD provides a 328-meter wide-screen coverage with SideScan, while DownScan™ provides a detailed view of the bottom structure and fish passages directly below the boat up to 92 m. StructureScan 3D is a multi-beam sonar technology that allows you to observe the structure and geomorphological features of the bottom in 3D.



ЕВРОПЕЙСКИ СЪЮЗ
ЕВРОПЕЙСКИ ФОНД ЗА
МОРСКО ДЕЛО И РИБАРСТВО



МИНИСТЕРСТВО НА ЗЕМЕДЕЛИЕТО, ХРАНИТЕ И
ГОРИТЕ



The "ReefMaster2.0.38.0" software was used to process and interpret hydroacoustic profile data (Fig. VI-XI).

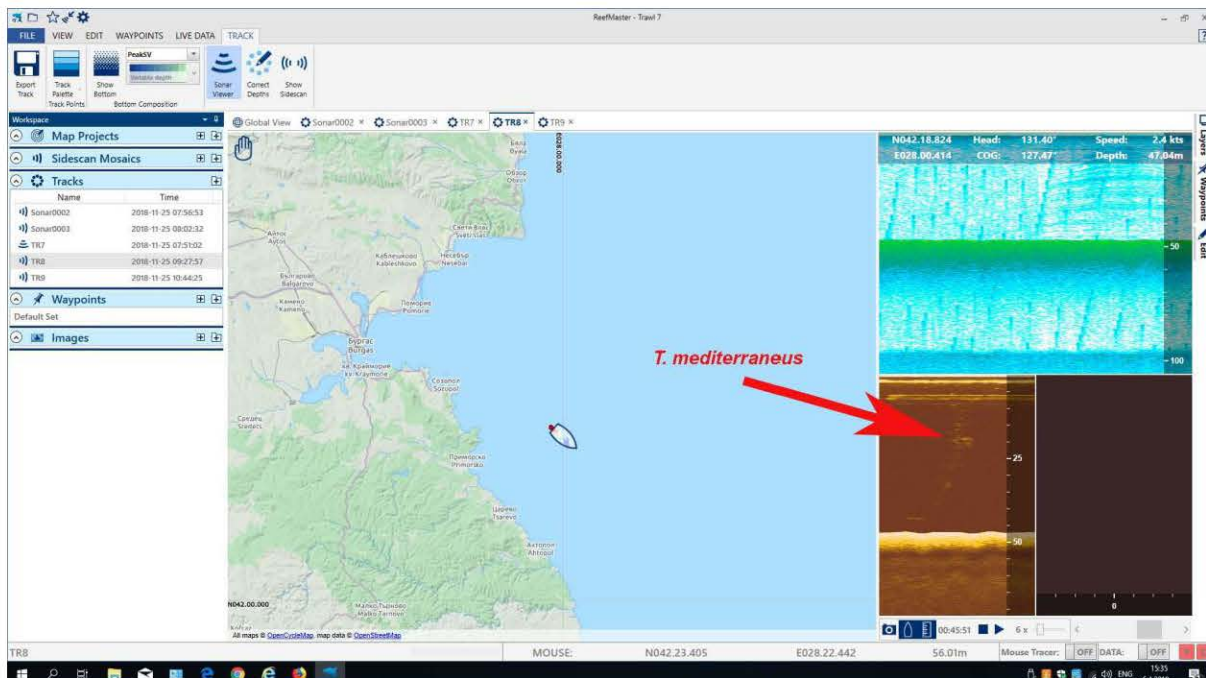


Figure VI. First Stage of survey



ЕВРОПЕЙСКИ СЪЮЗ
ЕВРОПЕЙСКИ ФОНД ЗА
МОРСКО ДЕЛО И РИБАРСТВО



МИНИСТЕРСТВО НА ЗЕМЕДЕЛИЕТО, ХРАНИТЕ И
ГОРИТЕ



1. First Stage

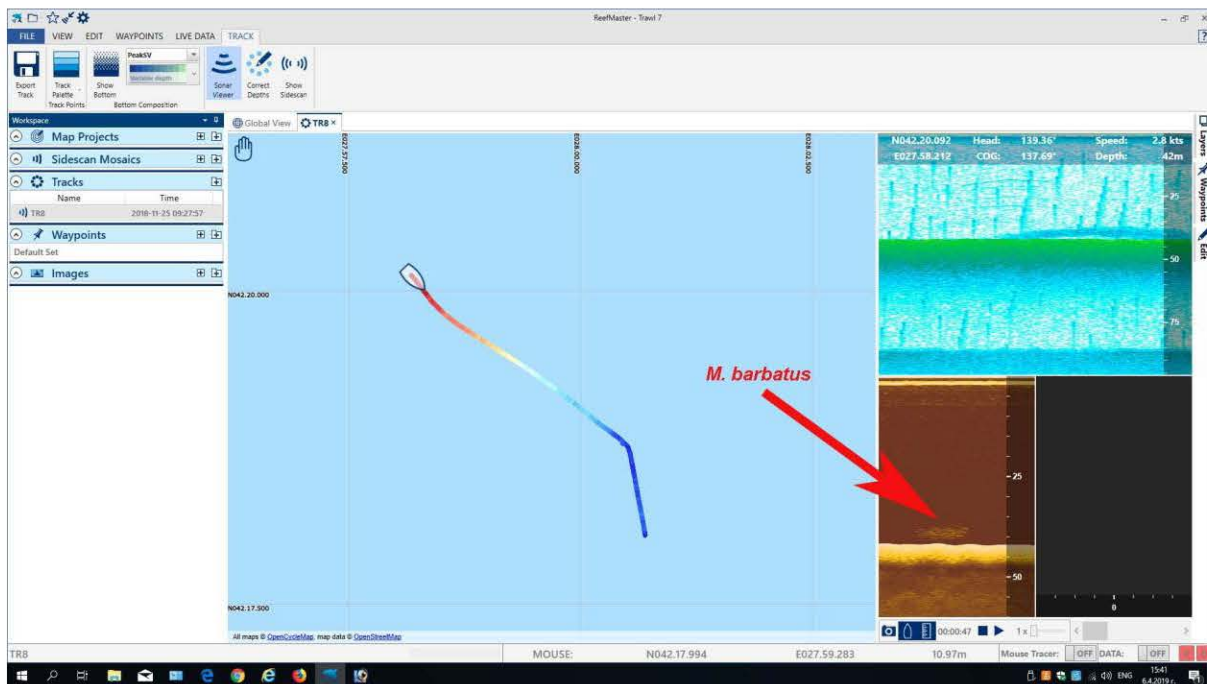


Figure VII. Trawl 8, situation – 1, start, fish cloud of *M. barbatus*



ЕВРОПЕЙСКИ СЪЮЗ
ЕВРОПЕЙСКИ ФОНД ЗА
МОРСКО ДЕЛО И РИБАРСТВО



МИНИСТЕРСТВО НА ЗЕМЕДЕЛИЕТО, ХРАНИТЕ И
ГОРИТЕ

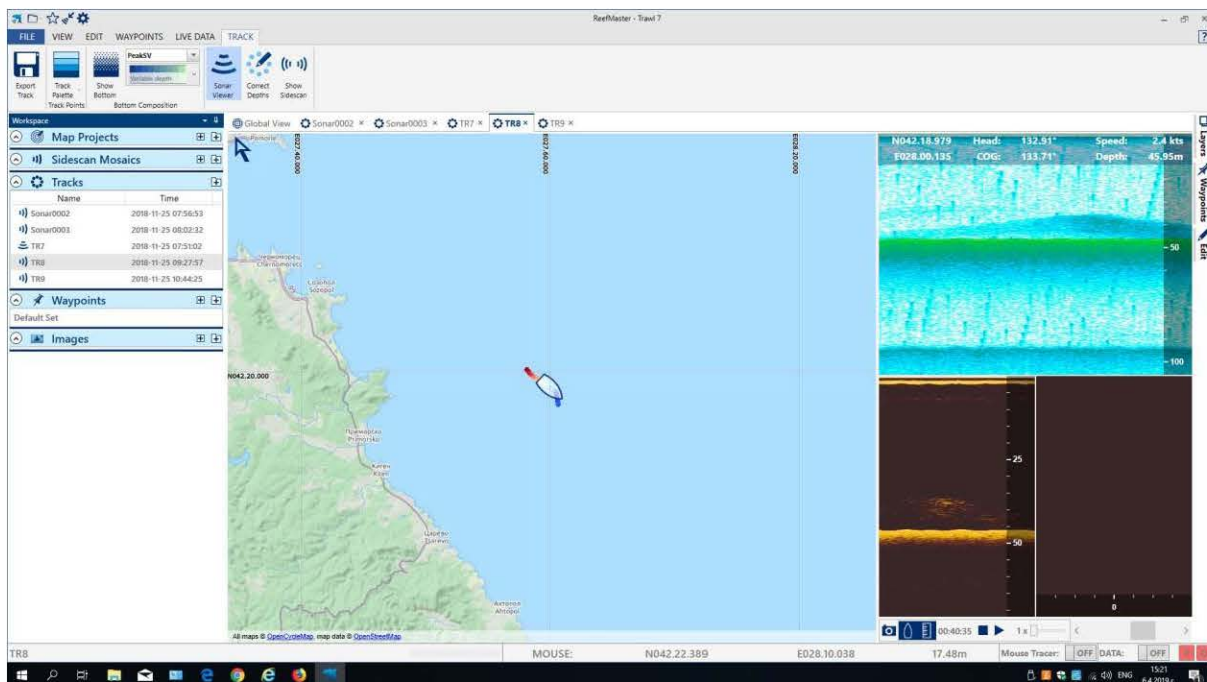


Figure VIII. Trawl 8, situation – 2



ЕВРОПЕЙСКИ СЪЮЗ
ЕВРОПЕЙСКИ ФОНД ЗА
МОРСКО ДЕЛО И РИБАРСТВО



МИНИСТЕРСТВО НА ЗЕМЕДЕЛИЕТО, ХРАНИТЕ И
ГОРИТЕ

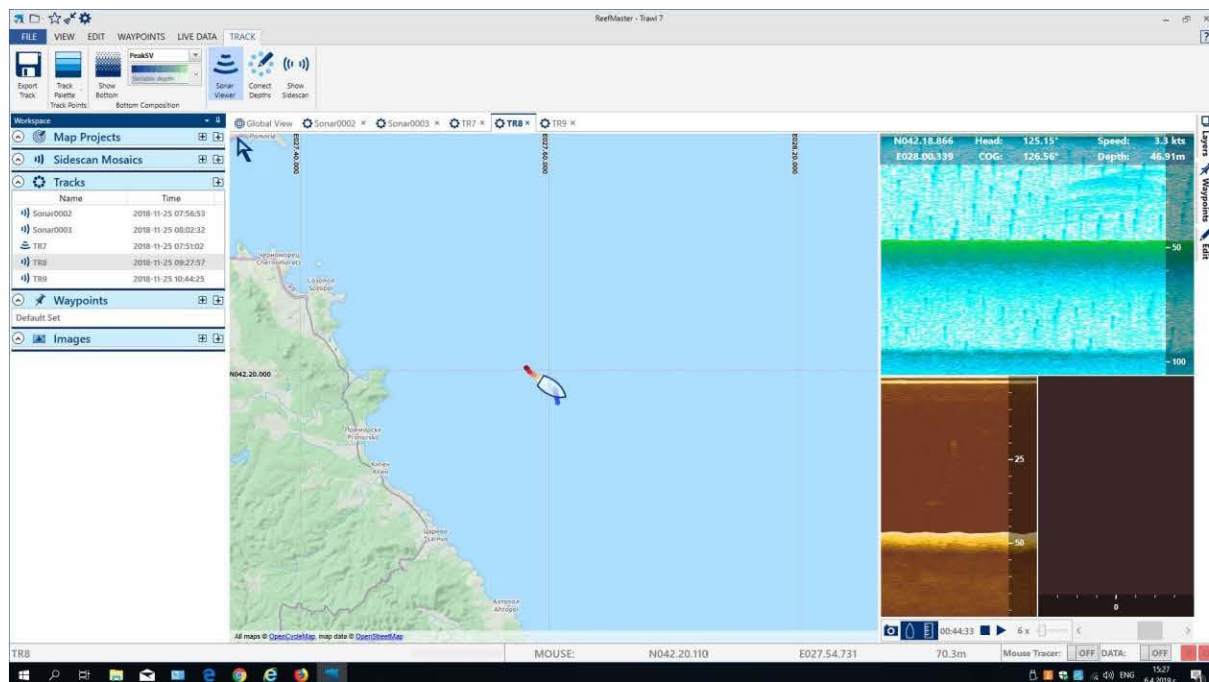


Figure IX. Trawl 8, situation – 3



ЕВРОПЕЙСКИ СЪЮЗ
ЕВРОПЕЙСКИ ФОНД ЗА
МОРСКО ДЕЛО И РИБАРСТВО



МИНИСТЕРСТВО НА ЗЕМЕДЕЛИЕТО, ХРАНИТЕ И
ГОРИТЕ

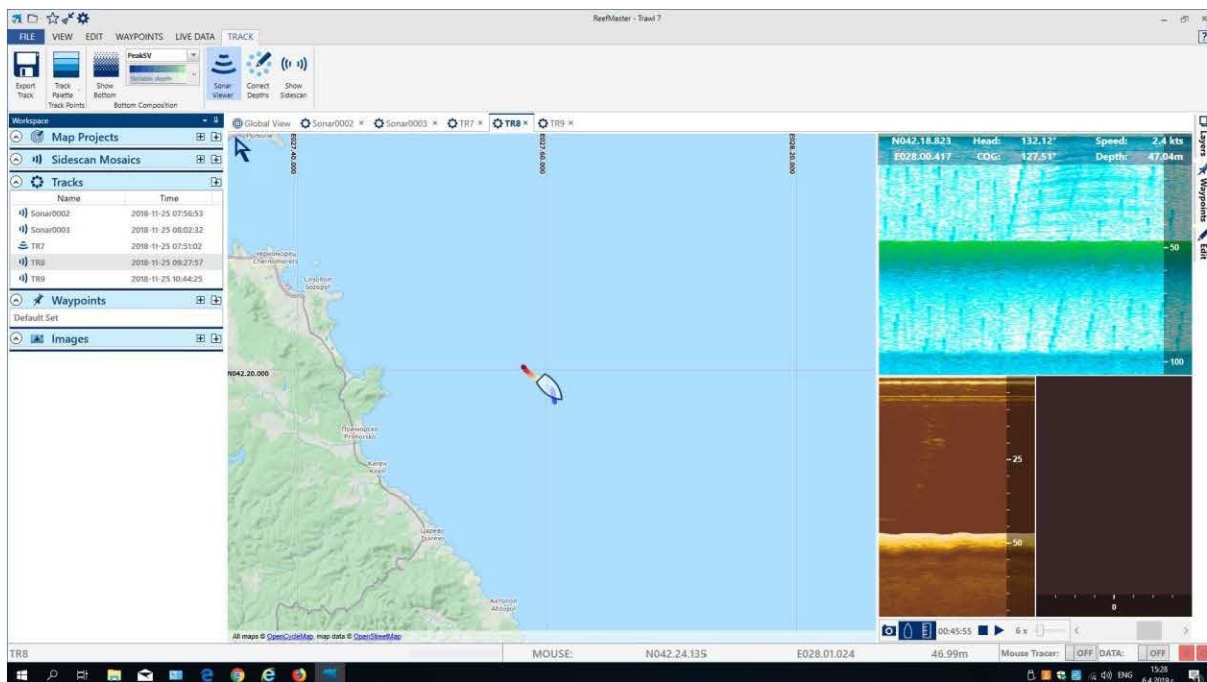


**Figure X. Trawl 8, situation – 4, fish schools of *M. barbatus*, *T. mediterraneus*,
*P. saltatrix***

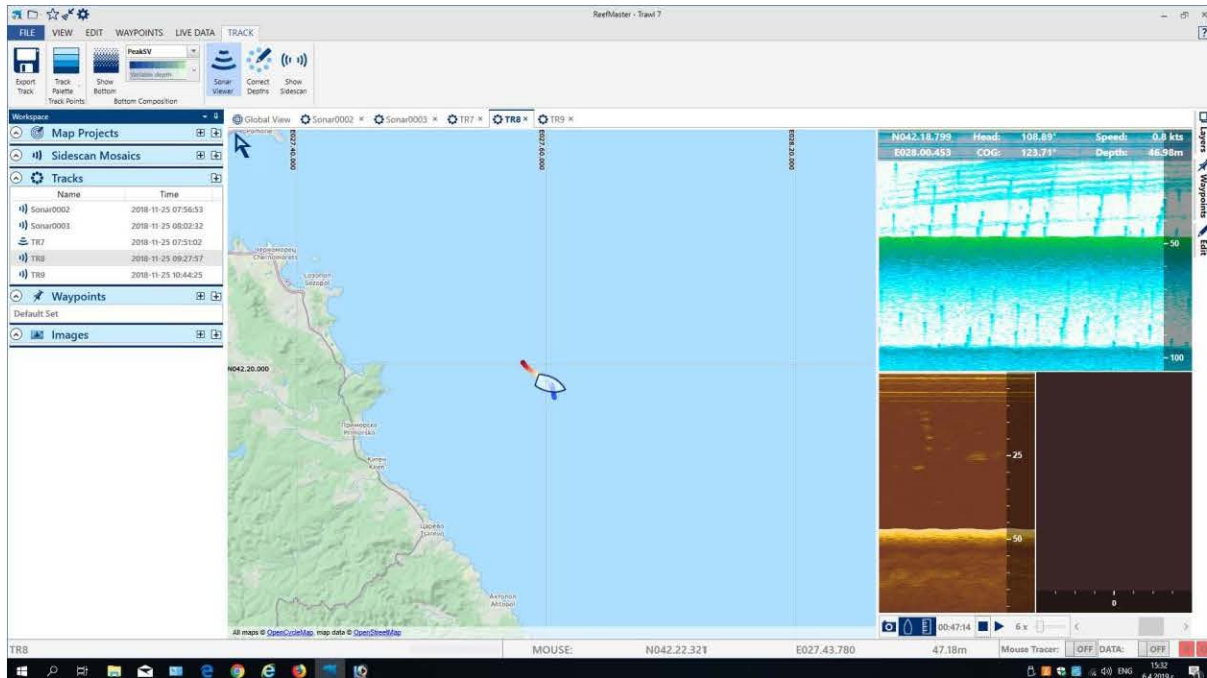


Figure XI. Trawl 8, situation – 5, end, catch - 20 kg *A. aurita*, 60 kg *M. barbatus*, 20 kg *T. mediterraneus*, 8 kg *P. saltatrix*

Softwares:

- [1] OpenCPN 4.8.0. <https://opencpn.org/OpenCPN/about/ver480.html>
- [2] Lowrance. 2018. <https://www.lowrance.com/lowrance/series/hds-carbon/>
- [3] SIMRAD. 2018. <https://www.simrad-yachting.com/simrad/series/nso-evo3/>
- [4] ReefMaster Software Ltd. 2018. <https://reefmaster.com.au/>



ЕВРОПЕЙСКИ СЪЮЗ
ЕВРОПЕЙСКИ ФОНД ЗА
МОРСКО ДЕЛО И РИБАРСТВО



МИНИСТЕРСТВО НА ЗЕМЕДЕЛИЕТО, ХРАНИТЕ И
ГОРИТЕ



Pictures



Photo 1. Catch in the codend



ЕВРОПЕЙСКИ СЪЮЗ
ЕВРОПЕЙСКИ ФОНД ЗА
МОРСКО ДЕЛО И РИБАРСТВО



МИНИСТЕРСТВО НА ЗЕМЕДЕЛИЕТО, ХРАНИТЕ И
ГОРИТЕ



Photo 2. Bycatch



ЕВРОПЕЙСКИ СЪЮЗ
ЕВРОПЕЙСКИ ФОНД ЗА
МОРСКО ДЕЛО И РИБАРСТВО



МИНИСТЕРСТВО НА ЗЕМЕДЕЛИЕТО, ХРАНИТЕ И
ГОРИТЕ

ПРОГРАМА ЗА
МОРСКО ДЕЛО И
РИБАРСТВО



Photo 3. *Sc. maximus*, *P. saltatrix*



ЕВРОПЕЙСКИ СЪЮЗ
ЕВРОПЕЙСКИ ФОНД ЗА
МОРСКО ДЕЛО И РИБАРСТВО



МИНИСТЕРСТВО НА ЗЕМЕДЕЛИЕТО, ХРАНИТЕ И
ГОРИТЕ



Photo 4. Catch and bycatch



ЕВРОПЕЙСКИ СЪЮЗ
ЕВРОПЕЙСКИ ФОНД ЗА
МОРСКО ДЕЛО И РИБАРСТВО



МИНИСТЕРСТВО НА ЗЕМЕДЕЛИЕТО, ХРАНИТЕ И
ГОРИТЕ



Photo 5. Catch and bycatch